Technical Report Documentation Page

1. Report No.	2. Government Accession No.	3. Recipient's Catalog No.
Preliminary Review Copy		

4. Title and Subtitle	5. Report Date
AN EXPLORATION OF LATERAL LOAD DISTRIBUTION IN A GIRDER-SLAB BRIDGE IN GATESVILLE, TEXAS	**September 2000**
	6. Performing Organization Code

7. Author(s)	8. Performing Organization Report No.
S. M. Barney, K. H. Frank, J. A. Yura, M. E. Kreger, and S. L. Wood	Research Report 2986-4

9. Performing Organization Name and Address	10. Work Unit No. (TRAIS)
Center for Transportation Research The University of Texas at Austin 3208 Red River, Suite 200 Austin, TX 78705-2650	11. Contract or Grant No. Research Study 7-2986

12. Sponsoring Agency Name and Address	13. Type of Report and Period Covered
Texas Department of Transportation Research and Technology Transfer Section, Construction Division P.O. Box 5080 Austin, TX 78763-5080	Research Report (9/95-8/99)
	14. Sponsoring Agency Code

15. Supplementary Notes

Project conducted in cooperation with the U.S. Department of Transportation

16. Abstract

Older bridges currently in service can be tested to determine if the bridges behave as originally designed. Many current design methods are overly conservative. This research shows the results of the instrumentation and testing of the Leon River Bridge for its lateral distribution of live load. Tests were conducted to determine the response of the bridge to normal and overweight vehicles and to explore static and dynamic effects. Data was acquired in a simple and logical manner that gave insight into bridge behavior. This research also shows the benefits of computer modeling using SAP2000 and BRUFEM in this process. The actual moments from the test runs, estimated moments from BRUFEM, and design moments from various codes are compared in order to draw conclusions about the performance of the bridge, quality of the estimates, and the adequacy of accepted design tools.

17. Key Words	18. Distribution Statement
	No restrictions. This document is available to the public through the National Technical Information Service, Springfield, Virginia 22161.

19. Security Classif. (of report)	20. Security Classif. (of this page)	21. No. of pages	22. Price
Unclassified	Unclassified		

Form DOT F 1700.7 (8-72) Reproduction of completed page authorized

An Exploration of Lateral Load Distribution in a Girder-Slab Bridge in Gatesville, Texas

by

S. M. Barney, K. H. Frank, J. A. Yura, M. E. Kreger, and S. L. Wood

Research Report 2986-4

Research Project 7-2986

BRIDGE LOAD TESTING PROGRAM

conducted for the

Texas Department of Transportation

in cooperation with the

U.S. Department of Transportation
Federal Highway Administration

by the

CENTER FOR TRANSPORTATION RESEARCH
BUREAU OF ENGINEERING RESEARCH
THE UNIVERSITY OF TEXAS AT AUSTIN

September 2000

Research performed in cooperation with the Texas Department of Transportation and the U.S. Department of Transportation, Federal Highway Administration.

ACKNOWLEDGEMENTS

We greatly appreciate the financial support from the Texas Department of Transportation that made this project possible. The support of the project director, Mike Lynch (BRG), and program coordinator, Ron Koester, is also very much appreciated. We thank Project Monitoring Committee members, XXXXXXX.

DISCLAIMER

NOT INTENDED FOR CONSTRUCTION,
PERMIT, OR BIDDING PURPOSES

K. H. Frank, Texas P.E. # 48953
J. A. Yura, Texas P.E. #29859
M. E. Kreger, Texas P.E. #65541
S. L. Wood, Texas P.E. #83804
Research Supervisors

TABLE OF CONTENTS

LIST OF FIGURES

LIST OF TABLES

SUMMARY

Older bridges currently in service can be tested to determine if the bridges behave as originally designed. Many current design methods are overly conservative. This research shows the results of the instrumentation and testing of the Leon River Bridge for its lateral distribution of live load. Tests were conducted to determine the response of the bridge to normal and overweight vehicles and to explore static and dynamic effects. Data was acquired in a simple and logical manner that gave insight into bridge behavior. This research also shows the benefits of computer modeling using SAP2000 and BRUFEM in this process. The actual moments from the test runs, estimated moments from BRUFEM, and design moments from various codes are compared in order to draw conclusions about the performance of the bridge, quality of the estimates, and the adequacy of accepted design tools.

CHAPTER 1: INTRODUCTION TO BRIDGE TEST

1.1 BACKGROUND

The F.M. Highway 1829 Bridge crosses over the Leon River in Gatesville, Texas. This bridge was included in a testing program organized by the U.S. Army and New Mexico State University. The Leon River Bridge is a 3-span, continuous steel girder bridge with a reinforced concrete slab. The University of Texas, with support from the Texas Department of Transportation (TxDOT) took advantage of the opportunity to perform testing on the unit. In addition to the scheduled test vehicle (a military heavy equipment vehicle loaded with a M113 Armored Personnel Carrier), the University of Texas included a 3-axle dump truck provided by TxDOT for the purposes of this research. The test was performed on 18 September 1998.

The primary goal of this research was to investigate the distribution of live load laterally across a steel girder bridge. In the course of this research, comparisons were made between the actual lateral distribution of live load and the distributions indicated by computer methods and by the empirical equations for lateral load distribution factors (LLDFs), given by various design codes. The actual distribution of load across three different bridge sections was obtained by the vehicle tests. The TxDOT dump truck was used to concentrate load on the exterior girders, whereas the military HETS vehicle was used to provide a case of distribution under an oversized vehicle.

1.2 BRIDGE DESCRIPTION

The Leon River Bridge was erected in 1955. The bridge was designed and built to fulfill H15-44 loading in accordance with the 1953 AASHTO Standard Specifications. A profile of the center span of the bridge is shown in Figure 1.1.

Figure 1.1: Profile view of center span of Leon River Bridge

1.2.1 Geometry

The F. M. Highway 1829 bridge is a 230-foot, three-span, continuous unit. The unit is orientated in an approximately north-south direction on F.M. 1829. The spans are 70'-90'-70' in length. The bridge consists of 4 girders in the longitudinal direction spaced 6.67' on center. The roadway is 24' wide and carries two lanes of traffic. The bridge contains a total of 15 sets of diaphragms. The spacing of these girders and diaphragms is shown in Figure 1.2.

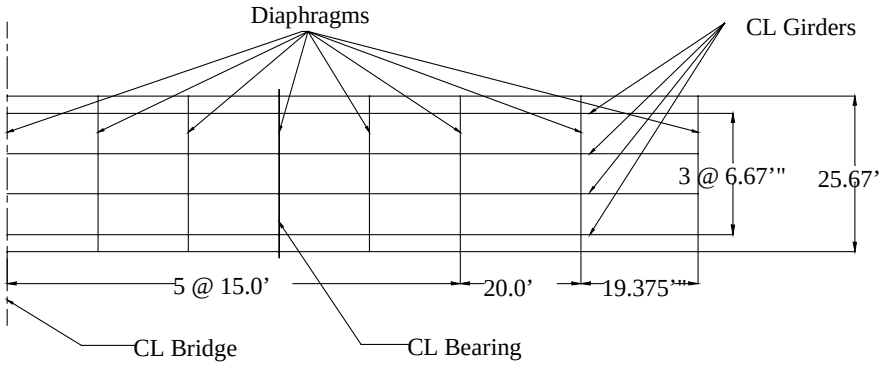

Figure 1.2: Plan view of girder and diaphragm centerline locations

1.2.2 Girders

The girders are supported on pin-and-rocker supports with one of the interior supports as a fixed shoe. One of the end supports is shown in Figure 1.3.

Figure 1.3: A rocker support at an abutment

W33x130 shapes are used in the end spans and are spliced to W33x141 shapes in the center span. The arrangement of wide flange shapes is shown in the half elevation given in Figure 1.4.

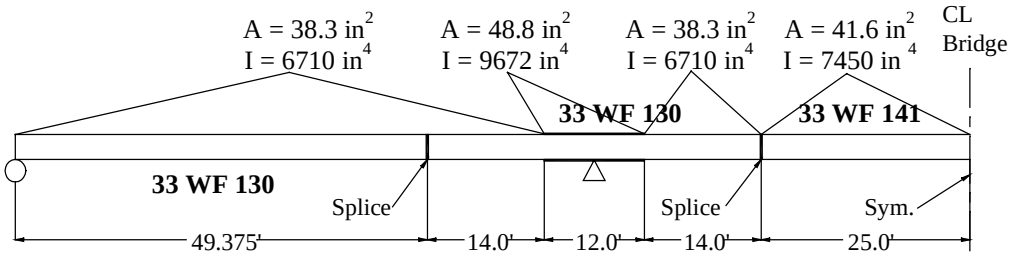

Figure 1.4: Half-elevation of the F.M. 1829 Bridge

The girders do not have shear studs to provide composite behavior with the deck slab. The girders do have 1.0" thick cover plates on the top and bottom of the W-shape at each pier location. These cover plates are 10.5"wide and 12' in length. The cover plates are also tapered at the ends, as shown in the cover plate detail of Figure 1.5.

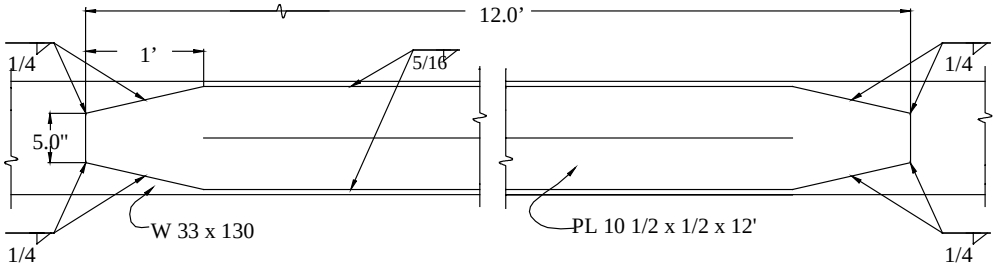

Figure 1.5: Detail of cover plate at support

Some of the dimensions of the girders were measured in the field. The dimensions of concern were the bottom flange thickness and web thickness. The top flange was embedded in the concrete deck and could not be verified by measurement. The nominal dimensions of the W33x130 shape are given in Figure 1.6.

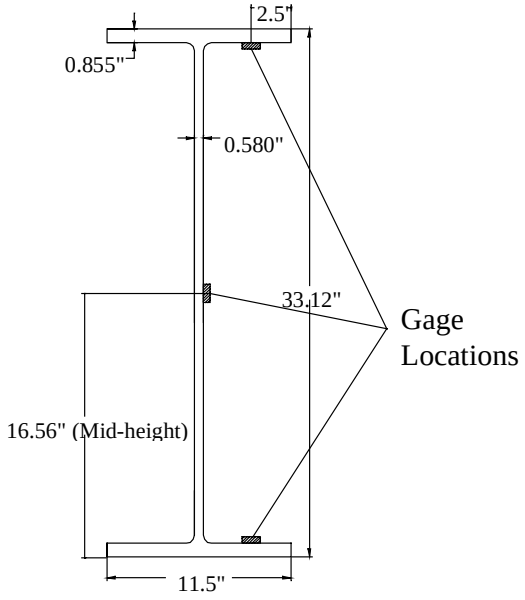

Figure 1.6: Nominal dimensions and gage locations for a W33x130 section

The nominal dimensions of the W33x141 are given in Figure 1.7. Field measurements on the W33x141 shapes were not taken because they were out of reach without special equipment for access.

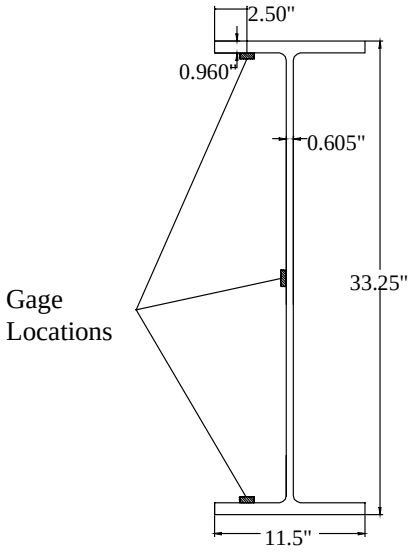

Figure 1.7: Nominal dimensions and gage locations for a W33x141 section

Table 1.1 below, shows the moments of inertia for the nominal and measured W33x130 sections. The largest percent difference was 1.4%. This small difference was within the experimental accuracy of the bridge measurements and software used for analysis. The nominal properties were used in the analysis of the bridge.

Table 1.1: Variation in moment of inertia for W33x130

Section	Moment of Inertia ($in.^4$)	Variation from Nominal
Nominal	6710.0	0.00%
Girder 1	6632.9	-1.15%
Girder 2	6795.6	1.28%
Girder 3	6804.0	1.40%
Girder 4	6677.1	-0.49%

1.2.3 Deck

The plans from 1955 state that the 6.0" deck is composed of 'Class A' concrete. The concrete was assumed to have a compressive strength of 4000psi. A cross section of the bridge is shown in Figure 1.8.

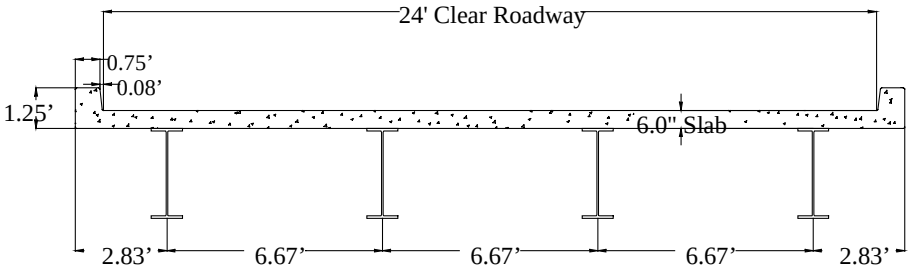

Figure 1.8: A complete Leon River Bridge section

1.2.4 Deck Reinforcement

The reinforcement in the deck slab is composed of reinforcing steel with a "design stress" of 20ksi. The use of structural grade reinforcing steel was not permitted. The typical mat consists of #5 bars spaced at 14". Some extra #5 bars are present at the curbs above every other diaphragm and are spaced at 7". The amount of reinforcement was assumed to be sufficient for the behavior considered in this research.

1.2.5 Other Bridge Components

This section contains details about the other features of the Leon River Bridge. These components include the railing, stiffeners, and diaphragms. The assumed contribution of each to the bridge behavior is also presented here.

1.2.5.1 Railings

The Leon River Bridge has a Texas Highway Department Standard Type II railing attached to the curbs on both sides. A picture of the railing and its attachment is shown in Figure 1.9.

Figure 1.9: A portion of the railing on the Leon River Bridge

The four bolt connection at every location was assumed to not be rigid enough to allow the railing to participate significantly in supporting moment. The railing was not considered in any models or calculations done for the bridge.

1.2.5.2 Diaphragms

Diaphragms are prominent in the bridge supporting structure. Of the 15 set of diaphragms used, there were three different types. Figure 1.10 shows a picture of a K-type diaphragm in the foreground and an X-type diaphragm in the background.

The steel components for all three types of diaphragms are shown in Figure 1.11.

Figure 1.10: K-type and X-type diaphragms

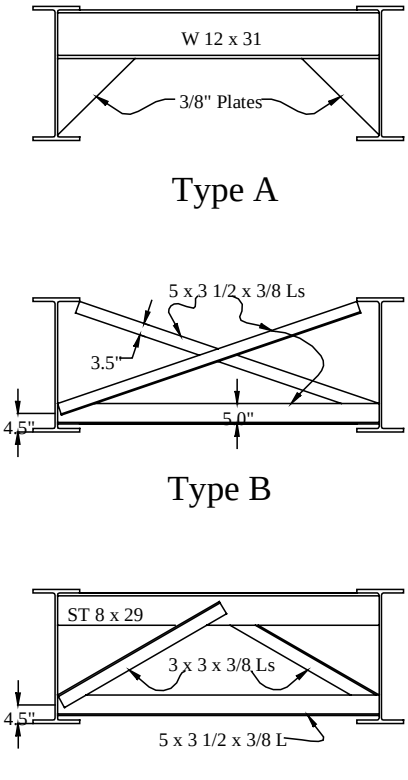

Figure 1.11: Three types of diaphragms used in the Leon River Bridge

The diaphragms were welded stiffeners welded to the W-shapes. The location of the welds is mentioned in Section 2.3.2.3 when the diaphragms are modeled in BRUFEM. Diaphragms are present at locations shown in Figure 1.2. Type A diaphragms were present only at the abutments. The rest of the diaphragms were either Type B or C and alternated starting with Type B as the first type of diaphragm off the abutment.

1.2.5.3 Stiffeners

Finally, web stiffeners were not used in the girders of the Leon River Bridge. However, the curbs were considered as a stiffening element for the exterior girders. The curbs contain approximately 81in^2 of material and are shown in Figure 1.8.

1.3 TEST INSTRUMENTATION AND DESCRIPTION

This section briefly describes the instrumentation and equipment used in the Leon River Bridge test. The focus is on the strain gauges, the gauge locations, and the load vehicles. Complete information on all the hardware and equipment used can be found in Jauregui (1999).

1.3.1 Instrumentation and Equipment

Strain gauges were set up at three sections along the bridge. One section was located at midspan of the 70' span, one at the midpoint of the 90' span, and one just before the start of the cover plate in the negative moment region of the first span. These sections are shown in Figure 1.12.

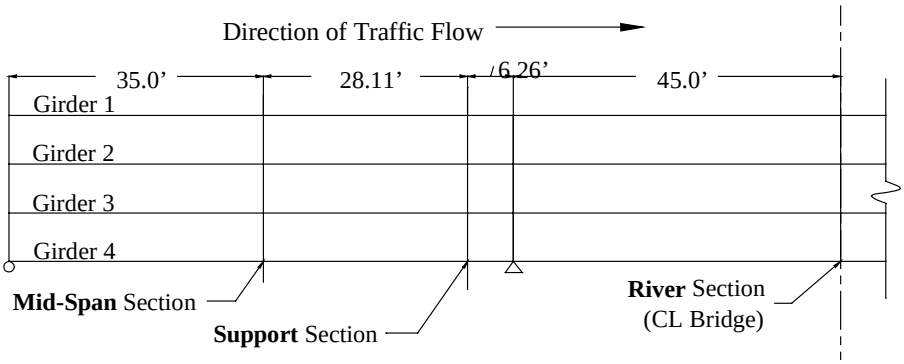

Figure 1.12: Location of gauging sections used in bridge test

The terms "Midspan," "River," and "Support" appear in Figure 1.12 and will be used throughout this research to refer to these sections. The River section was so named because it was located at the midspan of the 90'span over the Leon River, and required special equipment for access. The sections for gauging were chosen because they are locations of high positive and negative moment action. The larger the strains measured, the smaller the error induced by the precision of the data acquisition equipment.

1.3.1.1 The CR9000 and Related Equipment

A system of cables and junctions boxes was used in this test to carry the signals from the strain gauges to the data acquisition software. The signals were carried through a sequence that included the lead wires from the strain gauge, the terminal block, completion box, junction box, the interior cards of the Campbell Scientific CR9000C data logger, and the laptop computer. David V. Jauregui, Ph.D, originally developed the equipment.

The CR9000C is the hardware that receives data from all the gauges. The CR9000C has the capacity to receive data from eleven channels, each connected to five strain gauges. In this test, only 38 gauges were used, requiring ten of the eleven channels. Most channels did not have five active gauges. A more complete description of the CR9000 can be found in Jauregui (1999).

The important characteristics of this system include the precision of the data acquired and the sampling rate. The range of measurement for the gauges is $\pm$ 50mV. This was achieved with a noise level of $\pm$ 0.005mV ($\pm 2\mu\varepsilon$) for a typical test run. A sampling rate of 10 Hz was used for low-speed tests. A rate of 100Hz was used for high-speed tests.

1.3.1.2 Gauges and Gauge Locations

The strain gauges used in this test are 10mm long. They were self-temperature compensating. The lead wires were modified to fit the wiring scheme required by the CR9000C hardware. The gauge factor for the steel gauges was 2.11 and was acceptable for use in the range of temperatures experienced during the instrumentation and testing (20-40^{o}C). They were mounted in accordance with manufacturer specifications.

The number and locations of gauges needs explanation. Three gauges were placed at any given section, on any girder. One was located at midheight on the web one on the center of the top and bottom flanges on a given side. The typical locations on the girder are shown in Figures 1.6 and 1.7. Three gauges were used in this manner in order to accurately locate the neutral axis of the girder-slab system, therefore indicating whether or not noncomposite behavior exists. All of the girders at a section were gauged in order to obtain the total moment at that section. This total was checked with computer methods and was used to yield the distribution of lateral load at the section, the major goal of this research.

1.3.2 Load Vehicles

The Leon River Bridge was loaded with two different vehicles. The lighter vehicle was 3-axle TxDOT dump truck. A picture of the dump truck is shown below.

Figure 1.13: TxDOT dump truck

The total weight of the dump truck was 46.5k. The individual axle weights and wheel spacing are given in Figure 1.14.

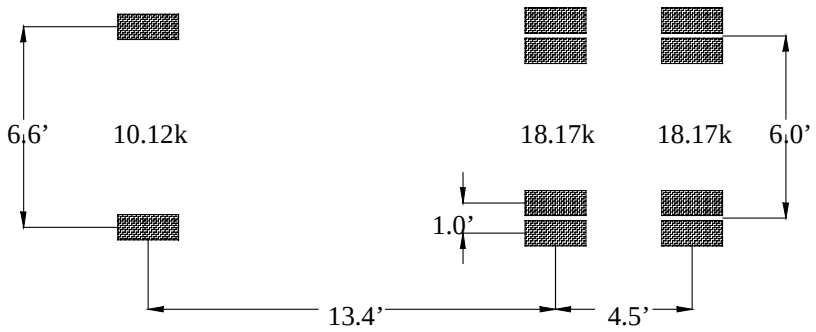

Figure 1.14: Dimensions and axle weights of the dump truck

The other load vehicle used was a military HETS vehicle. HETS is an acronym for "heavy equipment transport system." The HETS vehicle used was a U.S. Army M1070 trailer carrying a M113 Armored Personnel Carrier. It was obtained from the United States Army base at Ft. Hood, Texas. The HETS and personnel carrier are shown in Figure 1.15.

Figure 1.15: U.S. Army M1070 trailer with M113 armored personnel carrier

The total weight of this HETS vehicle with the personnel carrier was 110k. The individual axle weights and wheel spacing are shown in Figure 1.16.

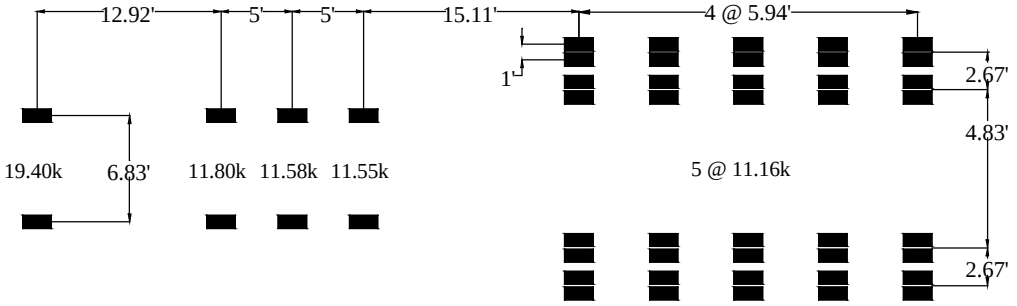

Figure 1.16: Dimensions and axle weights of the HETS load vehicle

1.3.3 Description of Loading

Although striped for two lanes of traffic, three load paths were used in the bridge test. The test lanes were marked with spray paint on the surface of the bridge. A picture of the roadway is shown in Figure 1.17.

The dump truck passes were made such that each outside girder of the bridge would carry a large portion of the load. The width of the bridge was such that only HETS runs down the centerline were practical. In addition, the dynamic runs with the dump truck were made down the center. Figure 1.18 shows a plan view of the three paths that were used.

Figure 1.17: The surface of the Leon River Bridge

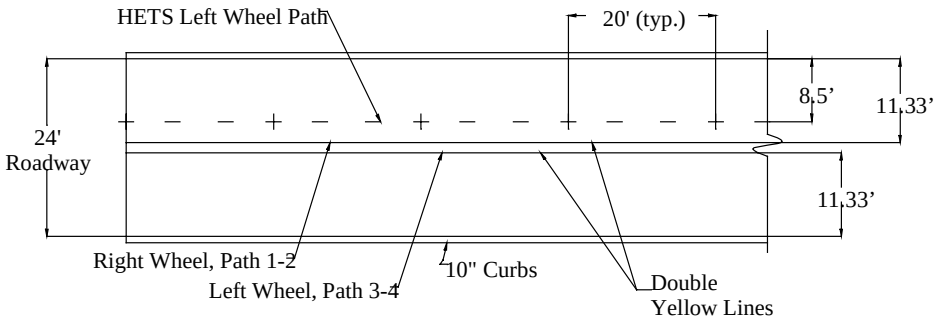

Figure 1.18: Diagram of the test paths on the surface of the bridge

The cross marks shown in Figure 1.18 were set 20' apart. Seventeen marks were made in all, beginning at the start of the bridge from the north, and covering the full length of the bridge plus some extra distance off the bridge. These marks were used in the correlation of computer data to truck position on bridge. An observer walked along the side of the vehicle using a manual switch to mark instances when the axle passed over a roadway mark.

A total of eight test runs was made. Five runs were done with the dump truck, and three were done with the HETS vehicle. The following table gives the notation for the eight vehicle runs.

Table 1.2: Notation for Leon River test runs

Test Notation	Test Description
D.T. 1-2a	First slow dump truck pass over girders 1 and 2
D.T. 1-2b	Second slow dump truck pass over girders 1 and 2
D.T. 3-4a	First slow dump truck pass over girders 3 and 4
D.T. 3-4b	Second slow dump truck pass over girders 3 and 4
D.T.H.S.	High speed dump truck pass over the center
HETS 1	First slow HETS pass over the center
HETS 2	Second slow HETS pass over the center
HETS H.S.	High speed HETS pass over the center

The two fast vehicle passes required some special treatment in order to be used in this research. This will be covered in Section 3.3.1.

CHAPTER 2: COMPUTER ANALYSIS METHODS

2.1 OVERVIEW OF TWO TYPES OF ANALYSIS METHODS

Computer programs were used to predict moments and stresses produced in the field by the test vehicles. The estimated stresses were compared to the measured stresses in order to determine whether or not the computer analysis gave viable results. An accurate, sophisticated method of computer analysis allows designers to design structures safely and with greater accuracy than design equations. The major computer package used in this research was BRUFEM (Bridge Rating Using Finite Element Methods) developed by the Florida Department of Transportation (FDOT). SAP2000 Nonlinear, a commercially available program, was also used. BRUFEM was used to generate lateral load distribution factors (LLDFs). SAP2000 was used to help reduce the data from the field tests.

2.2 ANALYSIS USING SAP2000

The SAP2000 software was used to perform a series of line girder analyses. A line girder analysis is a one-dimensional analysis used to obtain the total static moment present in a specific cross section of the bridge for any position of a load vehicle. This was accomplished through a series of steps. First of all, a model of one girder was made in SAP2000. Then the influence lines for each gauged section were generated. These influence lines were then used to generate moment histories for each section under the action of each load vehicle. A complete history of the total flexural moment at a given cross section was plotted as a function of vehicle position. This information was useful because it determined the vehicle positions in which the total flexural moment at a cross section was a maximum, minimum, or other significant value.

A full description of the procedure for a line girder analysis using SAP2000 Nonlinear can be found in Appendix A of McIlrath (1999). A computer package other than SAP2000 can be used, as long as it has the ability to generate influence lines. This section first outlines the element types, boundary conditions, and model details used in the SAP2000 line girder model of the Leon River Bridge. Then the method of obtaining the moment histories from the line girder model is covered.

2.2.1 SAP2000 Nonlinear Model Specifics

The first step in the line girder analysis was to model the properties of a single girder in SAP2000. The model included all the proper support conditions and section properties. Many properties for standard W shapes are automatically included in SAP2000. The section with the cover plates was user-defined and only required the cross-sectional area (48.8 in^2) and the moment of inertia about the primary bending axis (9672 in^4). Figure 1.4 in the previous chapter shows a half-elevation of the Leon River Bridge girder with the properties used for the SAP2000 model.

A girder with three spans (70’-90’-70’) was modeled with three-dimensional frame elements. Nodes were used to divide the girder into segments. A node was placed at every change in geometry of the girder, every support location, and at every location corresponding with one of the three gauged sections. Each segment created was divided with additional “output” nodes to give additional refinement to the model. The SAP2000 model used contained 14 joints, 13 basic frame segments, and 5,483 output segments. The output nodes were spaced such that the average length of any output segment was 0.0417 feet.

The travel lane and load vehicles needed to be defined in order to run the model. With this one-dimensional model, only one lane assignment existed. The lane was defined as the centerline of the line girder, moving from left to right. The load vehicles were defined in SAP2000 to check the model for errors by correlating moments generated in SAP2000 with those generated by other analysis software. Load vehicles were defined as single wheels spaced at the same spacing as the axles of the actual vehicles. Figure 2.1 shows the vehicles used in the SAP2000 model.

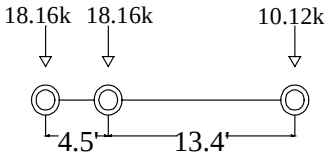

Dump Truck

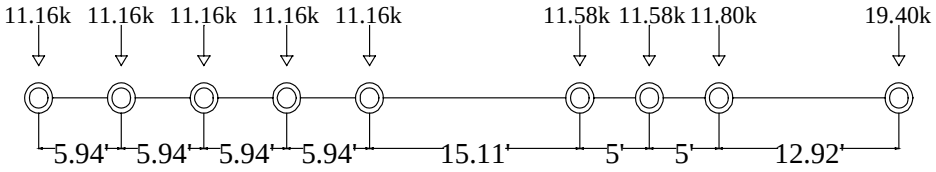

HETS Vehicle

Figure 2.1: SAP2000 load vehicles

Notice that each wheel in the SAP2000 load vehicle was given the load of the entire axle of the real load vehicle. This was necessary in order calculate total moment due to the whole vehicle, which was used in calculating LLDFs.

2.2.2 Using a Spreadsheet to Generate Moment Histories

SAP2000 was used to generate moment influence lines for three points on the line girder that correspond to Midspan, Support, and River sections on the bridge. The influence line values indicate the moment generated at the location of interest, from a unit load at any location along the girder. Using this concept, a spreadsheet program was used to generate the required flexural moment histories.

The spacing of the axles and the total axle weights were required to use this method. These were given in Figure 2.1. The resulting influence line values were tabulated at increments small enough that the amount of interpolation was minimized. The influence line increments in SAP2000 were 0.0417 ft. (0.5 in.). This high level of refinement was used because most of the axle spacings are evenly divisible by 0.5in.

Once defined, the axle weights were moved incrementally in the spreadsheet representing the path of the load vehicle. At each increment, the weight on the axle was multiplied by the influence line value to give a value of moment for that axle location. The effects of all the axles were summed up to get a moment value for the vehicle position. In the event that an axle did not line up with an influence line value, an average of the two closest values was used. This was acceptable because of the small length of output segments used in this method. The history of moment versus vehicle position was developed in this manner. This method worked well as long as the user kept track of which axles are on or off the girder.

2.2.3 Presentation of Moment Histories

A line girder analysis was performed using the 3-axle dump truck as well as the 9-axle HETS vehicle. The total length, axle-to-axle, of the HETS vehicle was longer than the dump truck (61.7’ compared to 17.9’). Therefore the method needed to be carried out until the front axle of the HETS was 290ft from the beginning of the bridge. At that point the rearmost axle was almost off the bridge and the moments generated were close to zero. The front axle of the dump truck only needed to be moved to 249ft from the beginning of the bridge to complete the traverse of the bridge. The moment histories for each section considering both vehicles are shown in the following figures.

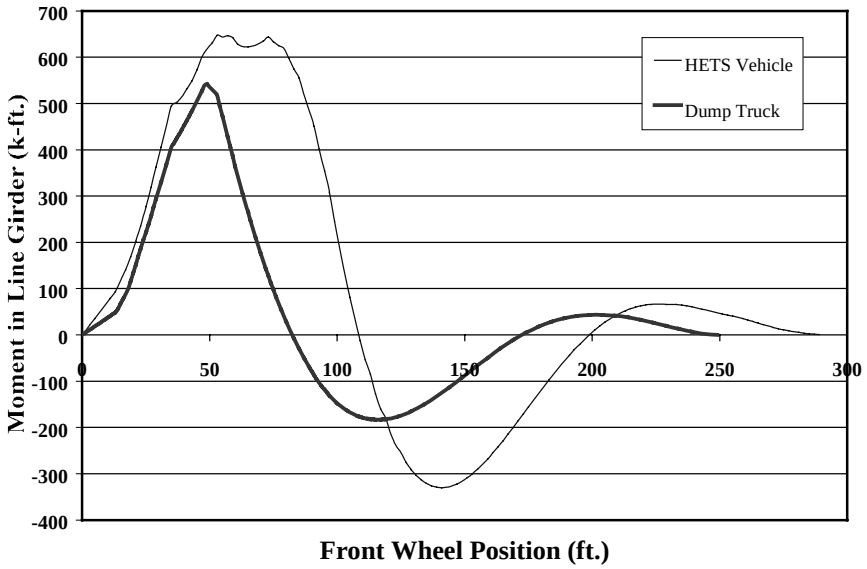

Figure 2.2: Total flexural moment at the Midspan Section caused by load vehicles

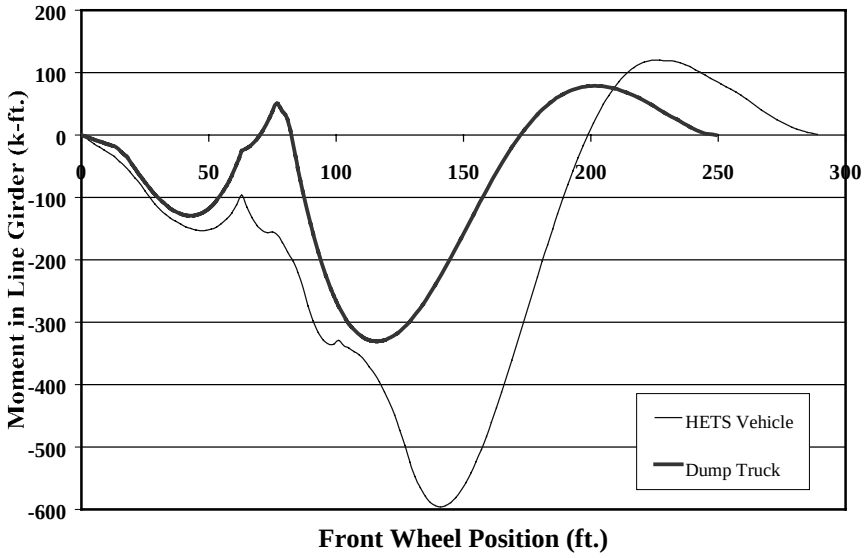

Figure 2.3: Total flexural moment at the Support Section caused by load vehicles

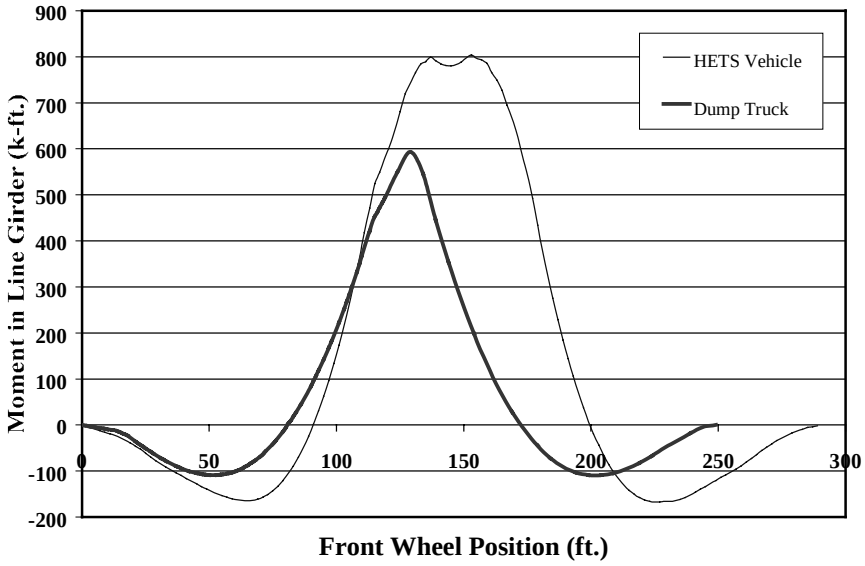

Figure 2.4: Total flexural moment at the river section caused by load vehicles

The line girder moment histories for the dump truck and HETS vehicle were similar in shape. The differences came from the different number of axles and different lengths of each vehicle. The HETS vehicle was longer and had more axles. The action of the additional axles going onto and off of spans created a history that is different from the dump truck.

The maximum static flexural moment in any one of the three sections caused by either vehicle was 804k-ft, in the River section when the HETS vehicle's front axle was 153ft from the beginning of the bridge. The other maximums and minimums for the dump truck and heavy vehicle are presented in Table 2.1 below.

Table 2.1: Maximum line girder moments in the Leon River Bridge

Vehicle	Maximum Positive/Negative Moments (k-ft.)	Maximum Moment Sections	Vehicle Front Axle Location at Maximum (ft.)
Dump Truck	593	River	129
	-331	Support	116
HETS	804	River	153
	-596	Support	141

Notice that neither of the maximum moment effects comes from the midspan section.

2.2.4 Truck Positions of Interest

Before the test data was reduced, the distribution of moment in the bridge was not known. It was expected that the vehicle position that gives the largest value of moment over a section might also give the largest value of moment experienced by any one girder. This was not a certainty. Table 2.2 contains the 7 different vehicle positions that were analyzed in detail in this research. The reasoning for selecting each vehicle position is also given in the table. For example, the front axle position of 57' was picked because it is at this location that the HETS causes the maximum positive moment in the Midspan section. Some other positions were chosen expecting a maximum negative value. Originally, 10 values were

chosen, including 3 locations where zero moment was expected. Locations at 80', 174', and 200' were discarded because of the numerical instability of the near-zero moment values.

Table 2.2: Representative vehicle positions selected from line girder analysis

Vehicle Front Wheel Position (ft.)	Significant Effect	Vehicle Causing Effect
50	Maximum Mid-span Positive Moment	Dump Truck
57	Maximum Mid-span Positive Moment	HETS
107	River Positive Moment	-
120	Maximum Support Negative Moment	Dump Truck
129	Maximum River Positive Moment	Dump Truck
139	Maximum Support Negative Moment	HETS
155	Maximum River Positive Moment	HETS

2.3 ANALYSIS PROCEDURE USING BRUFEM

In addition to line girder analyses from SAP2000, a three-dimensional finite element analysis was performed using BRUFEM. BRUFEM was developed by FDOT for use in analysis, rating and design of highway bridges. BRUFEM version 4.20 revised 30 August 1996 was used in this research. The package contains modeling capabilities that are tailored to various bridge types. The steel bridge modeling method was used in this research.

The BRUFEM software is contained in four FORTRAN programs, BRUFEM1, SIMPAL, BRUFEM3, and SMPLOT. The most important files used or generated by these programs are the HISTORY. PRE, BAR.DAT, VEH.DAT, and the BRATE.OUT file. These files will be mentioned in subsequent sections of this chapter in order to describe the BRUFEM model. BRUFEM1 creates the finite element model using interactive input from the user as well as prepared input files. The user-prepared BAR.DAT file contains the properties of the steel girders, and the user-prepared VEH.DAT files contain the description of the load vehicles. SIMPAL performs the finite element analysis and generates the output files and data files used in plotting. The actual bridge rating is performed by BRUFEM3. This program generates the LLDFs contained in a file named BRATE.OUT. The fourth program is SIMPLOT, which is used for plotting analysis results in a graphics environment. SIMPLOT was not used extensively in this research. More information on the BRUFEM package can be found in the BRUFEM manual by Hays (1994).

A major output of the BRUFEM package is lateral load distribution factors. These factors were generated for the three sections of the Leon River Bridge. They were compared with the distribution factors obtained from the test data. This comparison gave insight into how well the package works, and the usefulness of the package over accepted design equations.

2.3.1 Types of BRUFEM Analyses for Steel Girder Bridges

The basic BRUFEM model for a steel bridge contains the bridge girders and a deck slab. Additional elements such as parapets, diaphragms, and railings can be added to the basic model. The BRUFEM package can model a bridge system either compositely or noncompositely. For noncomposite action, the girder and slab elements act independently, and the centroid of the girder and slab coincide. The slab only undergoes plate bending and acts primarily to distribute the wheel loads to the girders. In modeling for composite action, the girder-slab interaction can be modeled one of two ways. The first method is the Composite Girder Model (CGM) and the second is the Eccentric Girder Model (ECM). A short comparison of the results from both methods is given in Chapter 5.

2.3.1.1 CGM

The CGM uses the properties of a composite girder in the analysis. The analysis is done in two dimensions and is akin to the composite modulus data reduction method that will be shown later in Section 4.2.3. The elements of the composite girder are modeled using frame (FRM3) elements. The slab is modeled using PLATE elements and is used to distribute wheel loads

The properties of the composite girder are computed in the classical elastic manner using the AASHTO effective width and a concrete section transformed by the modular ratio. The modular ratio *n* is given in Equation 2.1.

$$n = \frac{E_C}{E_S} \tag{2.1}$$

where: E_C = elastic modulus of the concrete deck slab

E_S = elastic modulus of the steel girders

E_S was taken as 29,000 ksi. E_C was calculated in BRUFEM using the AASHTO equation for normal weight concrete. The CGM assumes that centroid of the slab is at the same depth of the centroid of the composite section. A diagram of the CGM is shown in Figure 2.5.

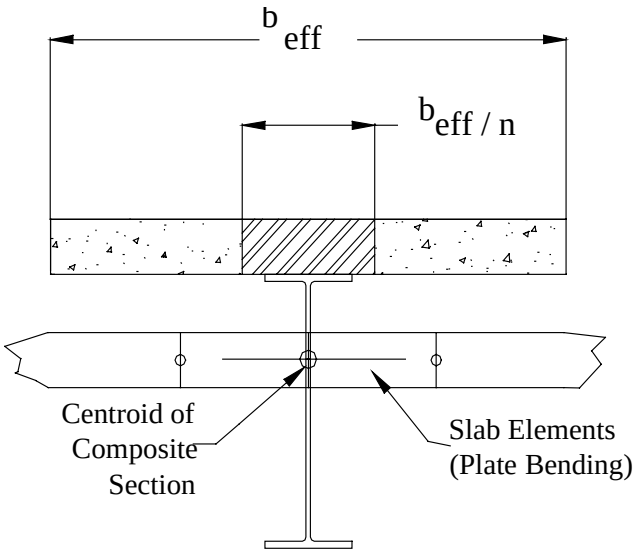

Figure 2.5: Modeling composite action using the BRUFEM composite girder model

In BRUFEM, the effective width of the concrete slab is also calculated using AASHTO recommendations.

2.3.1.2 EGM

This EGM uses a three-dimensional analysis and is similar to the Moment-Couple method of data reduction to be shown in detail later in Section 4.2.4. A full description can be found in Section 3.3.2 of the BRUFEM manual. This method models the bridge as FRM3 elements connected by rigid links to the slab. SHELL elements are used to model the deck slab. These elements exhibit membrane behavior to account for shear lag. A diagram of the EGM is shown in Figure 2.6.

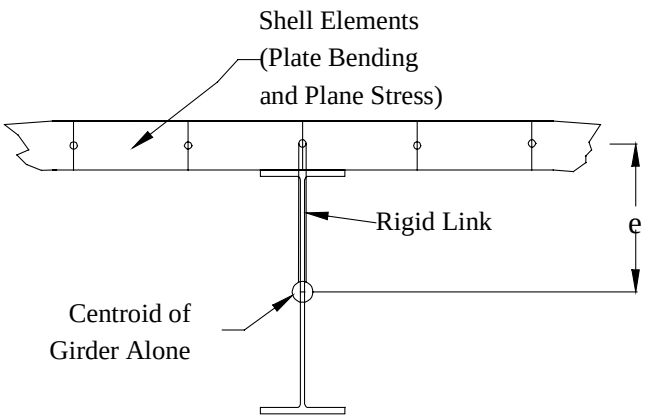

Figure 2.6: Modeling composite action using the BRUFEM eccentric girder model

According to the BRUFEM manual, the EGM is considered to be the more precise method as long as a sufficient number of elements are used in the longitudinal direction to attain strain compatibility between the girder and slab.

2.3.1.3 Modeling Diaphragms

In a study done during the development of BRUFEM, BRUFEM models containing diaphragms were considered slightly stiffer than other three-dimensional models without diaphragms. BRUFEM also only models X-type or steel beam type diaphragms. Appendix I of the BRUFEM manual gives a study on the effects of modeling using X-type diaphragms instead of K-type diaphragms. These two results indicate that in some cases, the BRUFEM models will underestimate the maximum girder moments and shears. BRUFEM corrects this in the post processor by increasing the live load moments and shears by 5%. Since this underestimation is slight in most cases, this 5% was removed from the BRUFEM results for this research.

2.3.2 Leon River Model

The primary purpose of this research was to explore moment distribution in the Leon River Bridge using the results of a BRUFEM model. In order to accomplish this goal, some simplifications in the Leon River Bridge model were made. All of the basic model parameters entered by the user for the bridge are found in the HISTORY.PRE files that are reprinted in Appendix A. This section will give an overview of the BRUFEM model that was used.

2.3.2.1 Geometry

A few simplifications were made to the bridge model for use in the BRUFEM system. The nominal span lengths are 70'-90'-70'. The centerlines of the supports at the abutments are located 0.625' from the end, which gives and actual end span length of 69.375'. The nominal span length of 70' was used in this analysis.

The finite element model used 1840 slab elements, and 460 beam elements. Each girder was subdivided in 115 elements. The two 70' spans each contained 35 elements in the longitudinal direction. The 90' interior span contained 45 elements. The recommended number of elements per span according to the BRUFEM manual is 20 in the longitudinal direction. The deck slab contained 16 elements in the lateral direction and 115 elements in the longitudinal direction. The typical slab element used was 2' x 1.67'.

BRUFEM models steel girders as built-up sections using FRM3 frame elements. The fillets in girders were ignored. The flange and web widths and depths for each W section were used to define the girders. The cover plates were treated as 10.5" x 0.5" x 12'-0" rectangles. The tapering of the cover plate at the ends was ignored. The BAR.DAT file contains the geometry of the steel girder and can be found in Appendix A.

BRUFEM allows for modeling deck material that extends beyond the centerlines of the exterior girders. A slab width of 2.83' was used in this analysis. The additional 81in^2 of concrete that comprises the curbs was not included in the model. The guardrails were also not modeled in BRUFEM.

2.3.2.2 Load Vehicles

The wheel configuration of the HETS vehicle could not be modeled exactly in BRUFEM. The axles of BRUFEM load vehicles are defined using representative distances on the axle. A schematic of a typical spacing is shown in Figure 2.7(a).

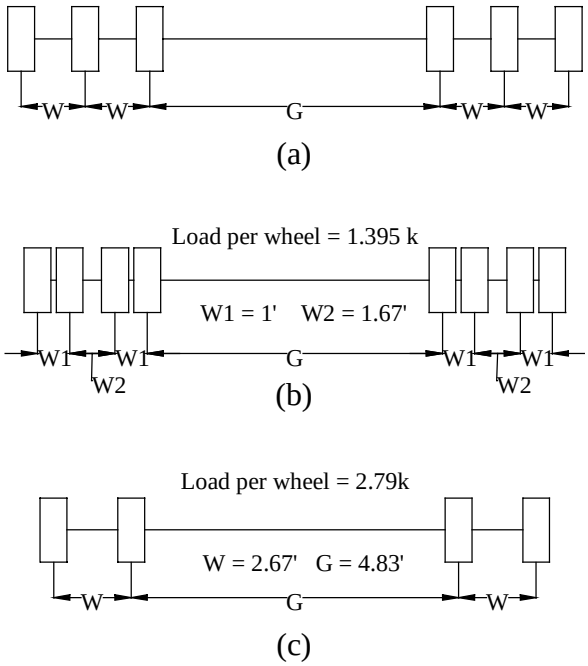

Figure 2.7: Typical axle modeling using BRUFEM

The gauge, *G*, is the distance between the two innermost wheels. The spacing between any of the wheels outside of the innermost two is given by *W*. In BRUFEM, *W* must be the same for all wheels on an axle. Figure 2.7(b) shows one the HETS axles. The spacings of all the wheels on the HETS axle are not the same. Some of the wheels on the HETS axle are spaced at 1.67', where others are spaced at 1'. The solution to this conflict was modeling each pair of wheels one foot apart as a single wheel, with double the load (Figure 2.7(c)). The full HETS wheel configuration used in BRUFEM is shown in Figure 2.8 below.

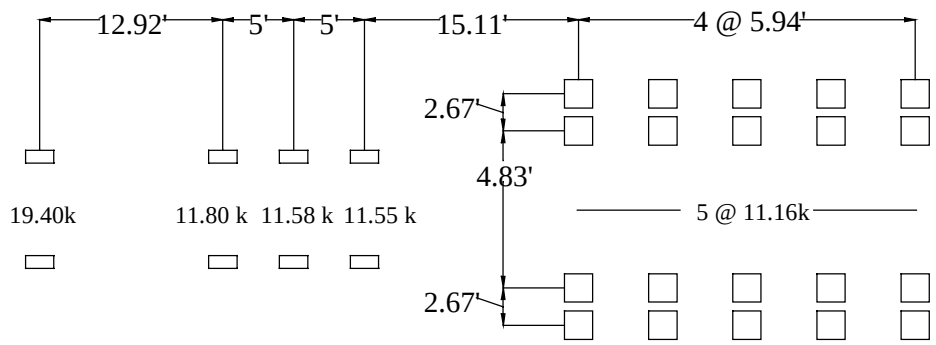

Figure 2.8: Modified HETS wheel pattern for BRUFEM modeling

The differences between the model HETS vehicle and the actual vehicle are subtle. The resolution of the finite element mesh is 1.67' in the lateral direction so modeling two loads spaced at 1' as one load was not crucial. This HETS and the dump truck modeling information are contained in the user-prepared VEH.DAT files that can be found in Appendix A.

2.3.2.3 Diaphragms

The results of Section 5.3.2 of this research conclude that diaphragms need to be included in the BRUFEM model. Section 1.2.5 contained the details regarding the three different types of diaphragms that exist in the Leon River Bridge. The bridge contains X-type, K-type, and steel beam type diaphragms. The BRUFEM model includes default diaphragms at support locations. These default diaphragms are 8 in. wide and are 80% as deep as the girder section. This default diaphragm is comparable in cross-sectional area to the Type A and Type C diaphragms given in Figure 1.11.

In BRUFEM, diaphragms at locations other than supports must be added. However, only the steel beam and X-type diaphragms are available. In the Leon River Bridge, all of the diaphragms not at support locations were either K-type or X-type. It was assumed that the *type* of diaphragms was not going to be crucial to the results of the BRUFEM analysis. Therefore, X-type diaphragms of *similar* cross-sectional properties and attachment locations were used throughout. Figure 2.9 shows the properties of the two types of diaphragms that exist at nonsupport locations of the Leon River Bridge and the composite diaphragm used in the BRUFEM model.

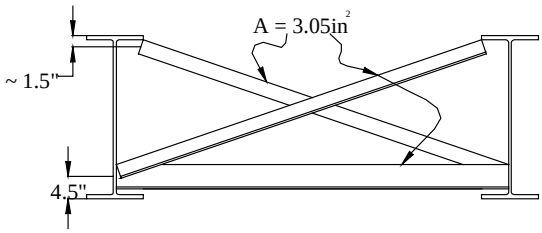

Type B Diaphragm

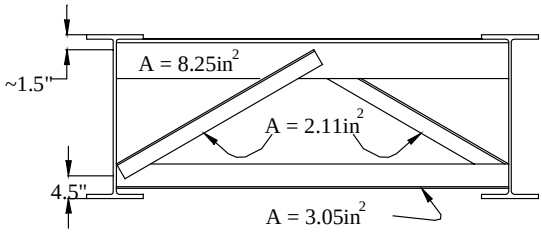

Type C Diaphragm

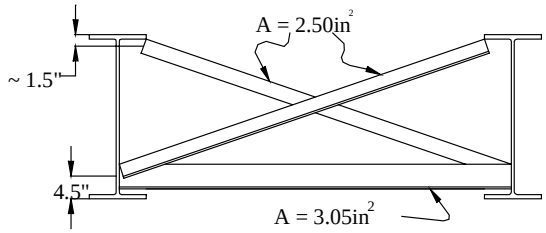

BRUFEM Diaphragm

Figure 2.9: Comparison of actual bridge diaphragms with the BRUFEM model diaphragm

2.3.3 BRUFEM Run Description

There are a few considerations that affected the number of BRUFEM runs that were needed. Recall that seven representative truck locations were chosen for analysis of moment distribution. In a single BRUFEM analysis, a load vehicle can be moved to all of these locations. Recall from Figure 1.18 that the two dump truck lanes were symmetric about the bridge's longitudinal centerline. Therefore, only one of the dump truck's lateral positions needed to be modeled. Thus, with only two BRUFEM analyses, one for the HETS and one for the dump truck, a full set of data for comparison was acquired.

For completeness, two BRUFEM runs were made using the CGM and two were made using the EGM method (one for each test vehicle). Since the ECM more accurately represents what is potentially happening in the slab-girder interaction, that method was chosen to investigate the behavior of the diaphragms and their role in the distribution of moment across the girders. A set of runs using the ECM was performed with the diaphragms removed in order to judge their importance to the model.

In summary, one run using the CGM, one using the ECM with diaphragms and one using the ECM without diaphragms was made for each vehicle. There were three major files that describe each run. These were the HISTORY.PRE, BAR.DAT, and VEH.DAT files. All essential BRUFEM files are included in Appendix A.

CHAPTER 3: INITIAL TEST RESULTS AND DATA REDUCTION

This chapter contains an explanation of the initial data reduction performed on the strains measured during the Leon River Bridge test. It also discusses some of the steps taken to put the initial strain data in usable format for the calculation of moments. The gauging scheme allowed for the calculation of moment in every girder of the bridge. The moment distribution factors were then computed using all the individual girder moments.

The initial data reduction problem was to determine the flexural participation of the slab with the girders. The bridge was designed noncompositely. The location of the neutral axis (N.A.) for a girder cross section was used to determine the degree of composite action of the system.

3.1 CALCULATION OF STRAIN

After field tests were completed, the first step in data reduction was to convert the test data acquired in millivolts into microstrain. This computation requires a gauge factor, *G.F.* supplied by the gauge producer. The governing equation for this first step is given in Equation 3.1.

$$\frac{Output\,(mV)}{Excitation\,(mV)} * \frac{4\,x10^{6}}{G.F.} \quad = \quad Microstrain\,(\mu\varepsilon) \qquad (3.1)$$

where $G.F. = 2.11$

The power for the system is a 12V battery, which is stepped down in order to provide a 5V excitation to the gauge system The excitation voltage was approximately 5,000 *mV* for all the tests. Typical output voltages for extreme strains were between –0.26 and 0.45 *mV* for the dump truck tests. This gave typical extreme strains between –150 and 200$\mu\varepsilon$. The output and input excitation voltage were provided in the data acquired by the computer. A spreadsheet was used to convert millivolts into microstrain for all test runs.

Plots were made of the raw data in microstrain. Figure 3.1 is a typical example of a plot from any of the low-speed test runs. The figure shows strains measured on one girder at the Midspan section (35’ from beginning of bridge). Extreme strains were recorded when the front axle of the dump truck was at approximately 55’. This makes sense because the rear axles are 13.4’ and 17.9’ from the front axle and carry the greatest load. When the front axle is at approximately 55’, the tandem was directly over the Midspan section.

More observations can be made from Figure 3.1. During positive moment action in the Midspan section (0’-87’), the bottom gauge registered a positive strain, and top gauge registered a negative strain. The gauge at midheight on the girder also recorded a strain of the same sign as the bottom gauge for most of the travel of the vehicle. This nonzero strain shows that the neutral axis of the girder is not at midheight, as it would be under noncomposite action. Note also that when the vehicle entered the center span (front axle at 87-150’), the strains switched sign because the top flange was in tension.

A few problems are also shown in Figure 3.1. At the location where the vehicle caused the strains to switch sign (a location where the truck causes zero moment at the section), a negative strain was recorded in all three gauges. This indicated some degree of interaction with the deck slab. After the vehicle moves far from the section (front axle position 150-250’), the web and top flange gages registered a positive strain value, also indicating some interaction with the deck. Oscillations could be seen in Figure 3.1 as well as most of the strain data, but were limited to $\pm 5\mu\varepsilon$ in most low-speed test runs.

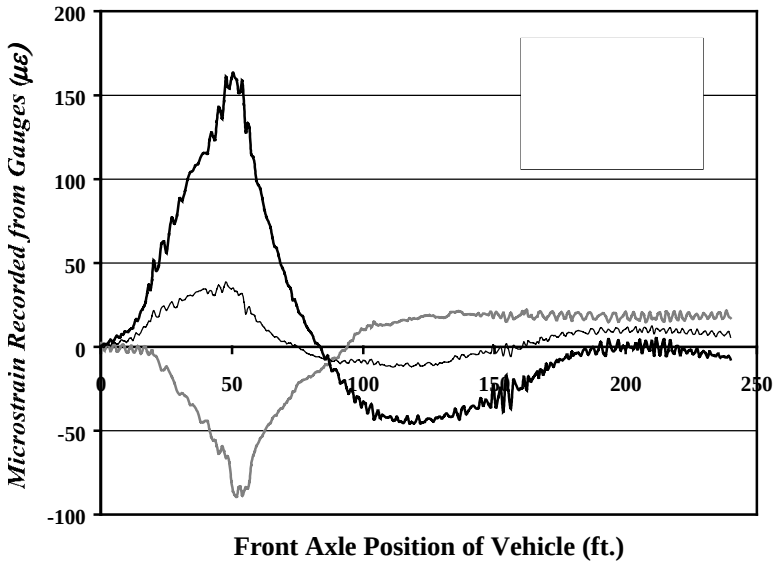

Figure 3.1: Strain history for girder 3 at the midspan section during Test D.T. 3-4b

3.2 CHANNEL SUMMARY

The system of gauges, completion boxes, junction boxes, and the CR9000 was complex enough that errors and malfunctioning channels could not always be remedied in the field. A total of thirty-six steel gauges were used in the Leon River test. Three gauges did not register strain readings for any of the tests. Two of the gauges were located on the bottom flange of girder 2, one at the Midspan location and one at the Support location. The other nonworking gauge was located at midheight on girder 1 at the Midspan section. The missing gauge data was estimated in a spreadsheet using similar triangles. This was done based on the assumption that plain sections remain plane. The calculation was done with confidence because two of the three gauges at each section still registered reasonable strain values.

3.3 NOTABLE TEST RUNS

If a problem with a vehicle test was noticed in the field, the vehicle was repositioned for a replicate run. There was one case where a problem was noticed upon review of the preliminary data. In addition, the high-speed runs had larger and quicker oscillations that needed special treatment. This section explains what was done to these test runs in order to make them usable for the rest of this research.

3.3.1 Fast Vehicle Tests

There were two sets of data that were acquired from high-speed vehicle tests. One run was done with each vehicle. The speed of the dump truck was approximately 55mph. The speed of the HETS vehicle was approximately 40mph. The impact of the vehicle with the bridge, the vibration of the vehicle, or some combination of both effects could have caused the vibration in the bridge system. The frequency of the oscillations caused by the dump truck was approximately 0.5hz. The HETS vehicle caused oscillations that were hard to distinguish from the typical noise of the data acquisition process.

Figure 3.2 is a sample of the data obtained from a high-speed run. Figure 3.2 shows the measured dynamic response in comparison with the predicted static response in terms of flexural moment. The flexural moments were calculated from measured strains using a method that is described later in Chapter 4.

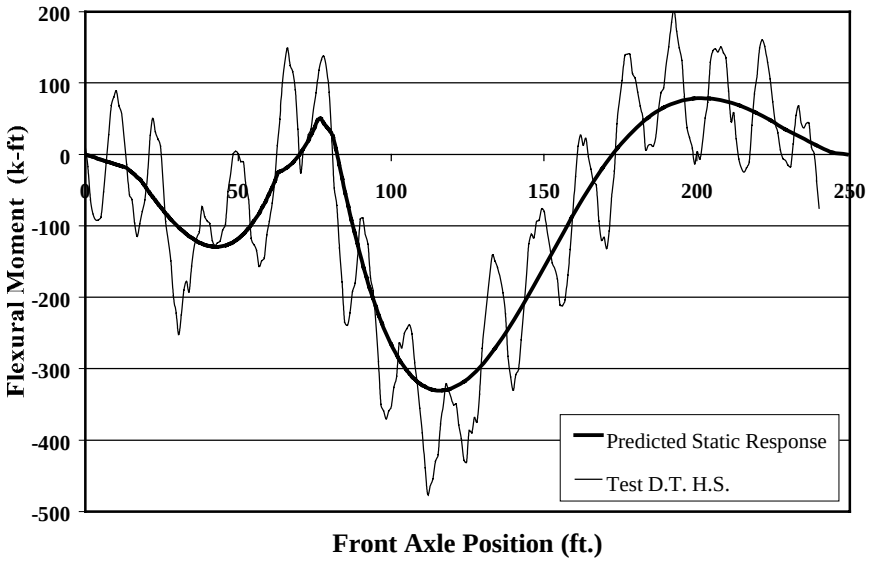

Figure 3.2: An example of vibration in a high-speed test

Note that the mean of the dynamic response follows the static response quite well. In order for the data from the high-speed tests to be usable for this research, the oscillations needed to be filtered out.

Figure 3.3 shows another example from high-speed dump truck run, this time showing the River section. Filtered data is also shown in Figure 3.3.

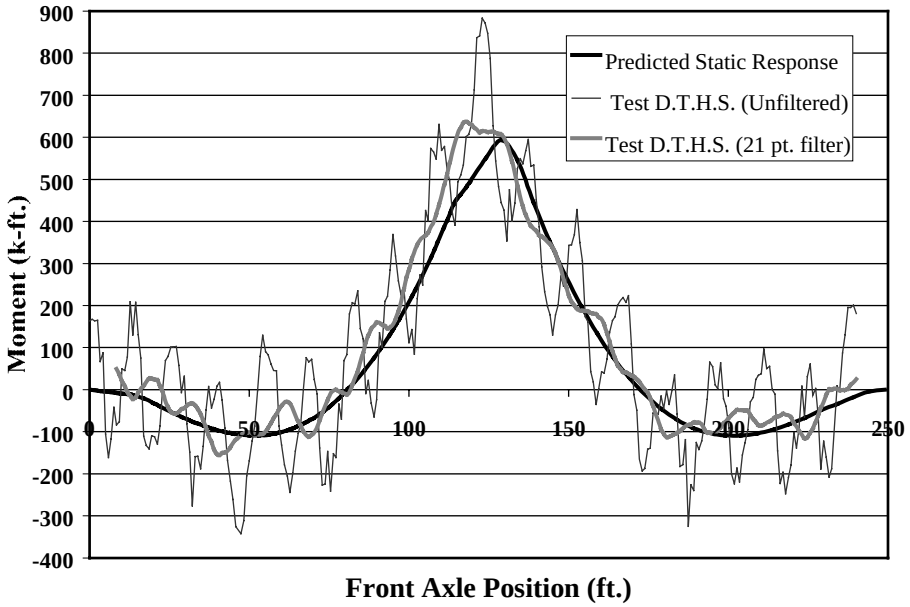

Figure 3.3: Total moment at the river section for a high-speed dump truck run

A 21-point moving average was used to filter the data. The technique gave a value that was equivalent to the average of the initial value and the ten preceding and ten subsequent values. This was important when discrete moment values were obtained. This technique did not fully eliminate the oscillations in the data,

but it did lessen the amplitudes. Unfiltered amplitudes for the fast tests were typically between 200 and 300k-ft. The 21-point moving average filter was applied to each moment record for each girder in deriving the lateral load distribution factors that appear in later chapters of this research.

3.4 CORRECTION OF FIRST DUMP TRUCK TEST

During vehicle test runs, a manual switch was used to mark the data records to indicate the vehicle position. An observer was placed in position to see the vehicle wheels cross the designated lane marks. The spacing of these marks was given in Figure 1.18. The observer opened the switch as the front wheel of the test vehicle passed a mark. The switch momentarily opened the excitation channel and produced a zero voltage. This effect was seen in the acquired data and was used data reduction. When test data was plotted against the line girder data for the same vehicle, the voltage marks were the method of plotting the acquired data with respect to the bridge features. The following plot was made of reduced data from the first dump truck tests.

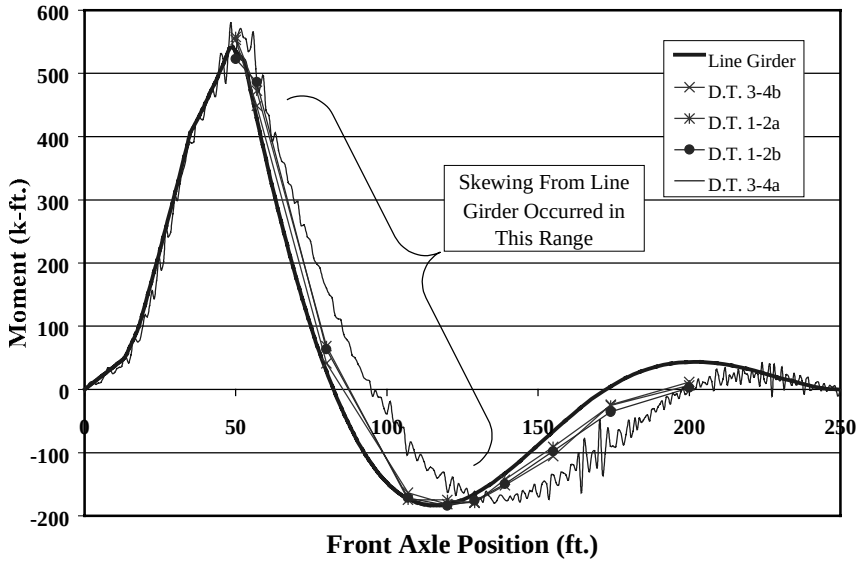

Figure 3.4: Total moment at midspan section showing skewed data

The data from test D.T.3-4a appears to skew from the other dump truck test and line girder moment. This is the *only* test that exhibited this behavior. Sample points taken from the other three dump truck tests fit the line girder analysis line well. Also note that a definite point at which the data starts skewing from the line-girder values is not visible. A solution was found in the voltage marks.

During a test, the vehicle tried to maintain constant speed. Therefore the number of data records between each voltage mark should have been somewhat constant. Each voltage mark signified 20' of travel. A summary of the number of data records per voltage mark for test D.T.3-4a is shown in Table 3.1.

Table 3.1: Manual switch data for Test D.T.3-4a

Actual # of Records per Mark	Distance Traveled (ft.)
26	20
26	40
24	60
19	***80***
21	***100***
18	***120***
22	***140***
25	160
23	180
29	200
27	220

The four values shown in bold italics are noticeably below the average number of records per mark given in the table. These values coincide with vehicle travel from 80' to 140', which is where the data for the test skews in Figure 3.4. Although the switch operator did not make any notes at the time of the test, it appeared as though and extra mark was added in this interval. The effect of this would be to gradually put the truck out of position over a span of 60' of travel.

A simple calculation was made to eliminate one mark and 20' of travel. The 60' of travel was reduced to 40'. Then the 40' of travel was distributed evenly to the 80 records that were affected. Then three marks were spaced evenly distributed such that number of records per click was nearly equal (27-27-26). Table 3.2 shows the result of this calculation that eliminated the assumed extra mark.

Table 3.2: Assumed records per mark for Test D.T. 3-4a

Assumed # of Records per Mark	Distance Traveled (ft.)
26	20
26	40
24	60
27	***80***
27	***100***
26	***120***
25	140
23	160
29	180
27	200

The affected marks are again shown in bold italic. Figure 3.5 is a plot of the corrected data.

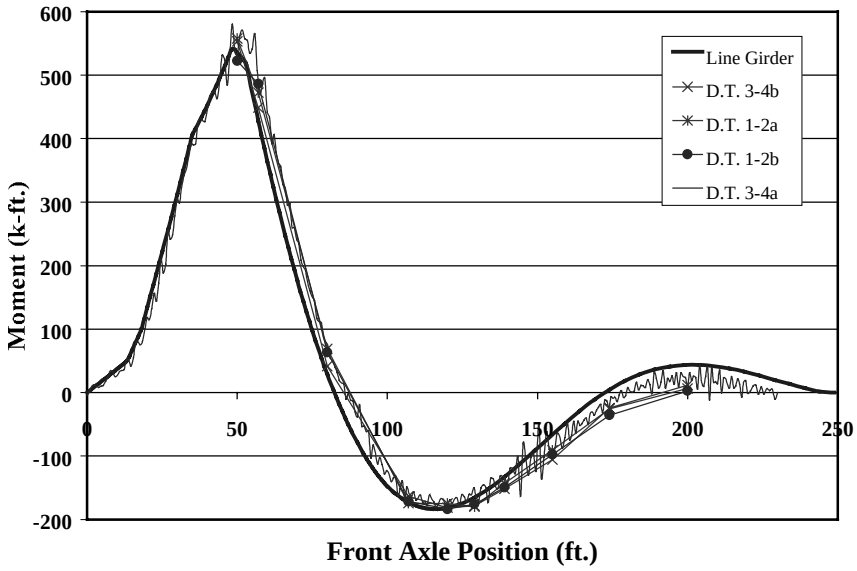

Figure 3.5: Total moment at midspan showing corrected D.T. 3-4a data

The adjustment provided a reasonable solution and test D.T. 3-4a was used with the same confidence as the other dump truck test runs.

3.5 LOCATION OF NEUTRAL AXES

The Leon River Bridge was designed and built to carry loads noncompositely. If loads were carried noncompositely, the data from any test performed should have given a N.A. location at midheight. This includes sections near the supports, because the cover plates were symmetric. This section contains an overview on how the N.A. locations were calculated, the values used in this calculation, and how the locations compared with expected values.

3.5.1 Neutral Axis Calculation

The following diagram shows how the neutral axis was calculated from the gauges on the top and bottom flanges using similar triangles. This method assumes that plane sections remained plane within the girder. Equation 3.2 shows how the neutral axis was calculated.

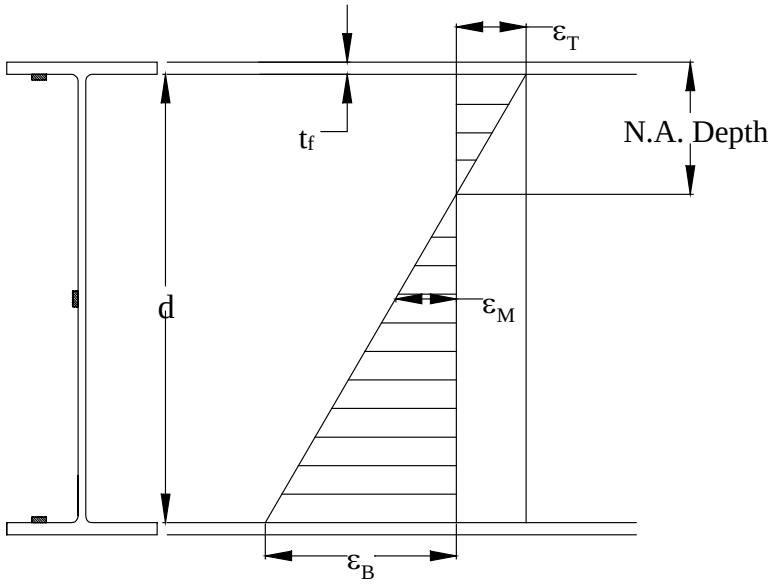

Figure 3.6: Neutral axis depth relative to measured strains

$$\left(d * \frac{|\varepsilon_T|}{|\varepsilon_T| + |\varepsilon_B|} \right) + t_f = N.A.Depth \tag{3.2}$$

where d = the depth of the web (in.)

ε_T = strain at the top gauge (in./in.)

ε_B = strain at the bottom gauge (in./in.)

ε_M = strain at the middle gauge (in./in.)

t_f = flange thickness (in.)

There was another indication of neutral axis position. Gauges were placed at the center of all girder sections. If the neutral axis were at midheight of the girders, there would have been zero strain at gauges placed at the center. Even if the electrical noise was considered, substantial strains were present in all of the gauges at midheight.

3.5.2 Values Used in Neutral Axis Calculation

The N.A. positions calculated using Equation 3.2 for the full length of travel of the test vehicle were not conclusive. Vibration, electrical oscillation, and changes in moment action seemed to contribute to this. A plot of the calculated N.A. position for the three girders with working gauges at the Midspan section is given in Figure 3.7.

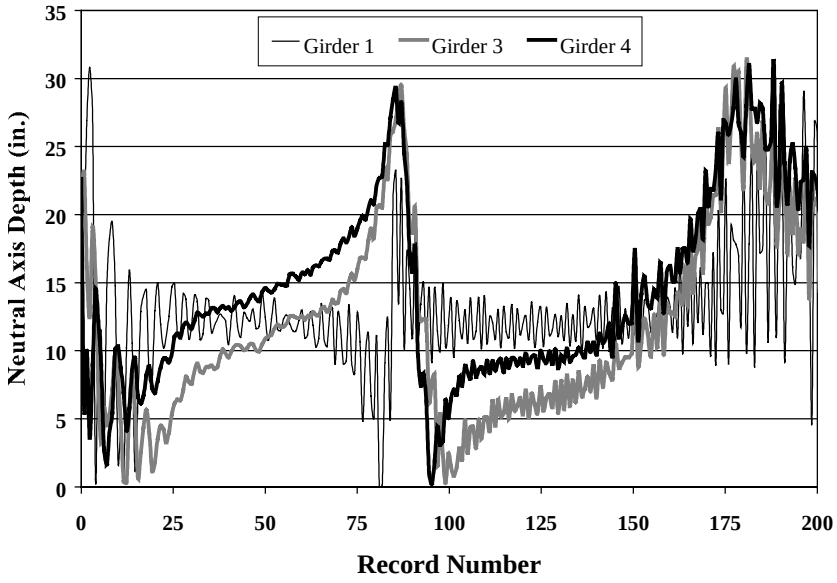

Figure 3.7: Neutral axis locations for Girders 1, 3, and 4 for the midspan section during Test D.T.3-4a

Under noncomposite action, the expected N.A. location was 16.5 in., which was at the midheight of the girder at this location. It was apparent that all of the girders' neutral axis depths were variable and none of them are located at 16.5in.

In order to be confident in the location of the neutral axes, data from only certain portions of the vehicle travel were used. Figures 3.8-3.10 show example strain histories for each of the three sections. The values used for N.A. calculation are those included in the shaded regions.

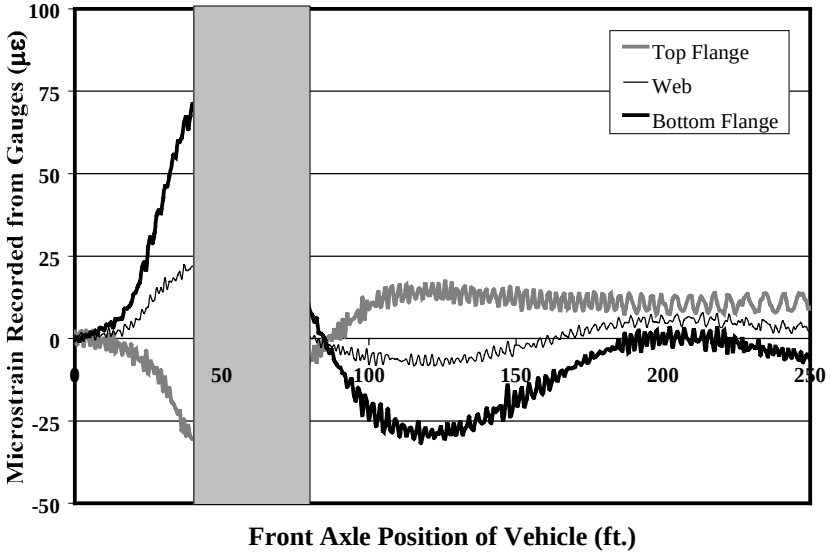

Figure 3.8: Girder 3 strains at the midspan section showing range of values used for neutral axis calculations

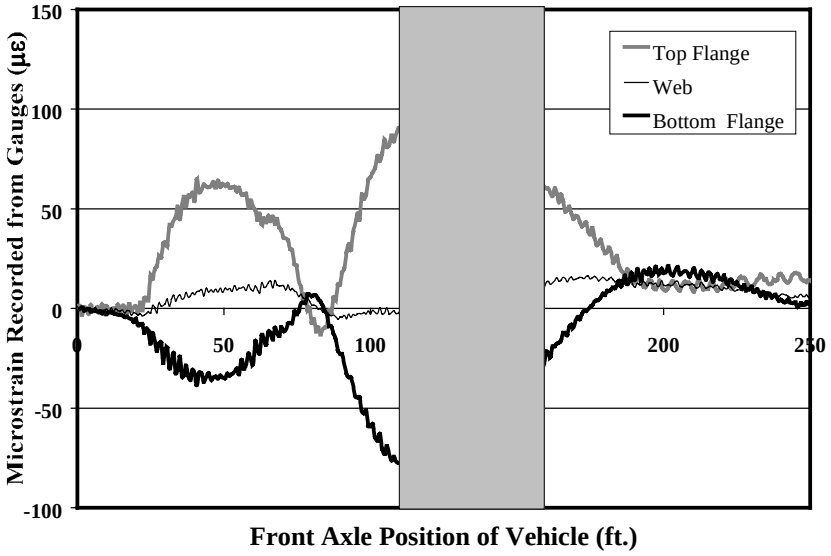

Figure 3.9: ***Girder 1 strains at the support section showing range of values used for neutral axis calculations***

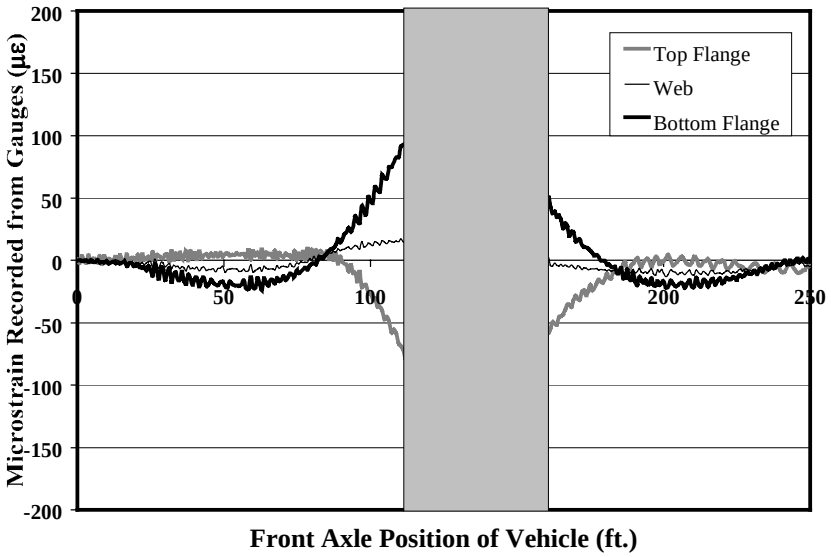

Figure 3.10: ***Girder 1 strains at the river section showing range of values used for neutral axis calculations***

The portions of travel chosen for the Midspan and River sections were 40'-80' and 110'-160' respectively. It is in these regions that strains were maximums. For the Support section, strains were the largest when the vehicle was in the 90-foot span, causing negative moment in the Support section. The region from 110'-160' was used for the Support section as well. The same regions fit well for the HETS tests and therefore were used for all N.A. calculations.

If some of the extreme values given at the River Section were ignored, the largest difference between any neutral axis value and the average for these intervals was 0.17in. Over 80% of the 144 samples had

deviations from the average that were less than 0.10in. These ranges were acceptable given the variability of the unfiltered data.

3.5.3 Comparison of N.A. Locations to Measured Values

A summary of the N.A. locations for all girders tested with low-speed runs is given below. Table 3.3 contains data for all girders that had reading for both the top and bottom flange gauges. Calculations for the Midspan and Support sections of girder 2 were not done because the bottom gauges at each location failed to register. It contains the average N.A. for the intervals just discussed, as well as the average for the girder throughout all tests. The expected value column is based on noncomposite action and is the distance from the top of the flange to the midheight of the girder.

Table 3.3: Neutral axis locations for all low-speed test runs

Section	Girder	Front Axle Position Sampled	Neutral Axis Depth for Vehicle Run (in.) D.T. 1-2a	D.T. 1-2b	D.T. 3-4a	D.T. 3-4b	HETS 1	HETS 2	Average for Girder (in.)	Expected Value (in.)	Difference (%)
Mid-Span	1	40'-80'	13.9	14.1	12.2	13.3	12.2	12.0	13.0	16.5	21.7
	2	N/A	-	-	-	-	-	-	-	-	-
	3	40'-80'	12.0	12.0	13.9	13.3	11.3	11.1	12.2	16.5	26.0
	4	40'-80'	8.4	8.7	17.1	14.2	11.0	10.7	11.7	16.5	29.5
Support	1	110'-160'	19.3	19.3	15.0	**5.8**	17.7	17.4	17.8	16.5	-7.3
	2	N/A	-	-	-	-	-	-	-	-	-
	3	110'-160'	15.0	15.6	15.9	15.5	14.3	14.3	15.1	16.5	8.7
	4	110'-160'	**7.9**	**4.1**	10.2	10.0	10.3	10.6	10.3	16.5	37.9
River	1	110'-160'	16.2	16.7	14.8	11.0	16.6	16.4	15.3	16.7	8.2
	2	110'-160'	15.4	16.0	17.0	17.6	14.5	14.8	15.9	16.7	4.6
	3	110'-160'	13.5	13.2	13.8	14.8	11.4	11.2	13.0	16.7	22.0
	4	110'-160'	9.4	9.0	13.8	13.1	9.4	9.2	10.7	16.7	36.0

The measured neutral axis depths differed from the expected depths by 19% on average. The difference indicated a higher neutral axis, which indicated some degree of composite action in most girders. A few extreme values are shown in bold. The most profound differences in every girder at a section were in the Midspan data for both the dump truck and heavy vehicle.

CHAPTER 4: MOMENT CALCULATION TECHNIQUES

The chapter will describe the calculation of moment from the strain data. The method of calculation depends on the assumed bridge behavior. The Leon River Bridge was designed noncompositely, but may not have behaved that way. The strain data needed a method of data reduction that was appropriate to the bridge behavior. In addition, the participation of the curbs in the flexural response of the bridge was in question. Therefore, a few different moment calculation techniques were used. The criterion for judging data reduction techniques was how well a summation of moments across a section matched the static line girder value.

4.1 SAMPLING INTERVALS

The summation of moments was done at the seven selected vehicle positions given in Table 2.2. The values of moment were based on an average to filter the noise in the data. The average moment value was calculated by averaging the three to four values that were contained within the range of data acquired one foot before and one foot after the vehicle location in question. In effect, for locations of maximum moment, the average moment underestimated the peak moment. The majority of the underestimates were within 5%, although some were as large as 15%. This effect was considered negligible since it eliminated some effects of oscillation and gave values acceptable for use in moment distribution factors.

4.2 MOMENT CALCULATION TECHNIQUES

There were two aspects of bridge behavior that needed to be dealt with when reducing the moments from the strain data. The first was the degree of composite action of the deck with the girders. The second was the contribution of the curbs if some composite action was assumed. The preliminary N.A. location information gave an indication that the girders and deck were acting compositely to some degree. The various ways to model the curbs is given first in this section before data reduction techniques are given.

4.2.1 Properties of the Contributing Curb Sections

The basis for the calculations in this section comes from the equation for moment given in Equation 4.1.

$$M = E\,\varepsilon\left(\frac{I}{c}\right) \tag{4.1}$$

where M = flexural moment in the girder (k-ft)

ε = strain at a given location on the girder (in./in.)

E = elastic modulus for steel = 29,000ksi

I = moment of inertia of the section (in^4)

c = distance from the neutral axis to the location of strain, ε (in.)

The critical value in the calculation of flexural response from the recorded strains was the value of I/*c* for the exterior girder sections. The value of I/*c* is called the section modulus, and will be referred to as S_{CG} to signify the use of the value of *c* that is the distance from the neutral axis to the location of the *gage*, not the extreme fiber. Four possibilities for S_{CG} were considered in this research. One was based on noncomposite action and three were based on composite action.

4.2.1.1 Calculation of S_{CG} for Noncomposite Sections

Where noncomposite behavior was assumed, the value of S_{CG} used for each W-shape was the standard value of I for the W-shape, divided by the distance from midheight of the W-shape to the location of the bottom flange gage, *c*. Gages were attached on the top of the bottom flange as shown previously in Figures 1.6 and 1.7. Therefore, considering noncomposite action, the values of *c* for the W33x130 and W33x141 alone were simply half the total height of the shape minus the thickness of one flange. The value of *c* was 15.69" for both W shapes. The value of I is 6710in^4 for the W33x130 and 7450in^4 for the W33x141. The value of S_{CG} was equal to 428in^3 for the W33x130 and equal to 475in^3 for the W33x141.

4.2.1.2 Calculation of S_{CG} for Composite Sections

For the interior girders, the effective width for composite action was taken as half the distance between the flanges on both sides, plus the width over the flange itself. However, the contributing concrete for an exterior girder was different. Figure 4.1 shows a section view of the deck material over an exterior girder.

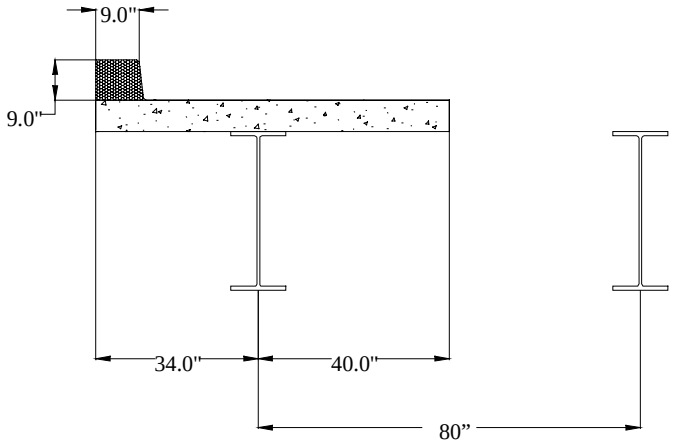

Figure 4.1: Section view of curb material

The slab extends past the centerline of the outer girders by 34", and parapets are present. The value of S_{CG} for the exterior girders was calculated three different ways.

One technique used to handle the parapets was to take the area of concrete contained in the parapet, and treat it like an extension of the slab. The 81in^2 of material shown in Figure 4.1 added 81/6 = 13.5in. of slab onto the existing 34in. This is shown in Figure 4.2.

The value of S_{CG} was also calculated using the full 80.0" width, ignoring the extra 7.5" of deck material. The 80" effective width was the same as the effective width for the interior girders.

A third composite technique did not manipulate the 81in^2 of material. Figure 4.3 shows the curb area with the 74" deck width.

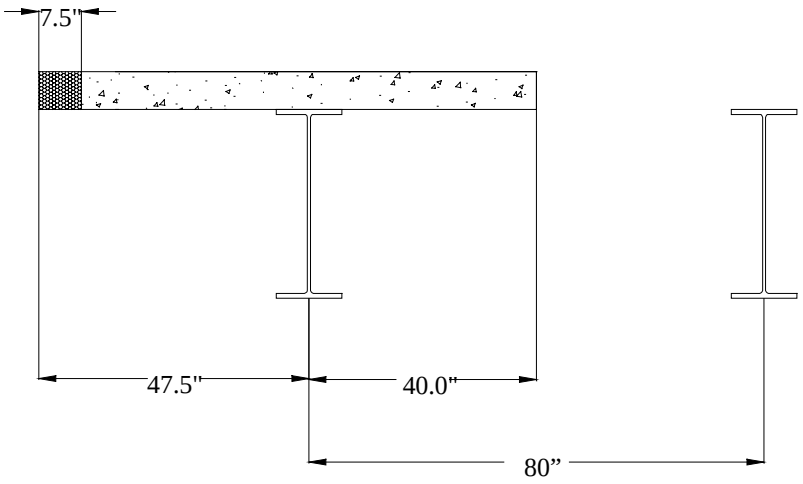

Figure 4.2: Curb area used as deck material

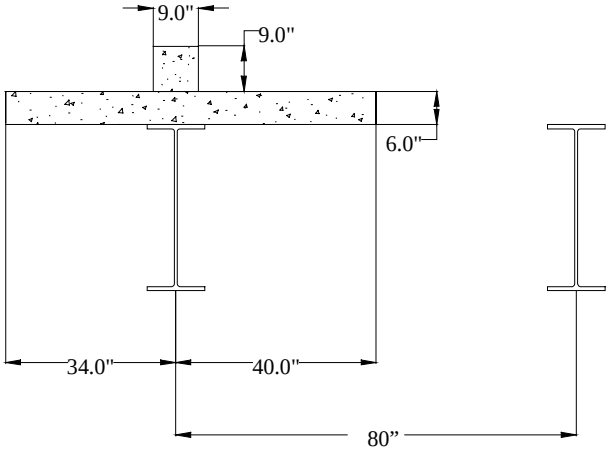

Figure 4.3: Effective concrete section including curb

For the calculation of I, the concrete was transformed by the modular ratio, *n*, assuming f’c = 4000psi, such that:

$$n = \frac{E_S}{E_C} = \frac{29000}{4000} = 7.25$$

For example, the effective width of transformed concrete for the 80” effective width was 80/7.25 = 11.03”. Table 4.1 below gives the values of S_{CG} calculated three ways for composite action.

Table 4.1: Summary of S_{CG} values for exterior girders

W-Shape	S_{CG} for Sections of Contributing Concrete (in^3)		
	80" x 6" Deck	87.5" x 6" Deck	73" x 6" Deck & 9" x 9" Curb
W 33 x 130	576	579	624
W 33 x 141	631	634	681
	Percentage Increase over S_{CG} for 80" x 6" Deck		
W 33 x 130	-	0.5	8.2
W 33 x 141	-	0.5	7.9

Notice that the extra 7.5" of deck material did not change the value of I/*c* significantly. However, the value of S_{CG} increased about 8% if the curb was treated in the position in which it exists. The largest values of S_{CG} most accurately depict the cross section and were used where appropriate in the calculations that follow.

4.2.2 Noncomposite Method of Moment Reduction

The first moment reduction technique assumed noncomposite action. Although the neutral axis locations indicated in Section 3.4.3 indicated a degree of composite action, the data was first reduced assuming no composite action, since that is how the bridge system was designed. The moment was related to strain by Equation 4.2.

$$M = \frac{\varepsilon_B * E_S}{12}\left(S_{CG}\right) \tag{4.2}$$

where M = total moment in the girder (k-ft)

ε_B = strain in the bottom gauge (in/in)

E_s = elastic modulus for steel = 29,000 ksi

S_{CG} = modulus for the W-shape alone (in^3) for strains at the top of the bottom flange

4.2.3 Fully Composite Method

A better technique used for data reduction is one that recognizes the neutral axis locations described in Section 3.4.3. Overall, the N.A. locations were higher than midheight. However, a wide range of N.A. depths are given in Table 3.3. The calculations of composite section modulus in Table 4.1 indicated a N.A. depth of approximately 4.7in when considering the 80" or 87.5" x 6" contributing slab. The N.A. depth was approximately 0.02in (practically at the interface of the steel and slab) for the 73" x 6" slab section and 9" portion of curb. These N.A. locations are higher than those indicated in Table 3.3.

Instead of trying a method of partial composite action to reduce date from girders that have varying N.A. depths, it was first assumed that all the girders behaved in a fully composite manner. The value of S_{CG} is the only variable that changes in this method from the noncomposite technique. The composite S_{CG} was calculated for both interior and exterior girders of both sizes. These were given in Table 4.1. Moment reduction was performed using Equation 4.2 and was the same as the CGM technique used by BRUFEM.

4.2.4 Moment-Couple Method

Another method of reducing the data in a fully composite manner was the Moment-Couple technique outlined in detail in Jauregui (1999). This method is similar to the EGM BRUFEM method discussed previously in Section 2.3.1.2. In this method, four assumptions were made:

1. Plane sections remained plane over the depth of the girder and tributary slab section, but not over the entire depth of the composite section. A strain discontinuity at the interface of the two materials was allowed.
2. The curvatures of the girder and tributary slab section were equivalent.
3. The tributary slab section stayed in contact with the girder but could move longitudinally relative to the girder flanges.
4. There was no net axial force at the girder cross section.

Under those assumptions, the total moment in the girder was equal to the sum of three moments: the moment resisted by the girder alone, M_g, the moment resisted by the effective slab width alone, M_s, and a moment from the equal and opposite axial forces acting on the girder and slab, M_c. The forces involved in M_c were caused by friction at the interface of the slab and girder. The moment comes from the equal and opposite forces acting at an eccentricity, *e*, which was equal to the distance between the neutral axes of the girder and slab. A diagram of the participating moments is shown in Figure 4.4.

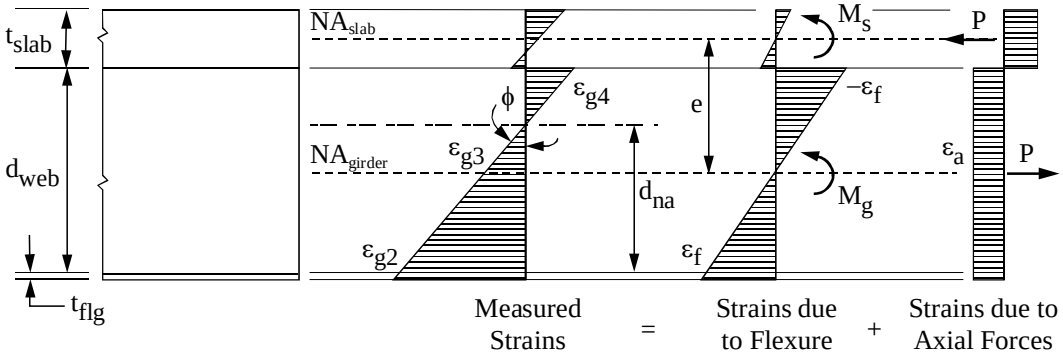

Figure 4.4: Assumed strain distribution for an interior girder section

There are many of strain equilibrium relationships that can be drawn from Figure 4.4. The relationships that were used involved the top and bottom strain gauges. This was done to eliminate error caused by oscillation or noise in the middle gauge, which had smaller strain readings than the other two. The following is a breakdown of the useful strain equations for the data reduction used in this research.

$$\varepsilon_f = 0.5\left(\varepsilon_{g2} - \varepsilon_{g4}\right) \tag{4.3}$$

$$\varepsilon_a = 0.5\left(\varepsilon_{g2} + \varepsilon_{g4}\right) \tag{4.4}$$

where ε_{g2} = strain on the top of the bottom flange (in./in.)

ε_{g4} = strain on the bottom of the top flange (in./in.)

ε_f = strain in pure flexure portion of girder action (in./in.)

ε_a = strain due to axial forces in girder (in./in.)

Given those strains, the participating moments were calculated by the following.

$$M_g = E_S \varepsilon_f \left(\frac{I_g}{c} \right) \tag{4.5}$$

$$M_s = M_g \left(\frac{E_c I_S}{E_S I_g} \right) \tag{4.6}$$

$$M_c = Pe = \left(E_S \varepsilon_a A_g \right) e \tag{4.7}$$

where I_s = moment of inertia of the slab of the slab alone (in^4)

I_g = moment of inertia of the girder alone (in^4)

P = axial force caused by girder-slab interaction (k)

A_g = gross area of the girder alone (in^2)

Using the above notation, the total moment at a girder section was calculated by Equation 4.8.

$$M_T = M_g + M_s + M_c \tag{4.8}$$

There again was the question of the exterior girders using this method. The calculations of moments of inertia used here needed to account for the increased eccentricity, *e* of the parapet portion. The normal participation of the 80" effective slab width was acceptable for *interior* girders, not the exterior ones. Therefore, the parapet was treated as an $81in^2$ area above the 74in wide section of deck material (Figure 4.3).

This technique required the moment of inertia of the slab, I_s. Table 4.2 below shows the values of I_s for the interior and exterior deck portions. Including the curb area also changed the eccentricity.

Table 4.2: Values of I and* e *used in the moment-couple technique

Section	Moment of Inertia for the Slab, I_s ($in.^4$)		Eccentricity,e (in.)	
	Interior	Exterior	Interior	Exterior
W 33 X 130	1440	5706	19.55	20.72
W 33 X 141	1440	5706	19.65	20.82

The inclusion of the curb area nearly tripled the value of I_s. The eccentricity between the two forces changed by only 6% for the exterior girder. The large increase in I_s for exterior girders only affected the M_s term in Equation 4.8 and did not have a large impact on the total moment. This was true because M_s was typically les than 10% of M_T.

4.3 COMPARISON WITH SAP2000

The major criteria used when judging the data reduction methods was how well moments summed across a section matched with the SAP2000 line girder moment. This was done for all six slow vehicle runs, at the seven selected vehicle locations. The three other zero moment locations were included as well

because they gave reasonable for total moment. Figures 4.7-4.24 show the results of moment reduction using all three methods discussed in Sections 4.2.2-4.2.4.

Figure 4.5 is an example plot. It was taken from the data for the dump truck over the River section. There a few key features that appear in the plot:

1. Each plotted point represents the total moment at the cross section for a single test run. This total was calculated using Equation 4.9.

$$M_{Tot} = \sum_{1}^{4} M_i \tag{4.9}$$

where M_t = Moment on a girder calculated from strains measured from the top of the bottom flange (k-in.)

M_{Tot} = Total moment at a cross section (k-in.)

2. The scatter of the values plotted at the same front axle location was small in general. This indicated a good degree of repeatability in the acquired data.
3. The predicted static response, "Line Girder," plotted near the test data or was contained within the range of test data for a given vehicle location.

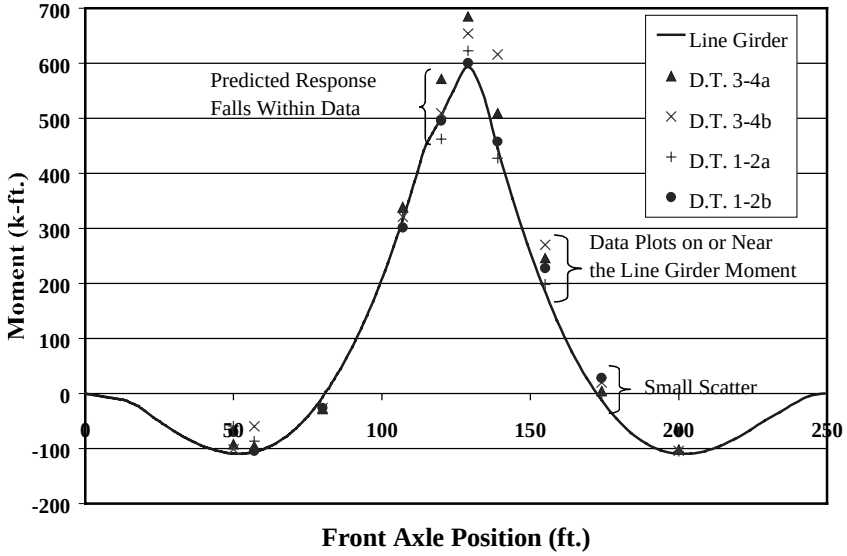

Figure 4.5: Example plot of total moment at river section for the dump truck using the fully composite method

When looking at the plots in Section 4.3.1, it is important to look at the same data plotted using each method. Figure 4.6 gives an example of moments calculated using the Noncomposite method, Fully Composite method, and the Moment-Couple method for one section and vehicle. Notice how the data from the Noncomposite method is not close to the line girder values. The data from the Moment-Couple method is closer to the predicted response. Finally, the data reduced using the Fully Composite method plots on the line girder value, or conservatively beyond it in regions of maximum moment.

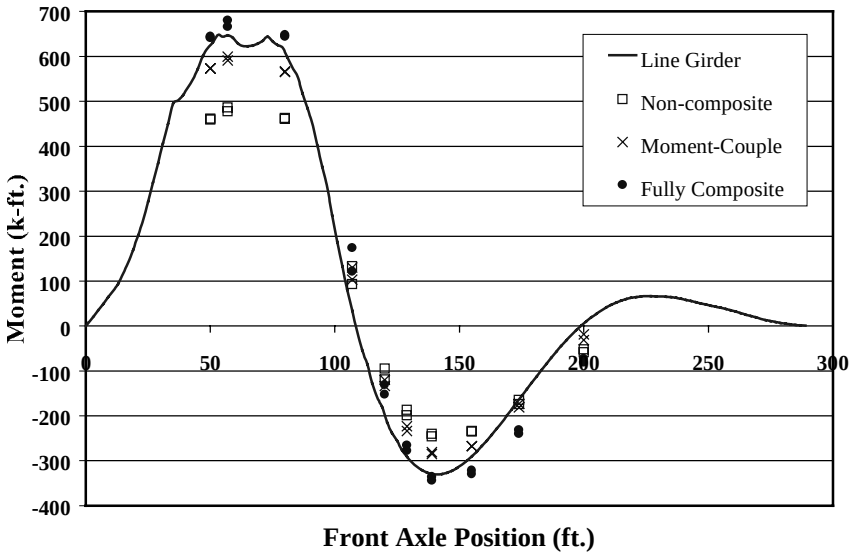

Figure 4.6: Data from a HETS vehicle test including all three data reduction methods (midspan section)

4.3.1 Slow Speed Vehicle Tests

The following nine pages contain the plots of total moment from the slow vehicle tests in comparison with the expected static line girder moments. The first three of the following nine pages contain the plots for the Midspan section for both vehicles. One of the three methods is shown on each page. The Support and River sections are presented in a similar manner.

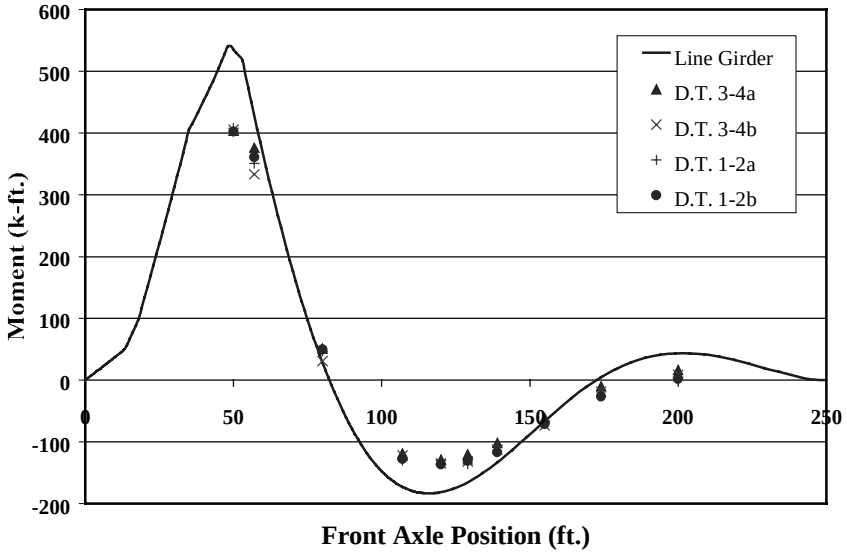

Figure 4.7: Total moment at the midspan section caused by dump truck loading (noncomposite method)

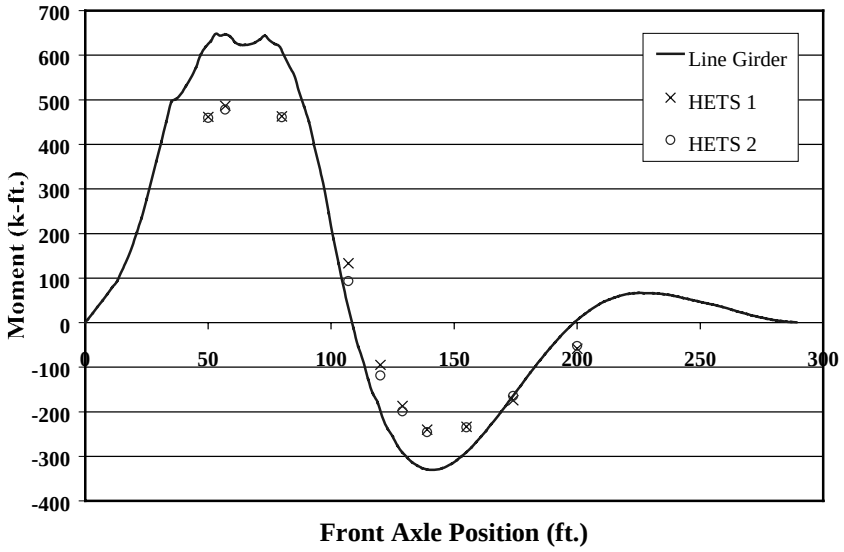

Figure 4.8: Total moment at the midspan section caused by HETS vehicle loading (noncomposite method)

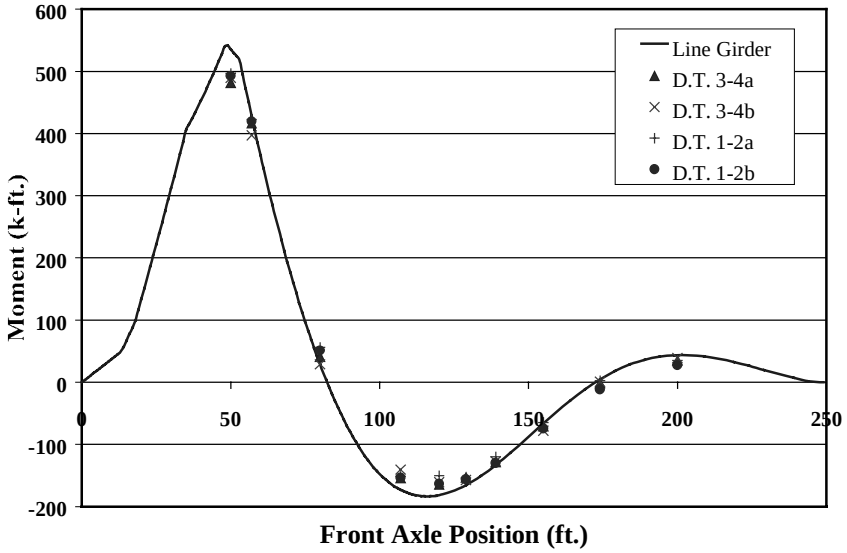

Figure 4.9: Total moment at the midspan section caused by dump truck loading (Moment-Couple Method)

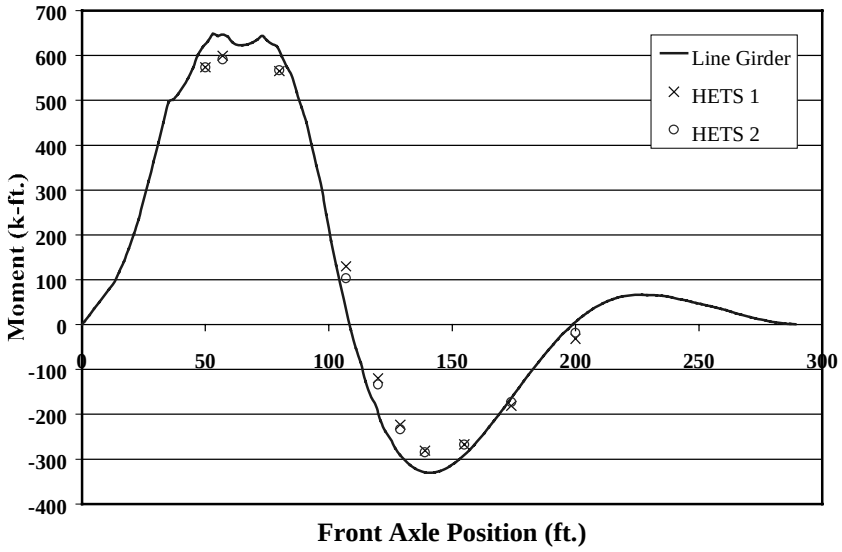

Figure 4.10: Total moment at the midspan section caused by HETS vehicle loading (Moment-Couple Method)

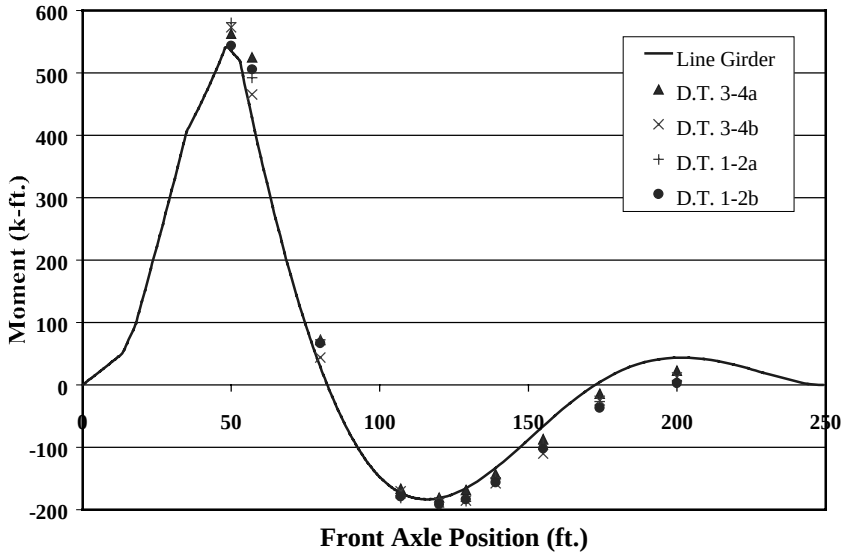

Figure 4.11: Total moment at the midspan section caused by dump truck loading (Fully Composite Method)

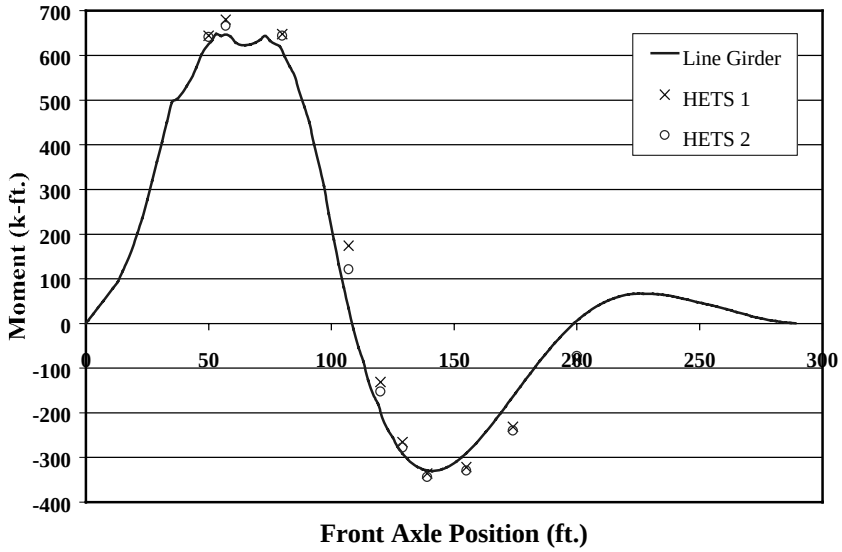

Figure 4.12: Total moment at the midspan section caused by HETS vehicle loading (Fully Composite Method)

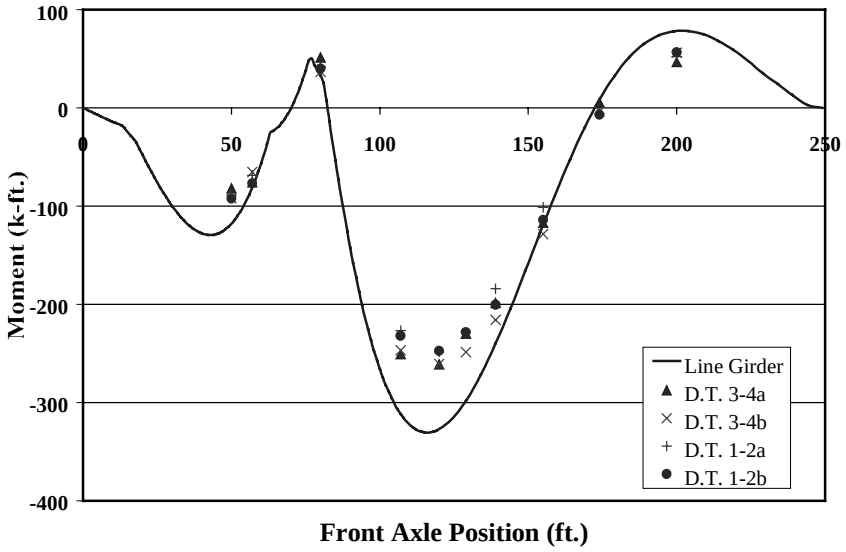

Figure 4.13: Total moment at the support section caused by dump truck loading (Noncomposite Method)

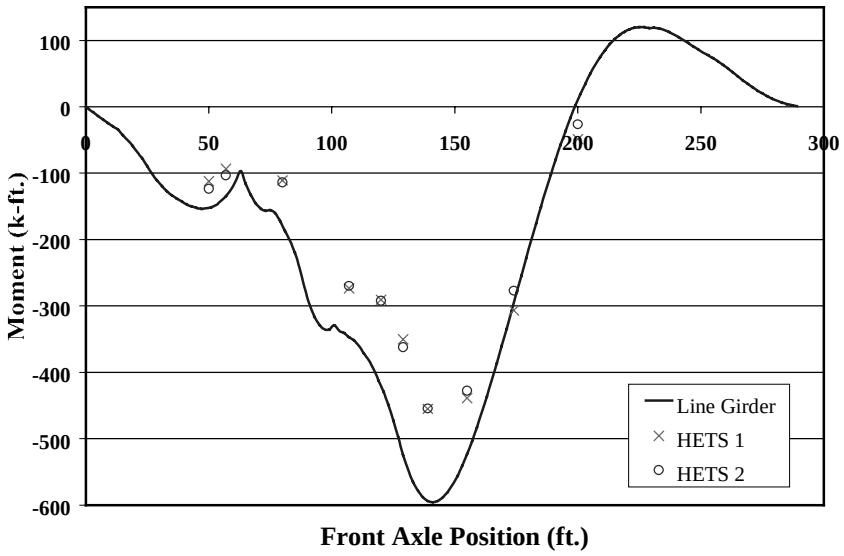

Figure 4.14: Total moment at the support section caused by HETS vehicle loading (Noncomposite Method)

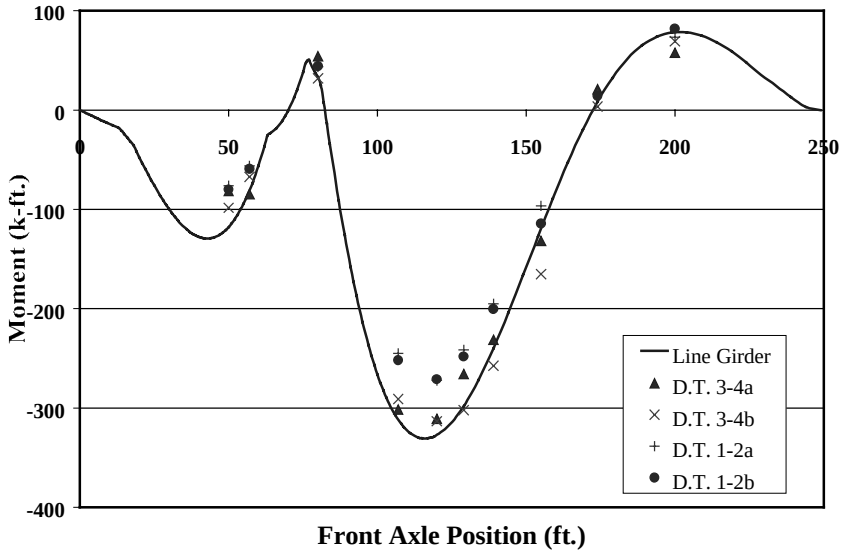

Figure 4.15: Total moment at the support section caused by dump truck loading (Moment-Couple Method)

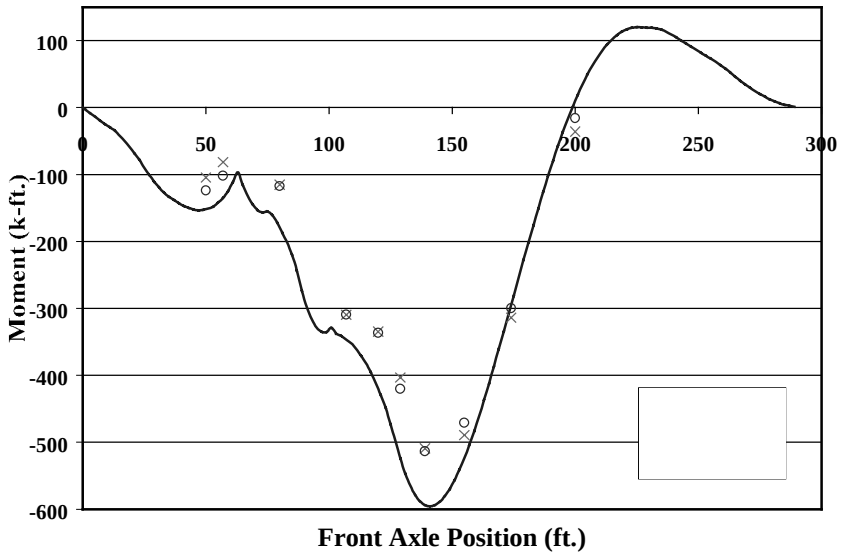

Figure 4.16: Total moment at the support section caused by HETS vehicle loading (Moment-Couple Method)

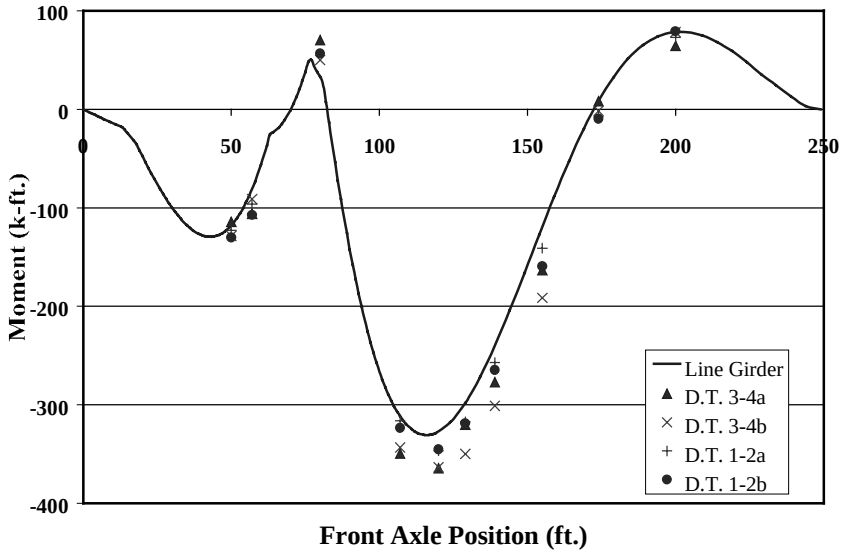

Figure 4.17: Total moment at the support section caused by dump truck loading (Fully Composite Method)

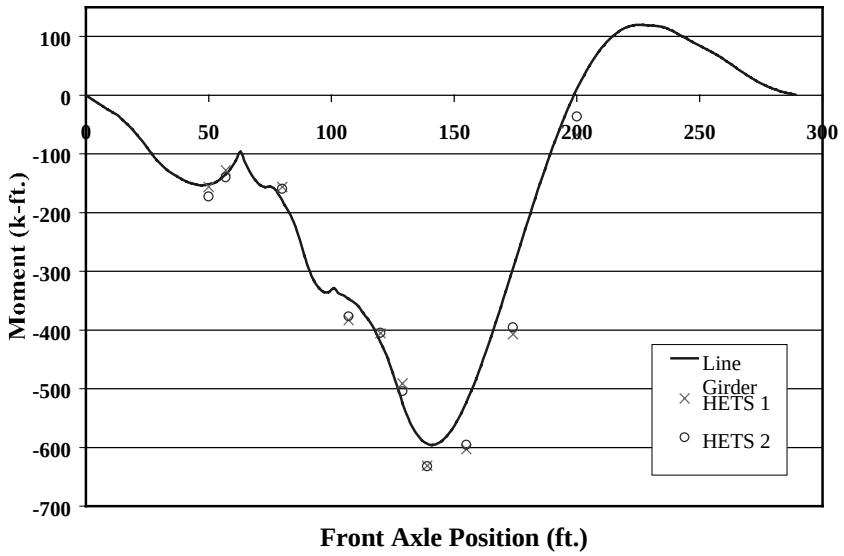

Figure 4.18: Total moment at the support section caused by HETS vehicle loading (Fully Composite Method)

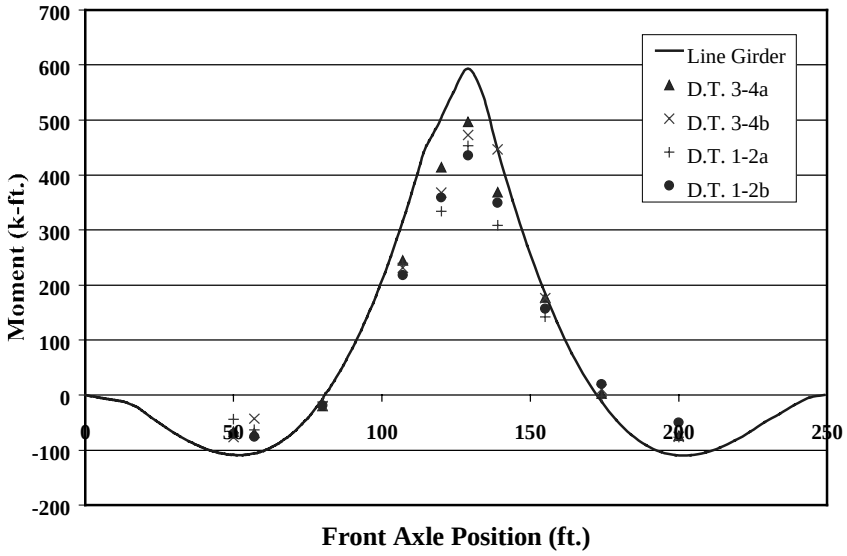

Figure 4.19: Total moment at the river section caused by dump truck loading (Noncomposite Method)

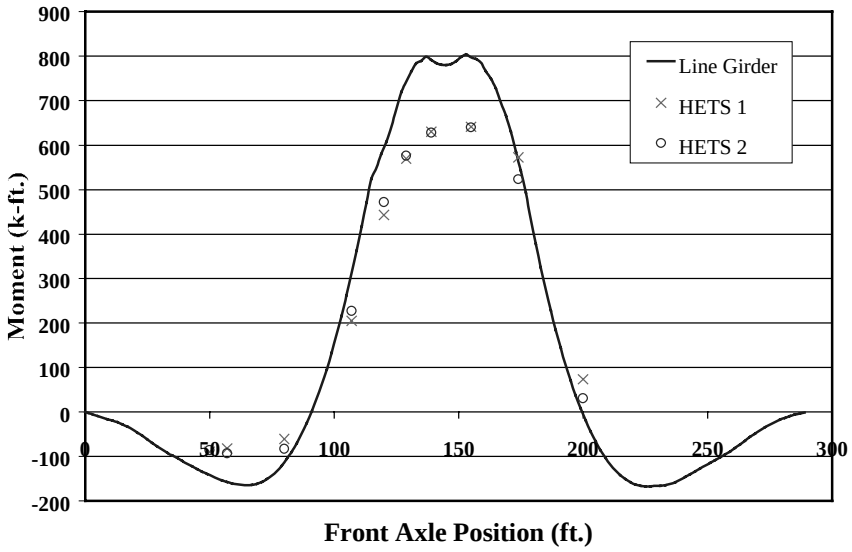

Figure 4.20: Total moment at the river section caused by HETS vehicle loading (Noncomposite Method)

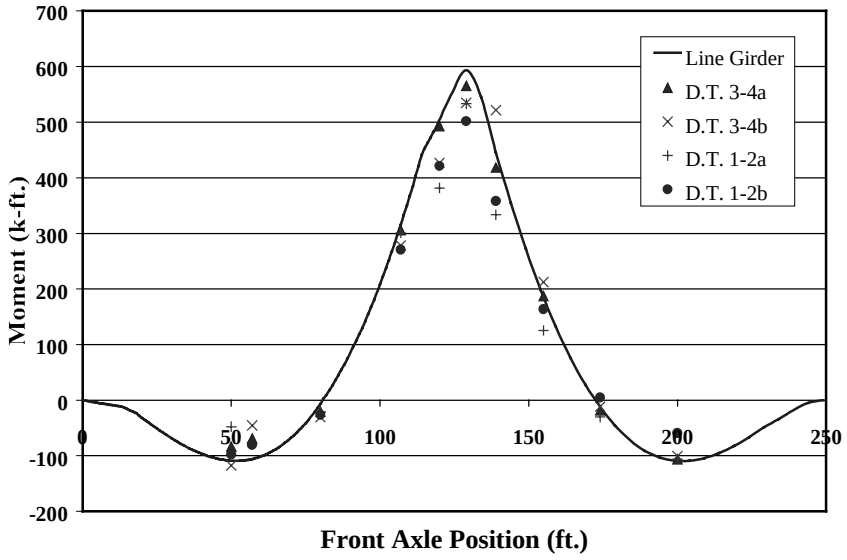

Figure 4.21: Total moment at the river section caused by dump truck loading (Moment-Couple Method)

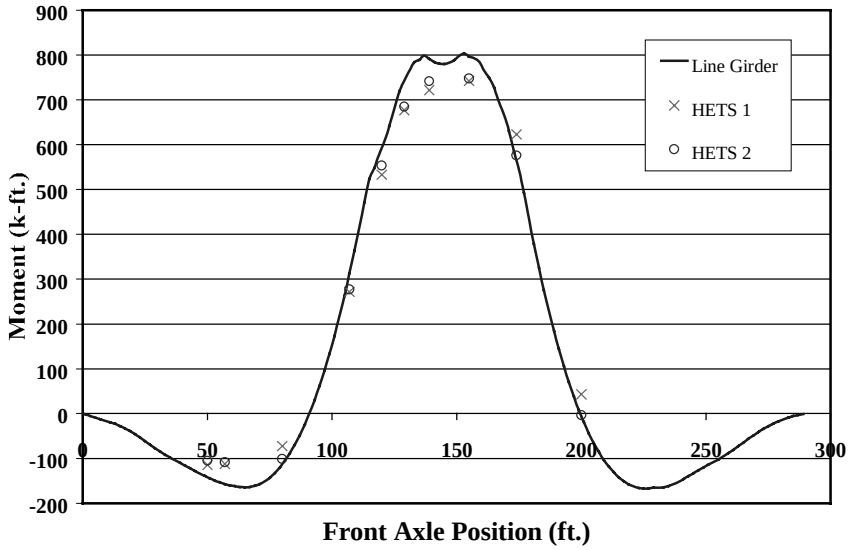

Figure 4.22: Total moment at the river section caused by HETS vehicle loading (Moment-Couple Method)

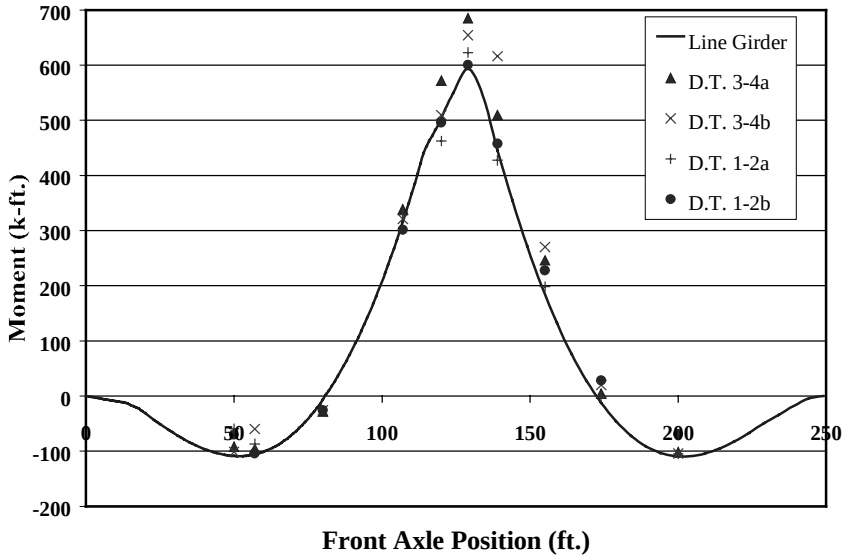

Figure 4.23: Total moment at the river section caused by dump truck loading (Fully Composite Method)

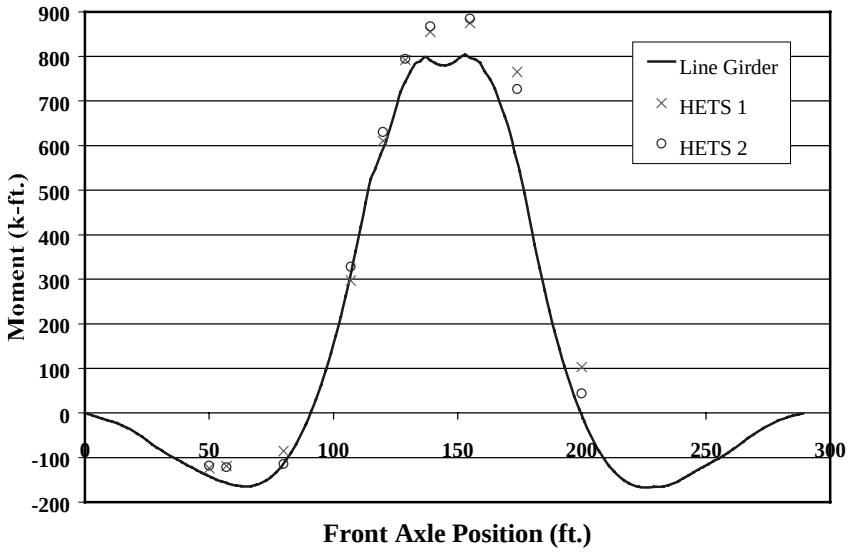

Figure 4.24: Total moment at the river section caused by HETS vehicle loading (Fully Composite Method)

The values from the Fully Composite method appeared to fit the line girder curves the best. Some values for repeated tests were greater than the line girder value, and some were less. In most cases, the line girder moment lied within the range of repeated tests done with the same vehicle. The values from the Noncomposite and Moment-Couple methods did not fit the line girder moment as well. This was especially prevalent in the Support section. The Fully Composite method tended to conservatively over-estimate the moment in region of maximum moment, but it fit well enough that a method of reduction using some degree of partial composite action was not made. Considering 5 locations of maximum moment for each vehicle (10 samples in all), the moment values given by the Fully Composite Method were conservative by 7.5% on average. This difference was deemed acceptable and the Fully Composite method was judged to be the best way to reduce the data.

4.3.2 High Speed Vehicle Tests

Although the low-speed tests were the primary focus of this research, some significant effects were noticed from the high-speed tests. It is important to realize that the data from the high-speed vehicle tests shown previously in Figures 3.2 and 3.3. was real data. Although the filtered high-speed data for the *total cross section* could be obtained, the important information was the additional moment present in *each girder* due to this dynamic effect. Table 4.3 gives the unfiltered maximum moments present in each girder for the HETS tests.

The maximum increase caused by dynamic loading was found in girder 2 at every section and ranged from 38-85%. The average increase in moment due to dynamic effects in all girders was 24%. According to AASTHO, in most field tests of highways bridges, "the dynamic component of the response does not exceed 25% of the static response." The HETS tests shown here exhibited behavior such as that seen by the developers of the AASTHO impact factors.

Table 4.3: Unfiltered maximum moments in individual girders from the HETS vehicle tests

Section	Girder	Test Run HETS 1 (k-ft)	HETS 2 (k-ft)	HETS H.S. (k-ft)	Max Increase in High Speed Over Low Speed Tests (%)
Mid-span Girders	1	175	172	217	26%
	2	157	160	217	**38%**
	3	213	208	201	-4%
	4	166	161	177	10%
Support Girders	1	-129	-130	-152	18%
	2	-187	-191	-283	**51%**
	3	-193	-193	-201	4%
	4	-161	-156	-162	4%
River Girders	1	227	231	249	10%
	2	247	254	457	**85%**
	3	228	228	272	19%
	4	256	258	330	29%

The high and low speed dump truck tests could not be compared as easily since different lateral positions of the truck were used. However, the dump truck tests could be included in comparisons of total moment *at each section*, since the same dump truck was used each time. Table 4.4 gives the unfiltered maximum totals moments across each section. The percentage increase in moment in the dynamic run over each low-speed run is also given.

Table 4.4: Unfiltered maximum total moments at each section for all test runs

Test	Mid-span Moment (k-ft)	Increase of High Speed over Low Speed Tests (%)	Support Moment (k-ft)	Increase of High Speed over Low Speed Tests (%)	River Moment (k-ft)	Increase of High Speed over Low Speed Tests (%)
D.T.H.S.	781	-	-489	-	905	-
D.T. 1-2a	584	**34%**	-355	**38%**	651	39%
D.T. 1-2b	595	31%	-367	33%	637	**42%**
D.T. 3-4a	600	30%	-377	30%	718	26%
D.T. 3-4b	580	35%	-385	27%	717	26%
HETS H.S.	741	-	-771	-	1074	-
HETS 1	694	7%	-669	15%	920	**17%**
HETS 2	685	**8%**	-660	**17%**	939	14%

The maximum increase in total moment due to dynamic effects from the dump truck was 42%. The maximum increase due to dynamic effects caused by the HETS vehicle was 17%, which was less than the unfiltered maximum increases per girder (38-85%) or the average increase per girder (24%).

CHAPTER 5: DISTRIBUTION OF MOMENT WITH VEHICLE POSITION

Information in Chapter 3 indicated that the Leon River Bridge exhibited some degree of composite action. The Fully Composite gave total moments that fit the line girder values very well. This method was applied to all the data used for the rest of this research. The distribution of moments in each girder was plotted against longitudinal position of the vehicle on the bridge. The results show that when the vehicle was directly above a section, the distribution of load in all girders at that section was the most disproportioned. As vehicle distance from the section increased, the load was distributed more evenly throughout the girders in the section.

This chapter shows this distribution of moment in two distinct manners, one using the full travel, and another using discrete values at selected locations. Section 5.1 contains plots of the moment in each girder as recorded during the entire travel of the vehicle. These plots were used to show the changing relationship of the moments in each girder with respect to one another. They were also used to show their summation in relation to the predicted static response. Section 5.2 explains how discrete moment values were obtained and shows how they were plotted effectively. Section 5.3 contains plots of this discrete type that were used to explore the differences in BRUFEM estimates using the CGM and EGM, as well as the effect of diaphragms in the model. Finally, Section 5.4 presents plots taken from a dump truck and HETS vehicle tests. BRUFEM plots for these test runs were also shown in order to show similarities in the measured and estimated data as well as how the distribution of moment changed with vehicle position.

5.1 PRESENTATION OF MOMENT HISTORIES

This section presents some plots taken from each type of vehicle test. Figures 5.1-5.3 show an HETS test presented first as an example. Then, after some points are made concerning key elements of the plots, selected figures from dump truck tests are shown. The moment histories from the dump truck tests most clearly show the difference in moment among girders since the dump truck was not centered laterally on the bridge.

5.1.1 Plots of Moment for a Complete HETS Run

Figures 5.1–5.3 show plots of the unfiltered data from one of the HETS vehicle tests. To create the plots, a value of moment was calculated using the Fully Composite method for each value of strain recorded for the entire traverse of the bridge by the load vehicle. The moment in each girder at a section was plotted as the vehicle moves across the bridge. The total moment, the sum of the four girder moments, and line girder moment are also shown for reference. Note that, all the girders experienced about the same moment action under HETS loading.

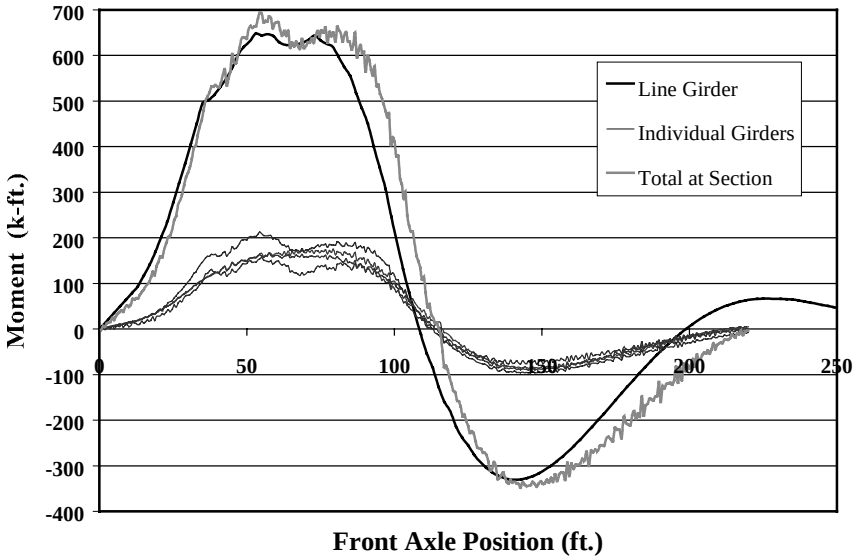

Figure 5.1: Moment at midspan section for Test HETS 1

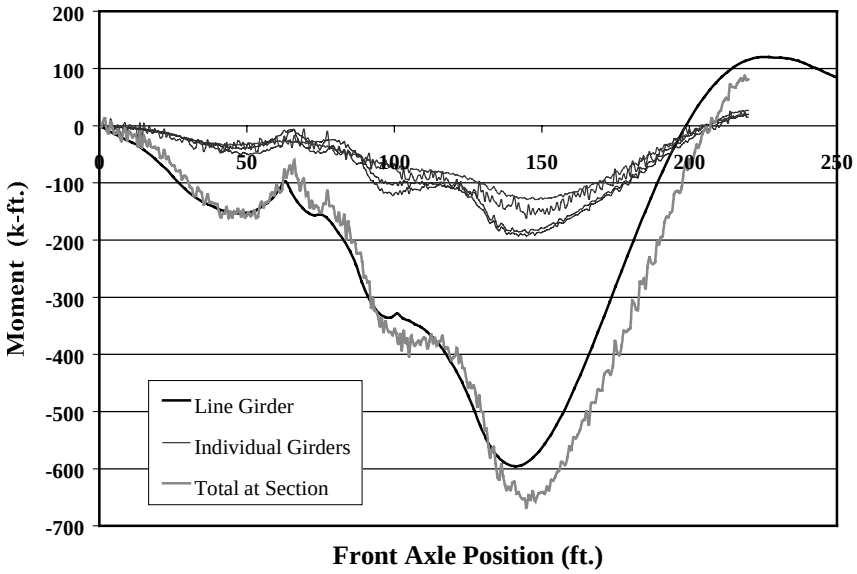

Figure 5.2: Moment at support section for Test HETS 1

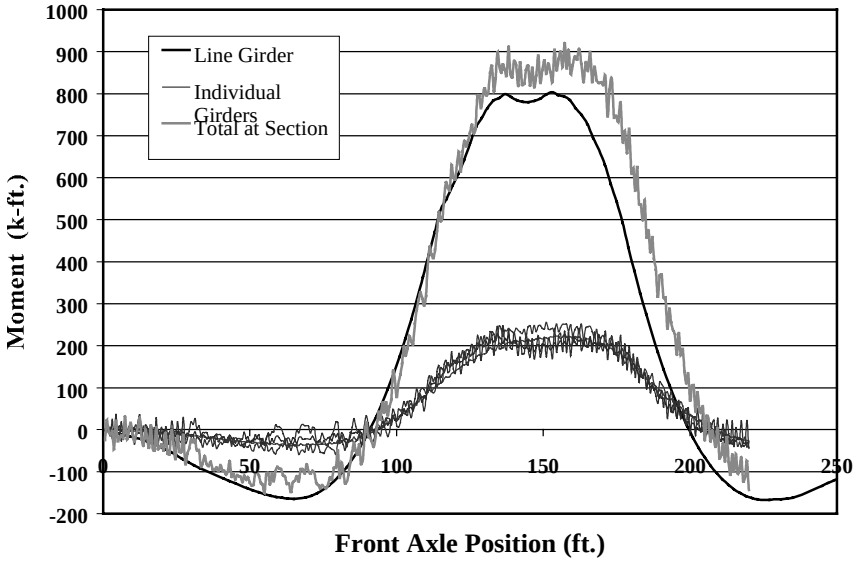

Figure 5.3: Moment at River Section for Test HETS 1

There were a few observations made from the plots in Figures 5.1-5.3. First of all, the total cross-sectional moment agreed very well with the line girder moment. The line girder moment represents the total moment applied to the bridge. The maximum line girder moment was less than the sum of the girder moments in some cases. There are a few possible reasons why the total moment did not match the line-girder exactly. They are given below.

1. The type of the data reduction technique. Perhaps a partially-composite method of data reduction would have given values closer to the line-girder values.
2. Human error or parallax because of the limited length of cord for the manual switch. In some instances the observer reached the limit of cord length or could not walk fast enough to obtain a good view of the vehicle axle. This would have caused the data to be skewed with respect to the line girder moment.
3. Noise and oscillation in the data acquisition system caused by exterior radio signals.
4. Moment carried by the slab that was not accounted for in spite of the data reduction method used.

More significant observations with respect to the plots for a dump truck test are given in Section 5.1.2.

5.1.2 Plots of Moment for a Complete Dump Truck Run

It was noted that the spacing between the individual moment histories for each girder changed as the vehicle moved across the bridge. The girders directly under the vehicles path carried a greater portion of the load when the vehicle is near the section than when the vehicle was far from the section. This was most evident in tests where the vehicle was not centered laterally on the bridge, such as the dump truck tests.

Unfiltered moment histories from tests D.T. 1-2b and D.T. 3-4a are shown in Figures 5.4-5.9. Girders 1 and 2 are shown in one color on the plots. Girders 3 and 4 are both shown in another. Recall that the D.T. 1-2b means that the dump truck was located on the side of the bridge over girders 1 and 2., likewise with D.T. 3-4a over girders 3 and 4. Since the truck positions were symmetric about the bridge centerline, the values appear to be exactly reversed when looking at both plots on a page at the same time. The values given for girders 1 and 2 in the plots for D.T. 1-2b should match the values given for girders 3 and 4 in plots of D.T. 3-4a.

Using Figures 5.4 and 5.5 as an example, the Midspan moments found in girders 1 and 2 for the D.T. 1-2 tests, and those found in girders 3 and 4 for the D.T. 3-4 tests were markedly higher than the other two girders for vehicle locations between 0' and 70' (in the same span as the instrumentation). The values of moment in all girders at the Midspan section became more equal to each other when the vehicle moved into the next span (between 70' and 160'). The values of moment in all girders were practically equal in value by the time the vehicle moved into the third span.

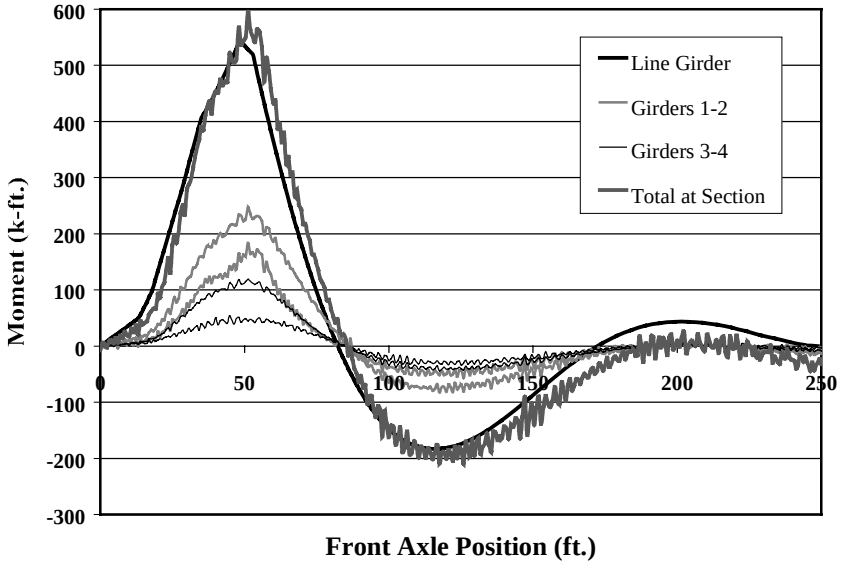

Figure 5.4: Moment at Midspan Section for Test D.T. 1-2b

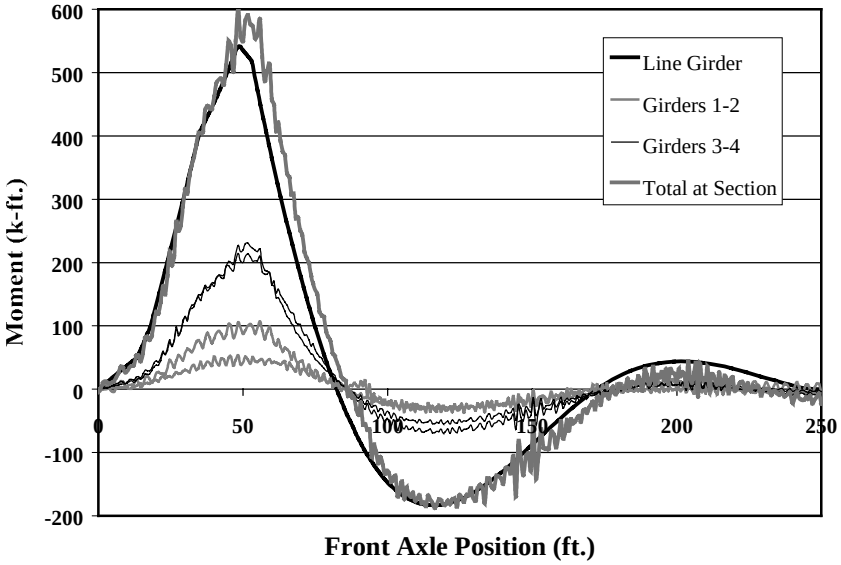

Figure 5.5: Moment at Midspan Section for test D.T. 3-4a

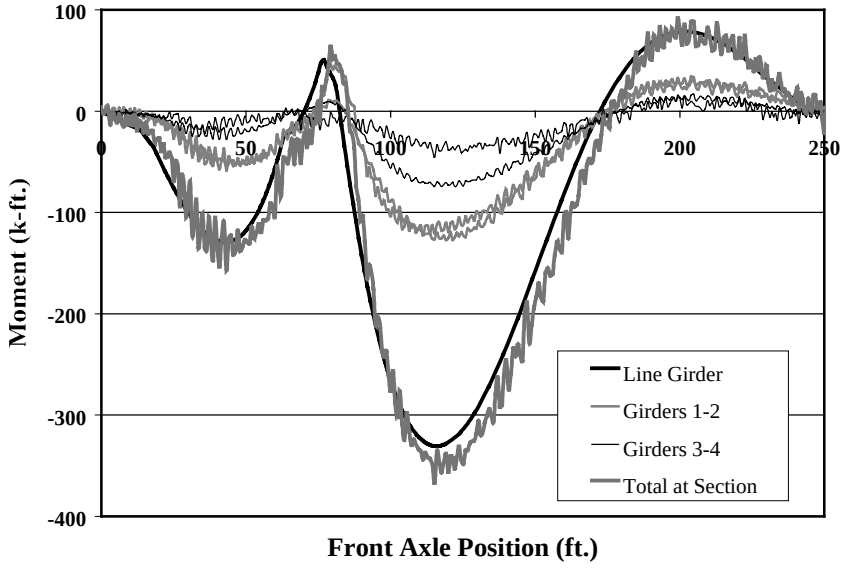

Figure 5.6: Moment at Support Section for test D.T. 1-2b

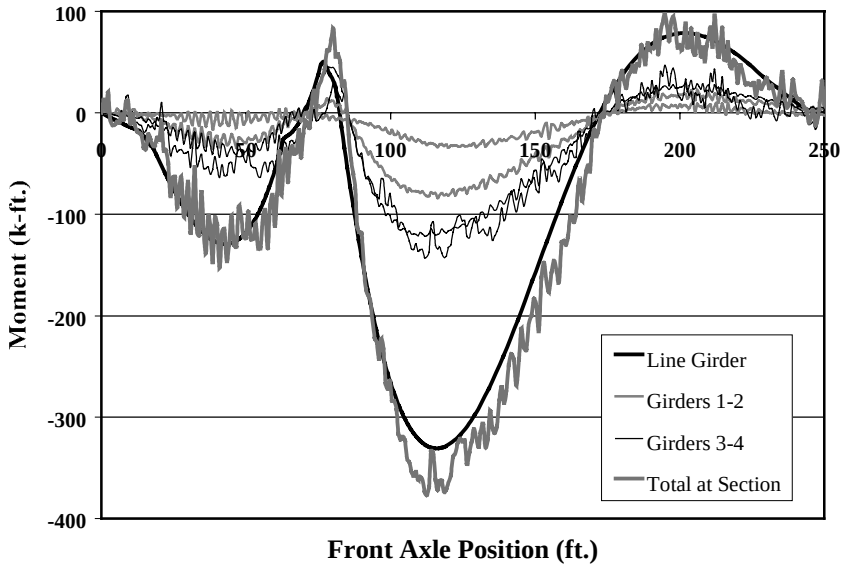

Figure 5.7: Moment at Support Section for test D.T. 3-4a

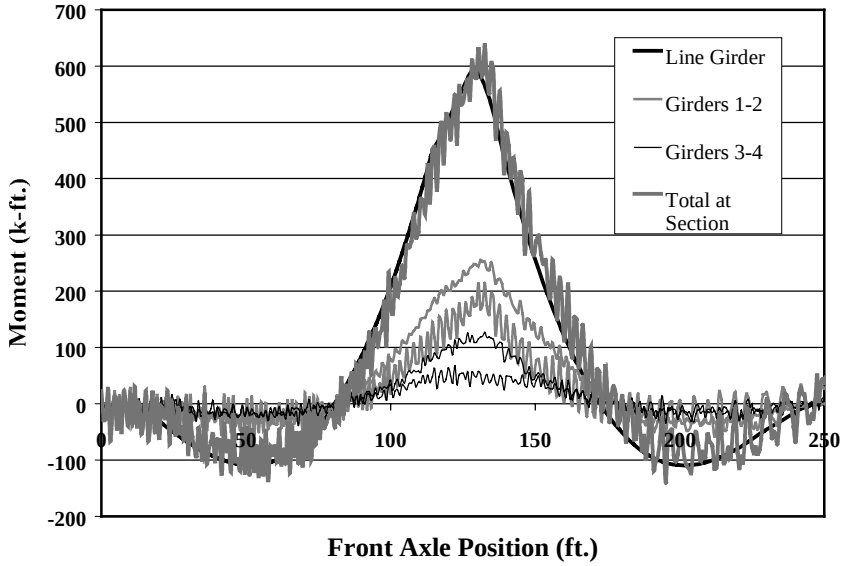

Figure 5.8: Moment at River Section for test D.T. 1-2b

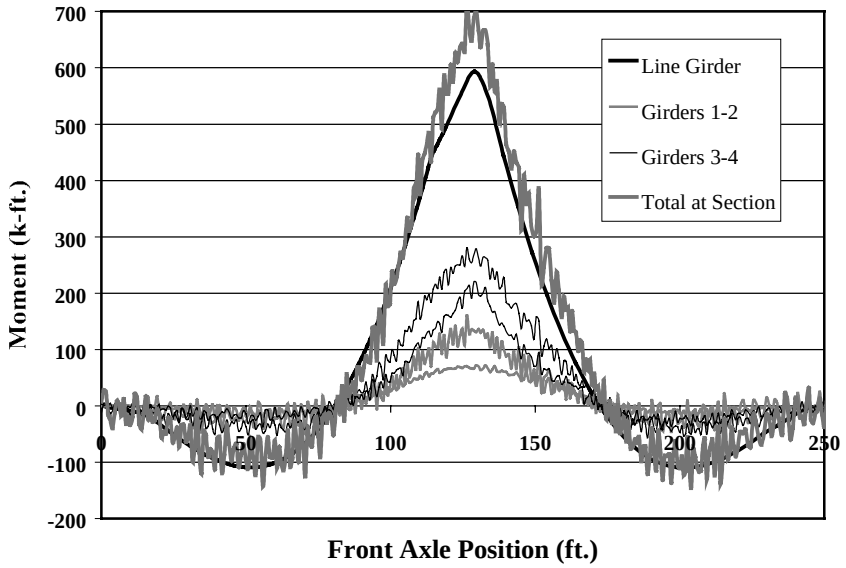

Figure 5.9: Moment at River Section for Test D.T. 3-4a

This apparent equalizing of the load among bridge girders required more exploration, and comparison with computer models. It was important to learn the degree to which a computer model could generate this action, and how the distribution of the live load would proceed if the computer model were used.

5.2 PLOTS OF DISCRETE MOMENT DISTRIBUTION VALUES

Instead of plotting moment distribution factors for every axle position in the style of plots given in the previous section, discrete values were calculated only for the moments at the seven locations named in Table 2.2. Live load distribution factors were calculated from the data from all eight tests. The LLDFs were calculated using Equation 5.1.

$$LLDF_g = \frac{M_g}{M_{sum}} \tag{5.1}$$

where $LLDF_g$ = live load distribution factor for girder

M_g = moment found in girder at a particular section

M_{sum} = sum of all four moments in the girders at the section

For example, for test D.T. 3-4a, the total moment at the Midspan section in all four girders was -180.5 k-ft when the dump truck was at position 120'. The moment in girder 3 alone was -53.1k-ft. Therefore, the LLDF for girder 3 at that position was 53.1/180.5 = 0.294 (29.4%).

The plots that appear in Sections 5.3 and 5.4 need explanation before going further. Figure 5.10 is an example plot. The value of 29.4% for girder 3 is located on the plot at the 120' position.

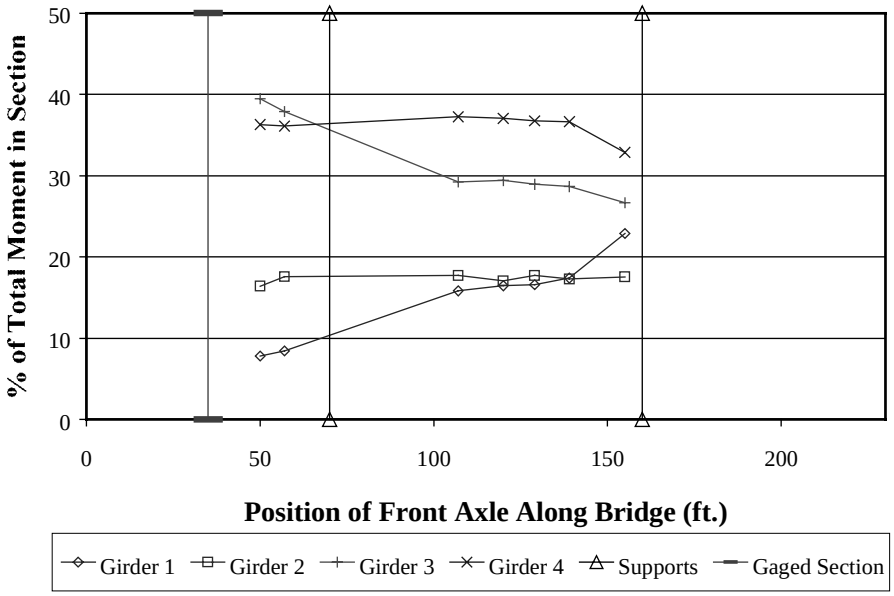

Figure 5.10: Example moment distribution plot taken from test D.T.3-4a

The units of the abscissa are feet along bridge. Vertical lines connected by hollow triangles show the locations of interior supports. Thus, these lines break the plots into three spans, just like the actual bridge. There is also a line indicating the location of the gauged section relative to the supports. The values plotted on the ordinate indicate the percentage of the total moment at that section that is found in each girder. Therefore, for any front axle position, the sum of all four plotted points equals 100%.

5.3 DISCUSSION OF BRUFEM MODELING ISSUES

Before BRUFEM was used to obtain moment distribution estimates for comparison to measured data, two inquiries were made with respect to BRUFEM modeling. A comparison of the Eccentric Girder Model and the Composite Girder Model was used to be sure that the choice of method had negligible impact on moment distribution. Also, a study of the effect of diaphragms was needed in order to see if they should be included in the BRUFEM model.

5.3.1 Comparison of EGM and CGM Methods

The BRUFEM modeling technique chosen for comparison was the CGM. This was done because the CGM uses a method of calculation similar to the Fully Composite method of data reduction. The EGM does not calculate values in the same manner that the CGM does, but is supposed to yield greater accuracy according to the BRUFEM manual. An investigation into the EGM was appropriate in order to show that the differences between the EGM and CGM were small. This validated the use of BRUFEM's simpler modeling technique.

Figures 5.11 and 5.12 show selected moment distribution plots for a dump truck and analysis performed in BRUFEM. The first plot shows the results using the EGM method, and the other shows the CGM method. The figures shown are representative of all of the test runs analyzed using both techniques. The plots are almost identical.

Out of all the runs performed using both the CGM and the EGM, the biggest difference in LLDFs was 11.2% (the difference between 3.78 and 4.25), with 90% of the repeated LLDF values having a difference of less than 3% between the EGM and CGM methods. The total static moments were equal using both methods. Therefore, the CGM was used for comparison in this research.

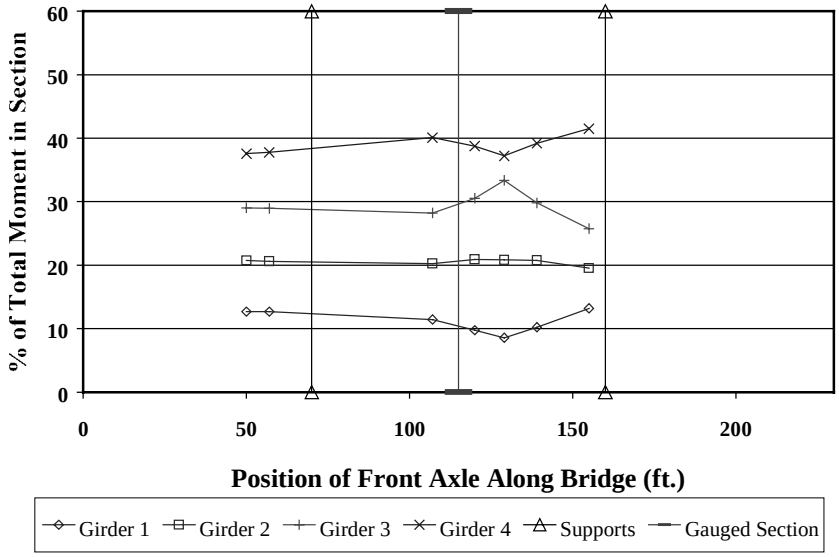

Figure 5.11: BRUFEM CGM moment distribution for a D.T. 3-4 Test, River Section

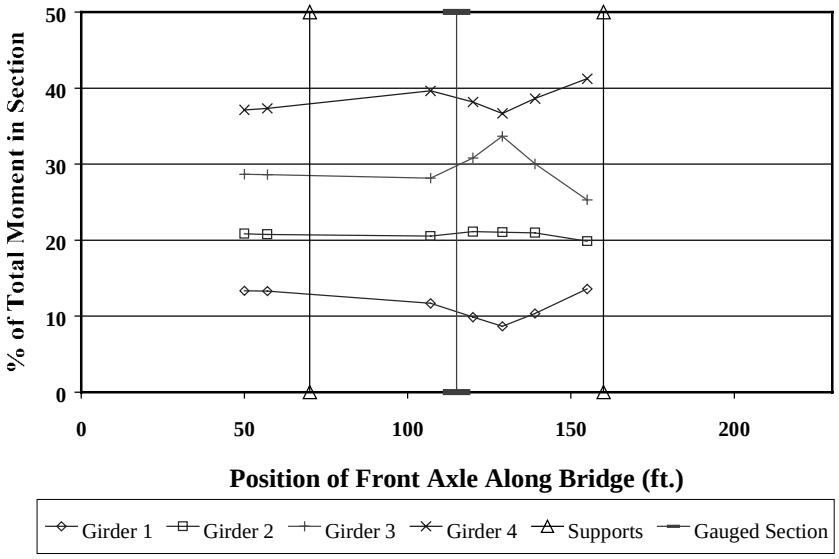

Figure 5.12: BRUFEM EGM moment distribution for a D.T. 3-4 Test, River Section

5.3.2 Effect of Diaphragms upon Analytical Results

Another aspect of the bridge system that was explored was the performance of the diaphragms. This was needed in order to determine whether or not the diaphragms were essential to the BRUFEM model of the Leon River Bridge. Duplicate sets of runs were made using the EGM with and without diaphragms. These were compared with plots made from measured data to determine which model most accurately represented the bridge. An example of each vehicle in the Support section is given here. Figures 5.13-5.15 contain distribution factors from the actual dump truck run, the BRUFEM model with diaphragms, and the BRUFEM model without diaphragms. Figures 5.16-5.18 show data from a HETS test in a similar manner.

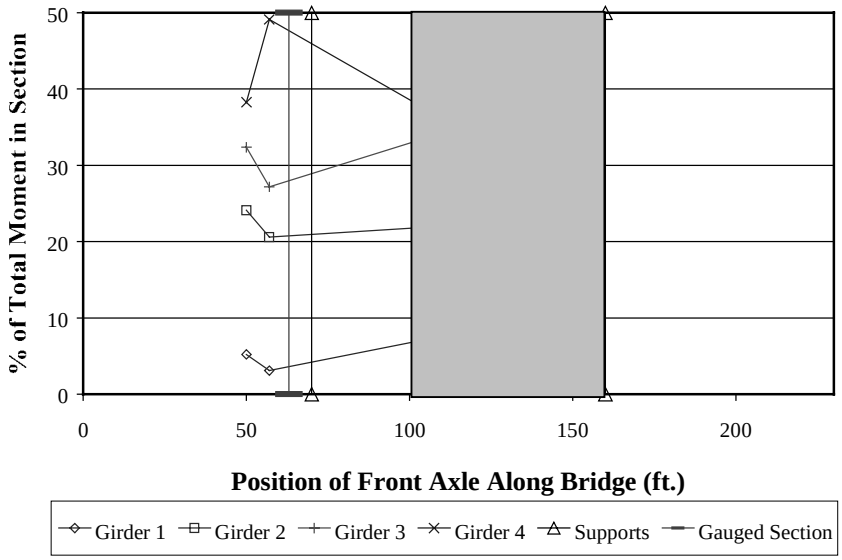

Figure 5.13: Measured moment distribution in the Support Section for Test D.T. 3-4a

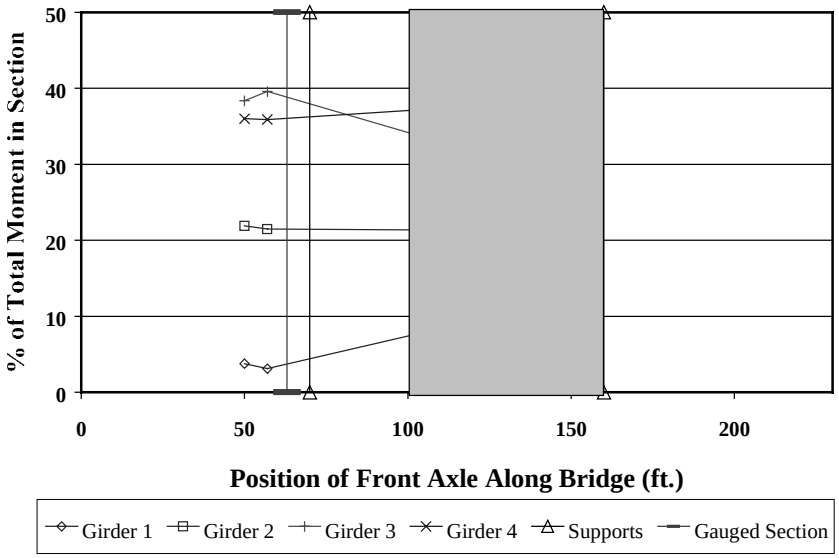

Figure 5.14: Moment distribution in the Support Section for BRUFEM EGM with diaphragms for Test D.T. 3-4a

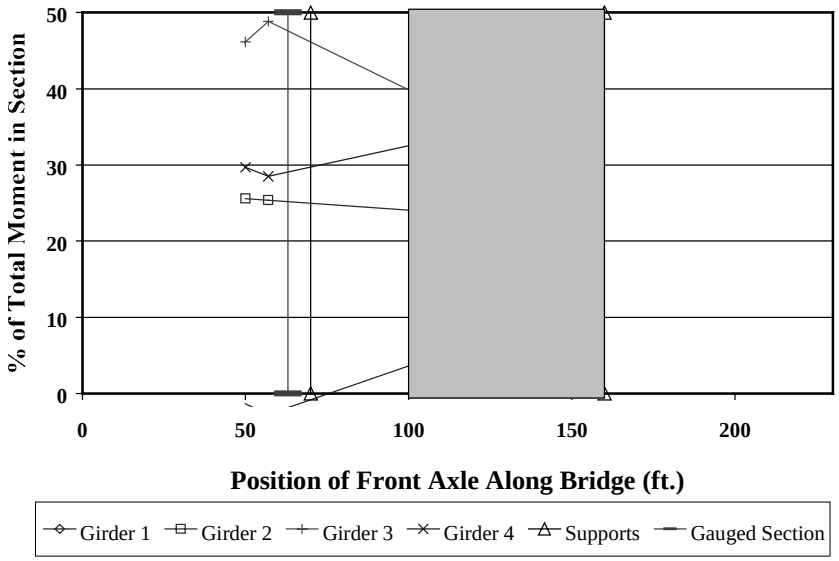

Figure 5.15: Moment distribution in the Support Section for BRUFEM EGM without diaphragms for Test D.T. 3-4a

Figures 5.13 through 5.15 appear very similar, especially in the shaded regions between 100' and 160', where the Support section experiences the largest negative moments from dump truck action (See Figure 2.3). This indicates that the presence of diaphragms in the BRUFEM model for the dump truck run does not cause much difference in the moments generated at the Support section. Some differences between the models with and without diaphragms can be perceived from Figures 5.16-5.18, which appear on the pages that follow.

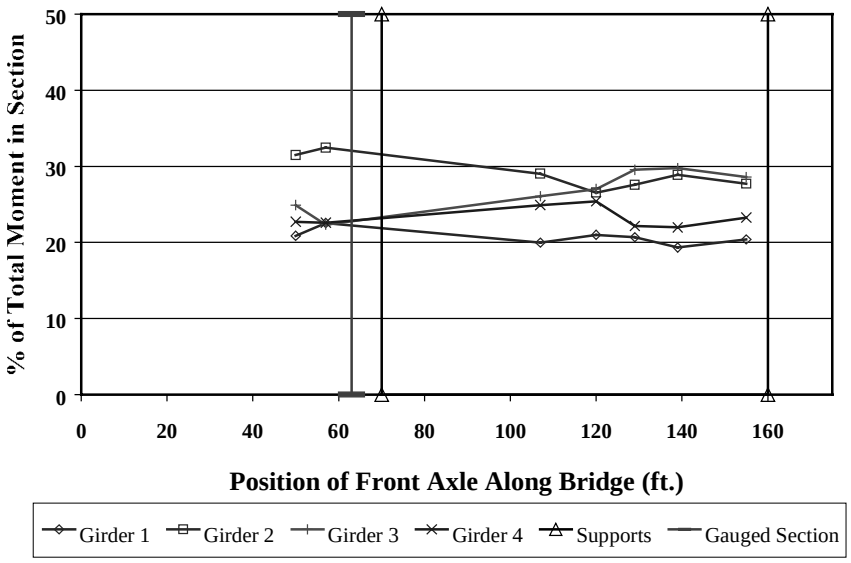

Figure 5.16: Measured moment distribution in the Support Section for HETS 1

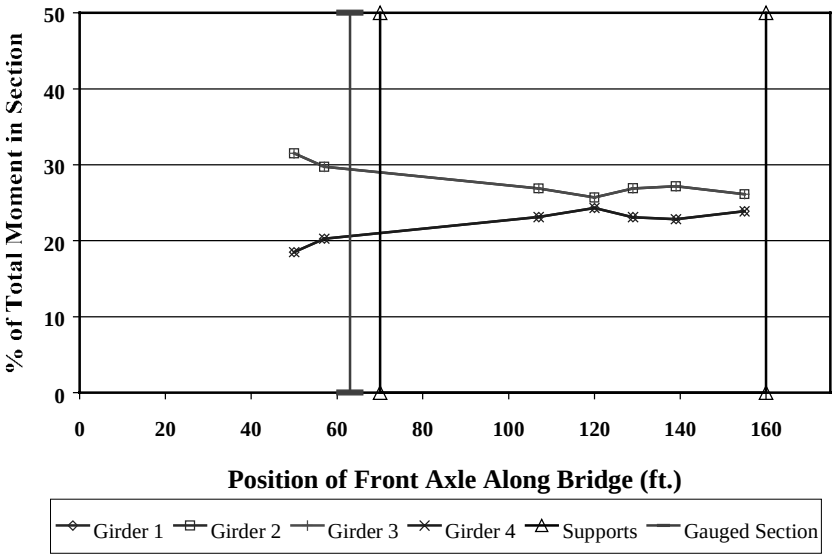

Figure 5.17: Moment distribution in the Support Section for BRUFEM EGM with diaphragms for HETS 1

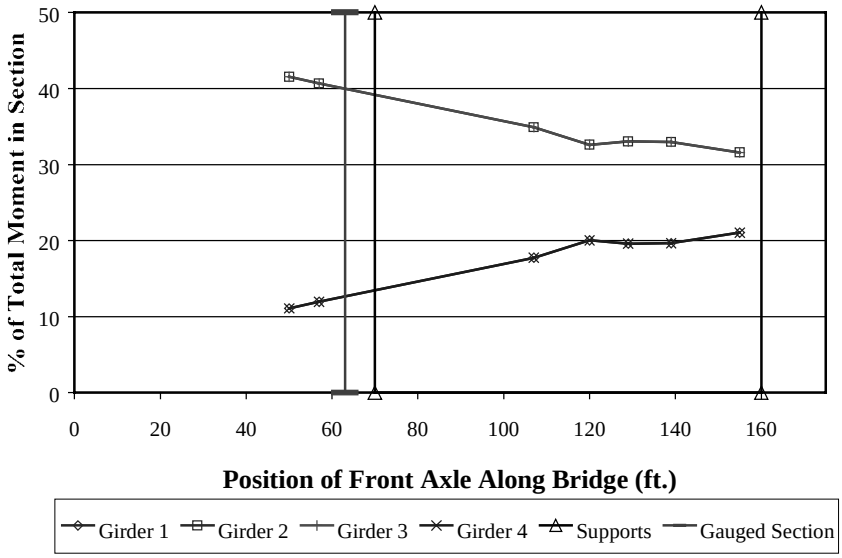

Figure 5.18: Moment distribution in the Support Section for BRUFEM EGM without diaphragms for HETS 1

The plots made using the EGM in the absence of diaphragms for the HETS example did not match the EGM with diaphragms or the actual data results very well. Figures 5.16 and 5.17 show rather equal moment distribution among all girders. Figure 5.18, shows a BRUFEM model without diaphragms and shows 60-80% of the load carried by the inner two girders. This kind of load distribution was not indicated by the test data given in Figure 5.16. When all the tests were considered, the factors from the EGM with diaphragms differed from the actual data by an average of 16% in the low-speed dump truck tests and by 10% for the low-speed HETS tests. The factors from the EGM without diaphragms differed by an average of 24% for dump truck tests and by 21% for the HETS tests. It was concluded that the diaphragms needed to be included in the BRUFEM model of the Leon River Bridge.

5.4 PRESENTATION OF MEASURED DATA AND BRUFEM ESTIMATES

The goal of this section is to compare the measured data to the estimates given from the BRUFEM CGM with diaphragms included. This section contains plots of moment distributions at each section for one example of each vehicle test. Two plots are presented on each page. The first was taken from an actual test run, and the second on the page was taken from the BRUFEM CGM data for the same vehicle and section.

5.4.1 Test D.T. 1-2b

Figures 5.19-5.24 contain data produced from test D.T. 1-2b. They were used to draw conclusions when compared with their respective BREUFEM counterparts. The outlined regions in Figures 5.19 and 5.21 show how the distribution in moment among all the girders at a section equalizes as the vehicle gets farther from the section. For example, the range in distribution factors for the front axle at 50', the left box in Figure 5.19, is 34% (42% for girder 1 and 8% for girder 4). When the vehicle is far from the gauge section, the range in factors was only 18% (36% in girder 1 and 18% in girder 4) as shown in the box on the right in Figure 5.19.

The outlined regions in Figures 5.23 and 5.24 show a good example of the similarities between the BRUFEM data and the acquired data. BRUFEM appears to model the change in moment distribution between girders well for the moment in the River Section. It is important to note that this behavior was

for uniform action in which the truck was always in the center span. Figures 5.19 to 5.24 are given on the pages that follow.

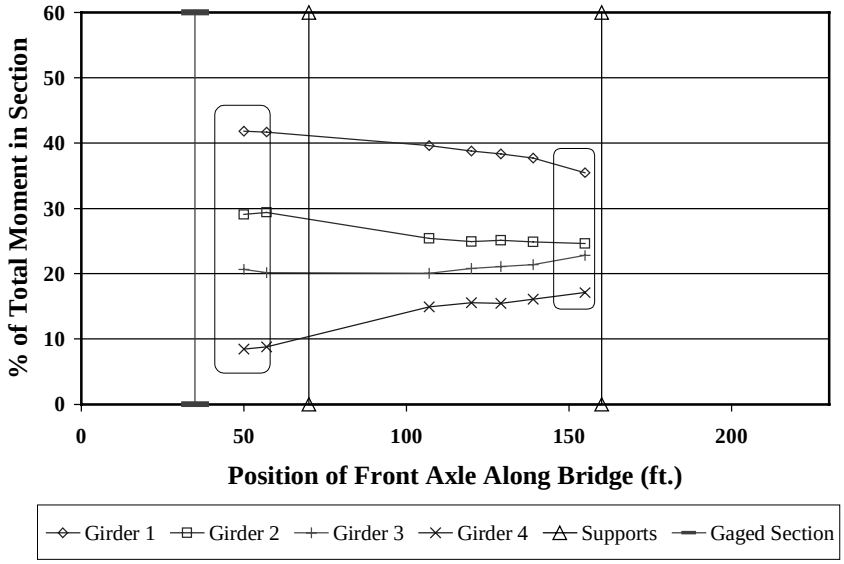

Figure 5.19: Measured distribution of moment in the Midspan Section for Test D.T. 1-2b

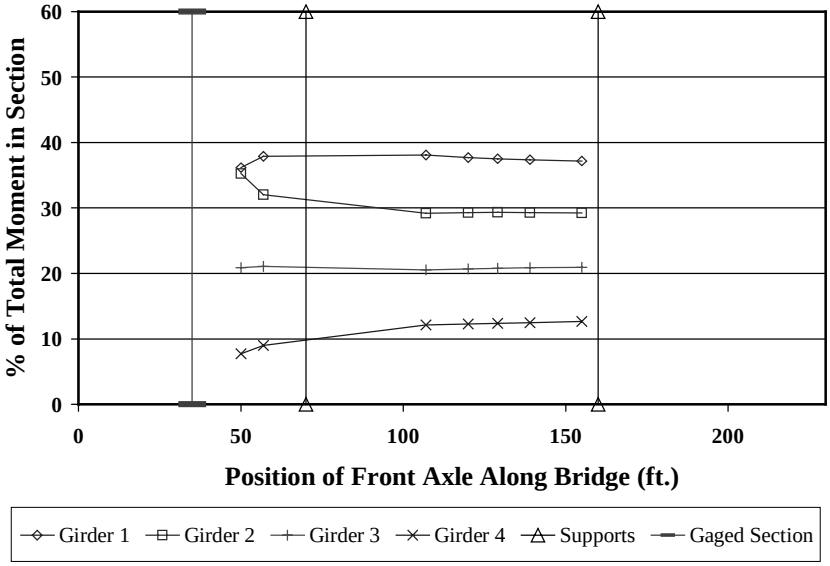

Figure 5.20: BRUFEM distribution of moment in the Midspan Section for Test D.T. 1-2b

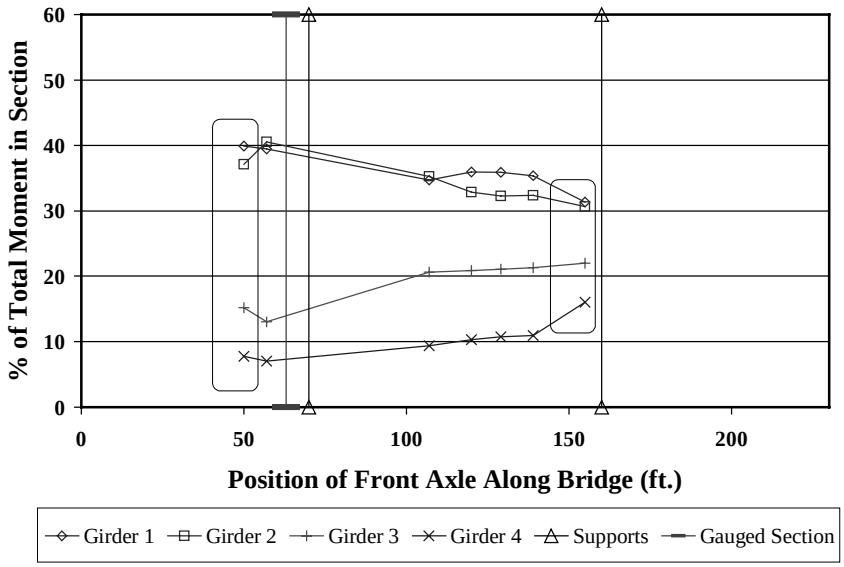

Figure 5.21: Measured distribution of moment in the Support Section for Test D.T. 1-2b

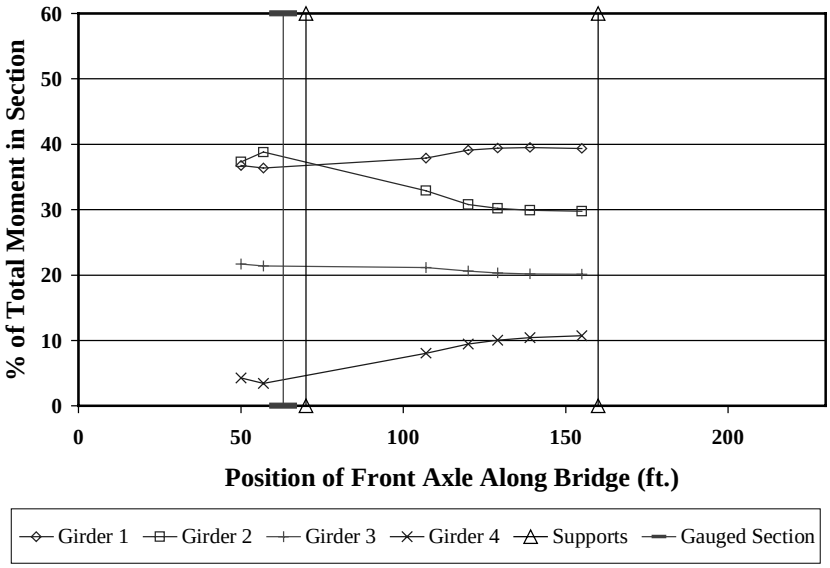

Figure 5.22: BRUFEM distribution of moment in the Support Section for Test D.T. 1-2b

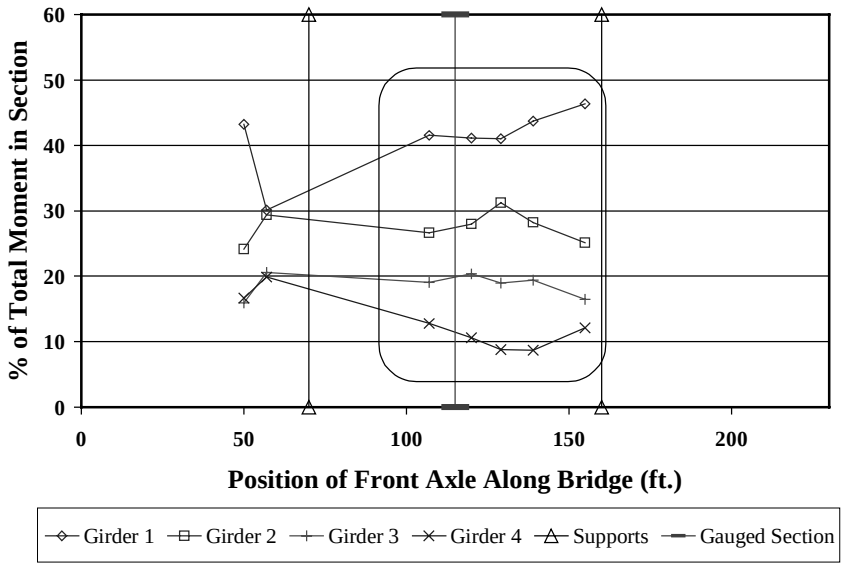

Figure 5.23: Measured distribution of moment in the River Section for Test D.T. 1-2b

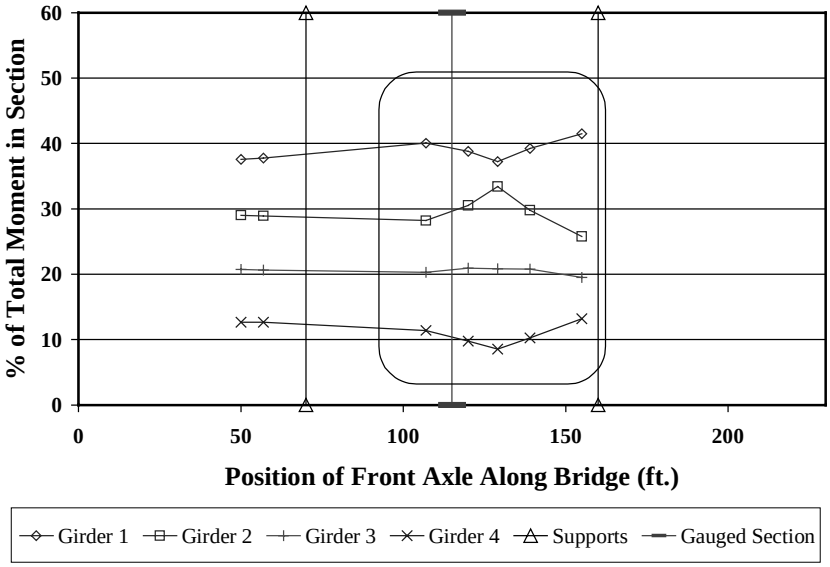

Figure 5.24: BRUFEM distribution of moment in the River Section for Test D.T. 1-2b

5.4.2 Test HETS 2

The next six figures give plots for the HETS 2 test in the same format as those given in Section 5.4.2. The distribution of load across the bridge section was more uniform since the HETS vehicle was aligned on the bridge centerline. Most LLDFs for all girders were bounded between 20% and 30%. Notice that the BRUFEM values for girders 1 and 4 and the values for girders 2 and 3 are equal due to this symmetry. The effect of load distribution with vehicle distance was not seen easily in these plots. These plots do show the good correlation between the acquired data and BRUFEM model data.

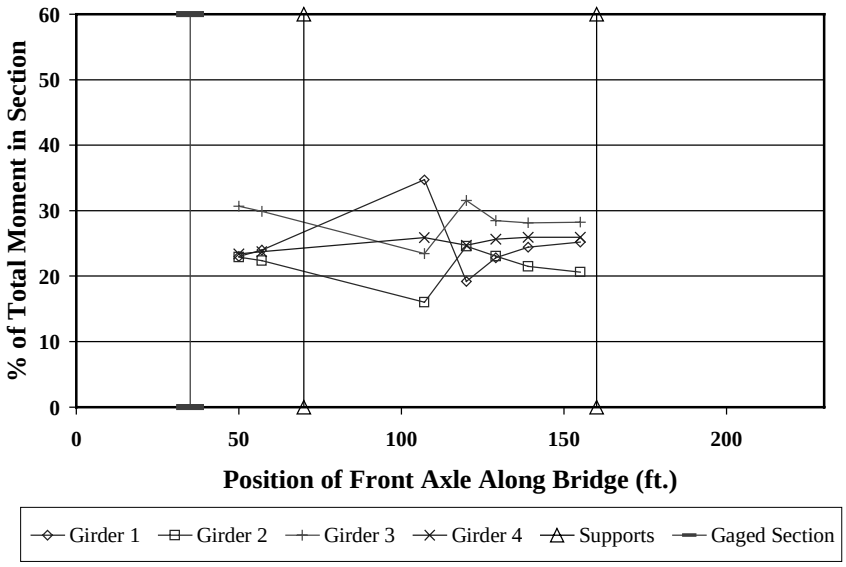

Figure 5.25: Measured distribution of moment in the Midspan Section for Test HETS 2

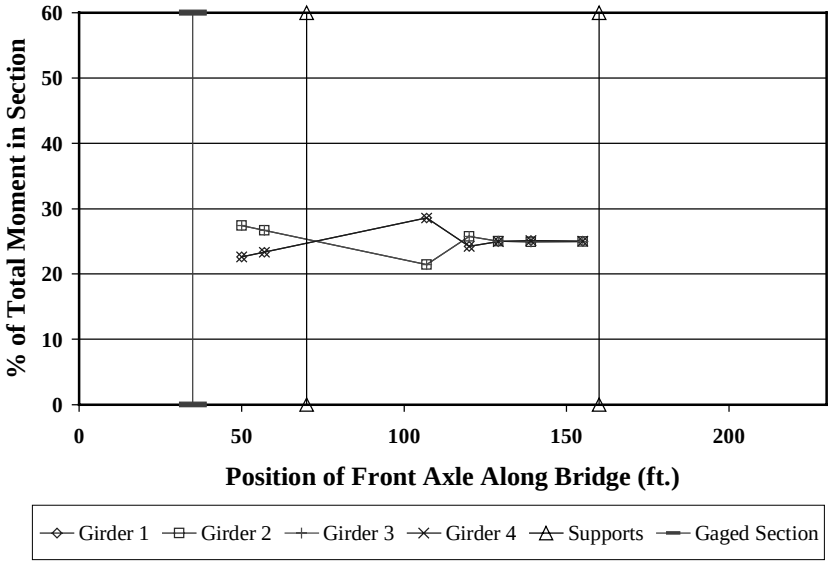

Figure 5.26: BRUFEM distribution of moment in the Midspan Section for Test HETS 2

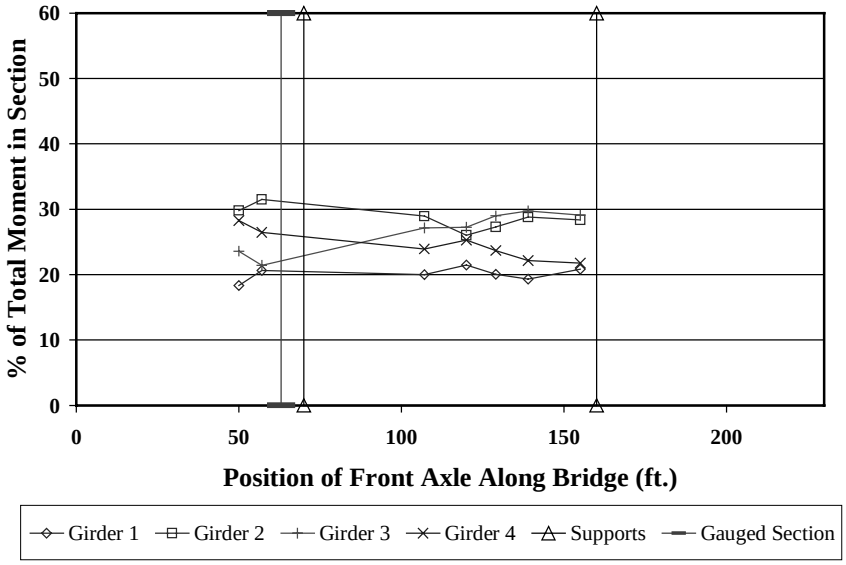

Figure 5.27: Measured distribution of moment in the Support Section for Test HETS 2

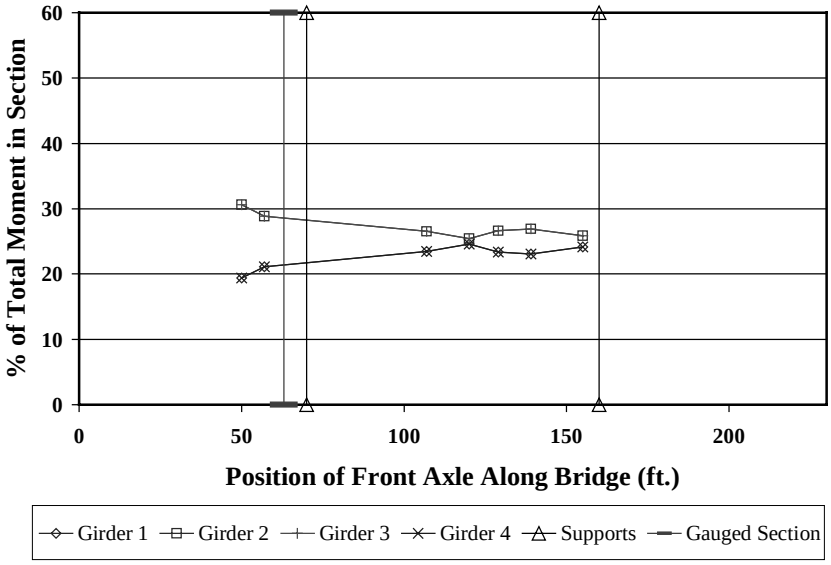

Figure 5.28: BRUFEM distribution of moment in the Support Section for Test HETS 2

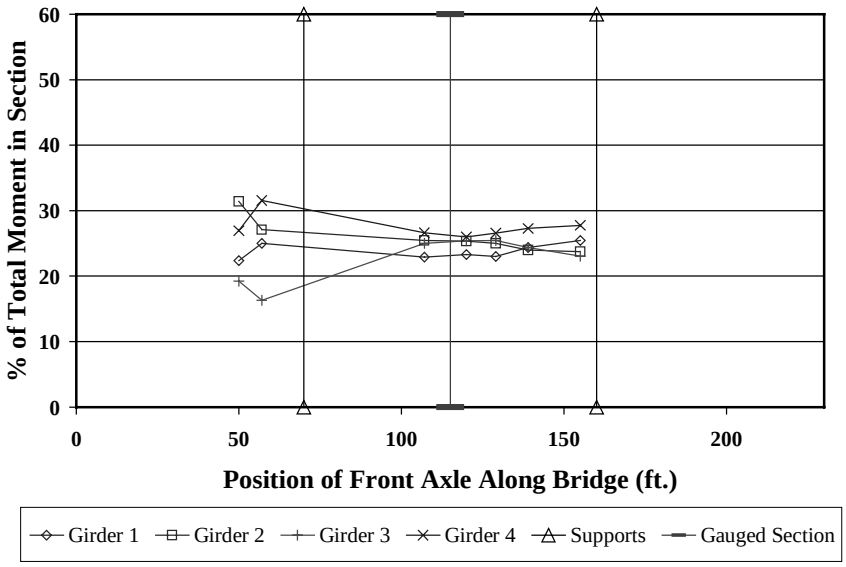

Figure 5.29: Measured distribution of moment in the River Section for Test HETS 2

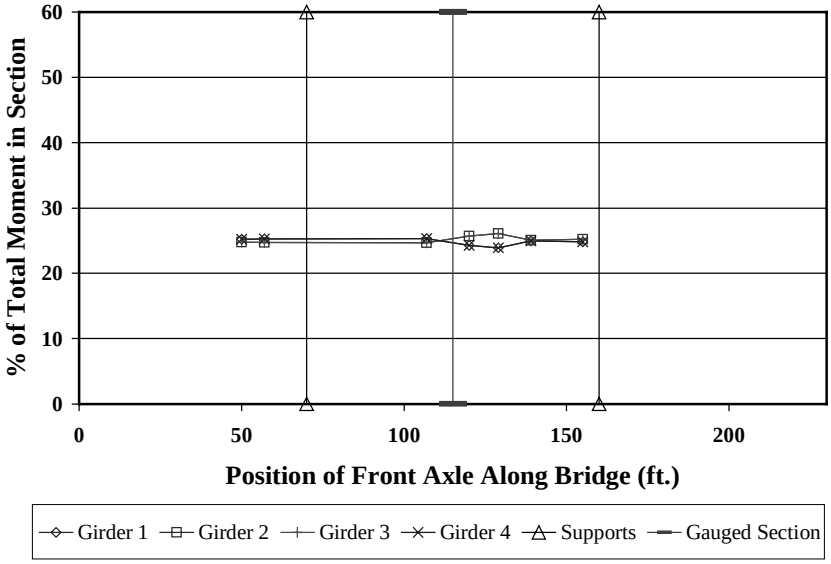

Figure 5.30: BRUFEM distribution of moment in the River Section for Test HETS 2

Overall, Figures 5.19-5.30 show very good correlation between the test data and BRUFEM predictions. The plots for dump truck action in Figures 5.19-5.24 show good results for the relationship between all four girders with a asymmetric loading. All the plots for the HETS shown in Figures 5.25-5.30 show fairly equal sharing of the load for the overweight vehicle on the center of the bridge.

CHAPTER 6: DESIGN LIVE LOAD DISTRIBUTION FACTORS

The acquired test data compared well with the output from BRUFEM. The next step was to compare the reduced data with the lateral load distribution factors found in the old AASHTO Working Stress Design (WSD) code and the new AASHTO LRFD code. Lateral load distribution factors for all sections were obtained for the vehicle positions of interest. The AASHTO LRFD design code contains a combination of empirical equations, approximate formulas, and special analysis techniques to determine live load distribution factors for use in design. The AASHTO WSD code contains a simpler equation for deriving LLDFs. These were utilized in order to see how well the design methods match what was obtained in the field.

6.1 METHOD FOR CALCULATING LLDFS

LLDFs from the test data and design codes were calculated in different ways. A single equation was used in the case of the actual data. Design LLDFs were found using a range of equations depending of the geometry and location of the girder. Also, the LLDFs from the test data were calculated only at the vehicle positions of interest, whereas the design LLDFs were applied to any vehicle location.

6.1.1 LLDFs from Test Data

Live load distribution factors were calculated from the data from all eight tests. The LLDFs were calculated using Equation 5.1 given previously in Section 5.2. Note that that method does not divide the moment in one girder by the line girder value at that section. Recall from the plots in Chapter 4 that fully composite behavior tended to over-estimate the predicted static response in regions of extreme strains. If the denominator of Equation 5.1 were replaced with the line girder value, the resulting LLDF would be increased. Although this would be conservative, Equation 5.1 was used to provide a consistent method of data reduction.

6.1.2 LLDFs from Design Codes

Some of the equations used to calculate LLDFs from the AASHTO design code include the effects of multiple vehicles on the bridge. In order to draw valid comparisons to the experimental LLDFs, some of the design equations needed to be modified. This was done to give the LLDF in terms of a single vehicle. These modification techniques are fully explained in McIlrath (1999) and were repeated in a succinct format in the appropriate following sections.

6.2 AASHTO LRFD LLDFS -INTERIOR GIRDERS

The AASHTO method for designing interior girders of a girder-slab bridge involves a single design equation that is not a function of vehicle location. This equation, referred to in Chapter 7 as the "Approximate Formula," modified for a single truck loading, is given in Equation 6.1.

$$LLDF = 0.06 + \left(\frac{S}{14}\right)^{0.4}\left(\frac{S}{L}\right)^{0.3}\left(\frac{K_G}{12.0Lt_S^3}\right)^{0.1}\left(\frac{1}{1.2}\right) \qquad (6.1)$$

where S = spacing of girders (ft.)

L = span length (ft.)

K_g = longitudinal stiffness parameter

t_s = thickness of the deck slab (in.)

$$K_G = n \cdot \left(I + Ae_g^2 \right) \tag{6.2}$$

where n = the modular ratio of steel to concrete = 7.25

I = moment of inertia of girder (in^4)

A = cross-sectional area of girder (in^2)

e_g = distance between the centers of gravity of the girder alone and deck slab alone (in.)

Equation 6.1 is valid for loading of one design lane in the category of bridges that includes the Leon River Bridge. This AASHTO equation has a built-in Multiple Presence Factor. The factor of (1/1.2) was applied to eliminate this effect and give a LLDF in terms of a single vehicle. The use of Equation 6.1 was only valid if the variables involved meet the range of applicability given in the AASHTO code. The bridge must have at least four girders and fulfill the other requirements given below.

$$3.5 \le S \le 16.0$$

$$20 \le L \le 240$$

$$4.5 \le t_s \le 12.0$$

$$10{,}000 \le K_G \le 7{,}000{,}000$$

The Leon River Bridge fulfilled all of these requirements.

The calculation of K_G can use *average* values for nonuniform cross sections. The K_G value for the W33x130 section included the area of the cover plates, since it was used for LLDF calculation in the negative moment region. The K_G value for the W33x141 included just the area of the W33x141 shape, since it was used for LLDF calculation in the center of the 90' span, the governing positive moment region. The values of Kg are calculated below.

$$K_G = 8 \cdot \left(6710 + (38.3 + 10.5) \cdot (19.55)^2 \right) = 202{,}892\, in^4 \qquad \text{(W33x130)}$$

$$K_G = 8 \cdot \left(7450 + (41.6) \cdot (19.65)^2 \right) = 188{,}102\, in^4 \qquad \text{(W33x141)}$$

Not only is K_G different depending on the section, the usable span length, L is also. The value of L can be taken as the average of two adjacent spans when considering a negative moment region near a support AASHTO (1998). In the calculation below, L for the negative moment region was taken as 80', the average of the adjacent span lengths.

$$LLDF = \left[0.06 + \left(\frac{6.67}{14} \right)^{0.4} \left(\frac{6.67}{80} \right)^{0.3} \left(\frac{202{,}892}{12.0 \cdot 80 \cdot (6)^3} \right)^{0.1} \right] \left(\frac{1}{1.2} \right) = 0.299$$

The AASHTO LRFD LLDF for interior girders in negative moment regions was 0.299. A similar calculation for the positive moment region using L = 90' and K_G = 188,102in^4 gave the AASHTO LRFD LLDF for interior girders in positive moment regions equal to 0.286.

6.3 AASHTO LRFD LLDFS - EXTERIOR GIRDERS

The Leon River Bridge is a zero-skew bridge with a cast-in-place deck on steel girders. AASHTO has three major methods for the design of the exterior girder for bridges of this type. The distribution of moment in the exterior girders is approximated by either the "lever rule," a method of rigid body analysis, or a factored version of the equation for interior girders.

6.3.1 Lever Rule

The lever rule is a method that uses statics alone to determine the distribution of load to the exterior girder of the bridge. The method assumes that a hinge is located at the next innermost girder. A summation of moments using this zero-moment location was used to determine the portion of the vehicle load, T, supported by the exterior girder. The reaction by the exterior girder was given as R. The value of R/T is the LLDF for the exterior girder. This was done for two different locations for each vehicle, the actual position and the AASHTO design case.

AASHTO requires that the vehicle be placed with its wheels no closer than 24" to the curb. This serves to give the largest and safest LLDF for design of exterior girders. The vehicle was also placed in the same lateral position that it was during the actual test. This does not give the worst possible LLDF, but was done to get a LLDF for comparison to the actual test data. The AASHTO and actual axle locations for the dump truck are shown in Figures 6.1 and 6.2. The AASHTO and actual axle locations for HETS are shown in Figures 6.3 and 6.4 respectively.

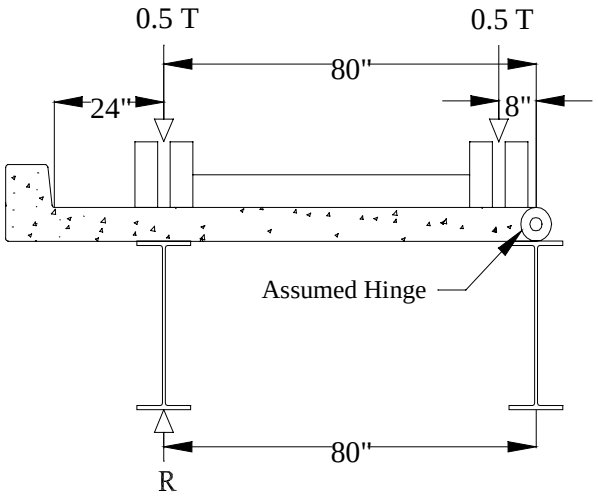

Figure 6.1: AASHTO lever rule dump truck position

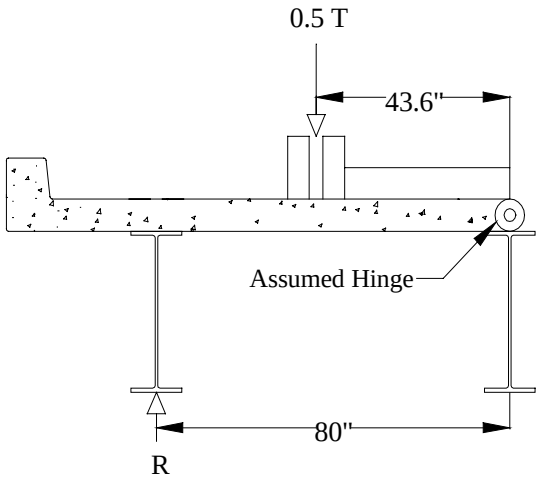

Figure 6.2: Actual dump truck lateral position

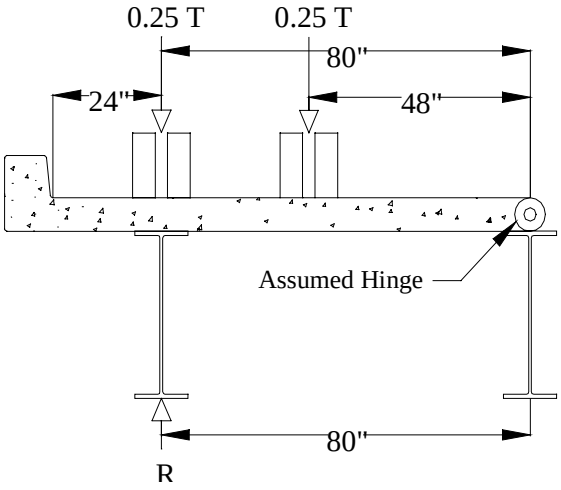

Figure 6.3: AASHTO lever rule HETS vehicle position

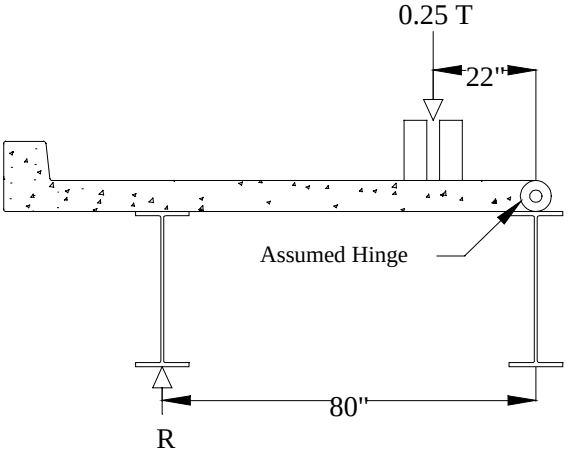

Figure 6.4: Actual HETS vehicle lateral position

The LLDFs for the vehicle positions shown in Figures 6.1 through 6.4 were found using a summation of moments about the assumed hinge location. For example, for Figure 6.1 the calculation is presented below.

$$\frac{1}{2}T(80)+\frac{1}{2}T(8)=R(80)$$

$$LLDF=\frac{R}{T} \quad \therefore \quad LLDF=\frac{44}{80}=0.55$$

No multiple-presence factors were included in these calculations. These values were compared to the largest LLDFs obtained for an exterior girder from the six slow test runs. The actual LLDFs and the design LLDFs for both vehicles and vehicle positions are given in Table 6.1.

Table 6.1: AASHTO LLDFs for exterior girders using the lever rule

Live Load Distribution Factor		
	Actual Position	AASTHO Position
3-Axle	0.273	0.550
HETS	0.069	0.400

Note that the AASHTO locations yielded much larger LLDFs than did the LLDFs for the actual vehicle positions. In the case of the HETS, the design vehicle location was not representative of the actual location. In practice, a vehicle as wide and as heavy as the HETS vehicle, would generally progress down the longitudinal center of the bridge. Thus, the AASHTO LLDF was conservative by a factor of 0.4/0.069 = 5.8 over the LLDF for the likely position of such an overweight vehicle.

6.3.2 Rigid Body Analysis

Another way AASHTO permits LLDF calculation for the exterior girders is by a rigid body analysis. In this method, the entire cross section is assumed to rotate about the longitudinal centerline of the bridge. The design vehicles were placed at the same design locations required by AASHTO (24" from the curb) and at the actual lateral locations used in the test runs. Equation 6.3 is the governing equation for this method.

$$LLDF=\frac{N_L}{N_b}+\frac{X_{ext}\sum_1^{N_L}e}{\sum_1^{N_b}x^2} \tag{6.3}$$

where N_L = number of loaded lanes under consideration

N_b = total number beams

e = eccentricity of a lane from the center of gravity of the pattern of girders (ft.)

x = horizontal distance from the center of gravity of the pattern of girders to each girder (ft.)

X_{ext} = horizontal distance from the center of gravity of the pattern of girders to the exterior girder (ft.)

The wheel locations and important dimensions for the dump truck and HETS loading are shown in Figures 6.5 through 6.8.

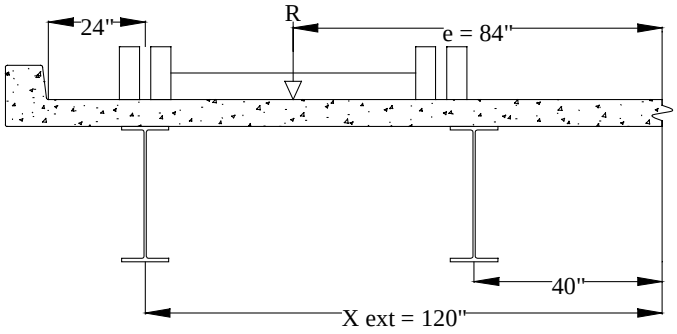

Figure 6.5: AASHTO dump truck position used in rigid body method

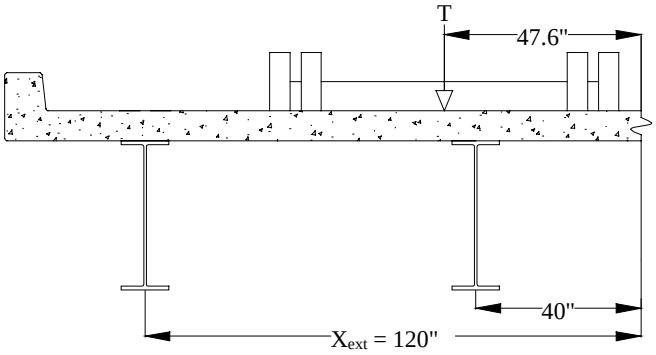

Figure 6.6: Actual dump truck position used in rigid body method

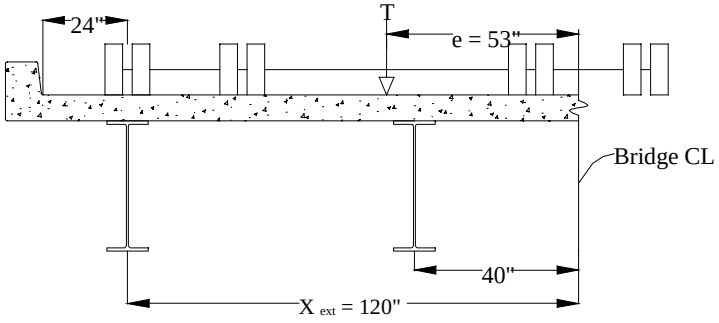

Figure 6.7: AASHTO HETS vehicle position used in rigid body method

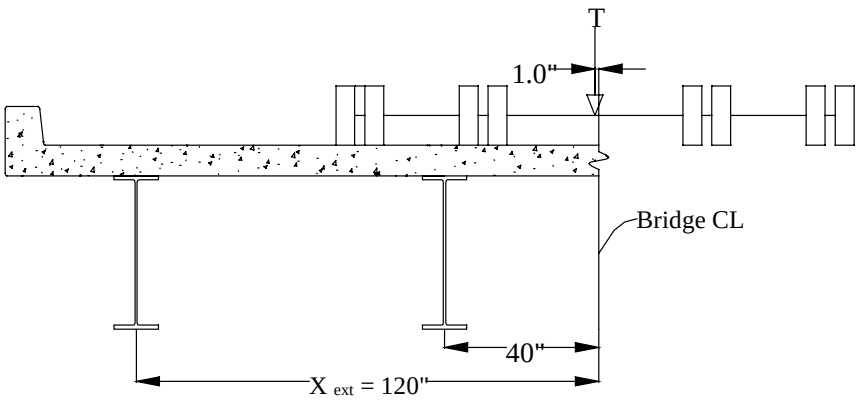

Figure 6.8: Actual HETS vehicle position used in rigid body method

The LLDF calculation proceeded as follows for the AASHTO position of the dump truck given in Figure 6.5.

$$LLDF = \frac{1}{4} + \frac{10 * \left| \frac{84}{12} \right|}{2 * \left[\left| \frac{40}{12} \right|^2 + \left| \frac{120}{12} \right|^2 \right]} = 0.565$$

Equation 6.3 was used to calculate all the other rigid body LLDFs for the exterior girders. Table 6.2 below gives these LLDFs.

Table 6.2: AASHTO LLDFs for exterior girders using rigid body analysis

Live Load Distribution Factor		
	Actual Position	AASTHO Position
3-Axle	0.429	0.565
HETS	0.254	0.449

The AASHTO LLDFs using rigid body analysis were still conservative by at least 30% over those for the actual position. They were not as conservative as the lever rule case because the calculation involves the vehicle position relative to the entire bridge cross section.

6.3.3 LRFD Exterior Girder Equation

The AASHTO method for design of exterior girders involves applying a correction factor, *e*, to the LLDF from the interior girder design as shown in Equation 6.4.

$$(LLDF)_{Interior} = e * (LLDF)_{Exterior} \tag{6.4}$$

The correction factor *e* is a function of d_e, which is the distance from the center of the exterior girder to the beginning of the curb. This correction factor is given in Equation 6.5.

$$e = 0.77 + \frac{d_e}{9.1} \geq 1.0 \tag{6.5}$$

where e = correction factor

d_e = the distance between the center of the exterior beam and the interior edge of the curb (ft)

Equation 6.6 is applicable only if d_e is between -1.0 and 5.5ft. The value of d_e for the Leon River Bridge from Figure 1.8 was 2ft. Therefore, the correction factor was 0.99 and taken as 1.0 according to Equation 6.5. In this case the LLDFs for the exterior girders are the same as those for the interior girders. The LLDF values were calculated in Section 6.2 and were 0.299 for negative moment regions and 0.286 for positive moment regions.

6.4 LLDFS FROM THE AASHTO WORKING STRESS DESIGN CODE

The empirical equations using the AASHTO LLDFs from the Working Stress Design code are simple. Depending on the number of lanes considered, either of two equations is used. Since a single truck load was used in the field tests, the equation for a single lane was used for comparison. Equation 6.6 from the AASHTO WSD specification is given below.

$$Wheel\ Load\ LLDF\left(One\ Design\ Lane\right) = \frac{S}{7} \tag{6.6}$$

where: S = girder spacing = 6.67ft

Equation 6.6 is in terms of wheel loads. Since the distribution factors given in this research were in terms of full vehicle loads, (in the same manner that the line girders were loaded with full axles), Equation 6.6 needed also to be given in terms of full axles. Therefore, a factor of 0.5 was applied to the above equation, which yielded Equation 6.7.

$$Truck\ Load\ LLDF\left(One\ Design\ Lane\right) = \frac{S}{14} \tag{6.7}$$

For the Leon River Bridge, S was equal to 6.67ft. Therefore the AASHTO WSD LLDF was 6.67/14 = 0.476. This factor only depends on the girder spacing, and therefore was valid in this research for both vehicles in positive and negative moment regions.

CHAPTER 7: COMPARISON OF LATERAL LOAD DISTRIBUTION FACTORS AND GIRDER MOMENTS

This chapter compares the LLDFs and design moments calculated from the field data, from the BRUFEM model, and from various design codes. Three criteria were used to organize the data. They were the type of load vehicle (dump truck or HETS), type of girder (interior or exterior), and moment region (negative or positive). A brief discussion of vehicle location is given before the LLDF data tables are presented. Trends in the LLDFs and design moments are summarized in the last section of this chapter.

7.1 LOCATIONS OF MAXIMUM STATIC RESPONSES

In Section 2.2.3 of this research, seven representative vehicle locations were selected. Six of those locations were chosen because they were close to extremes anticipated by the line girder analysis. However, the location of the vehicle that gives the maximum response may have been a few feet from the selected representative location. For example, one location for consideration was 139' when the absolute maximum response was given at 141' for the HETS. Small differences in distance were neglected, since none of the selected locations were farther than 4' from a location of expected maximum moment. Table 2.1 gave a summary of the extreme values of moment taken from the line girder plots of Chapter 2. All of the design LLDFs found in the next section were multiplied to the maximum moment values in Table 2.1 in order to obtain design moment values for comparison. For example, the maximum negative moment for the dump truck was -331k-ft. Applying the AASHTO lever rule LLDF of 0.550 gave a design moment of -331*0.55 = -182k-ft.

The dump truck values in Tables 7.5 and 7.7 contain two very different truck positions for maximum moment for repeated tests. There is a simple explanation for this. In the case of Table 7.5, the predicted static negative moments in the support section when the truck was at 107' and at 120' were -312k-ft and -325k-ft respectively. This is shown in Figure 2.4. Therefore, small changes in moment in the girders caused governing moments in Table 7.5 to come from either dump truck location. In the case of Table 7.7, Figures 2.3 and 2.5 show that the static moment in the Midspan section for the dump truck at 50' is only about 60k-ft from the value given at the River section for a dump truck location at 129' (535k-ft compared with 593k-ft). Small changes in distribution among girders caused some governing positive moments to come from either section.

7.2 COMPARISON OF ACTUAL AND DESIGN LLDFS AND MOMENTS

This section presents the results of all the LLDF calculations done throughout the course of this research. It also shows comparisons in terms of design moment. In the tables that follow, values from the measured data are given in the top portion. The values are averages from all the tests that involved the same vehicle and lateral location on the bridge. The analysis and design values are given in the lower portion. A moment value from design tools such as BRUFEM or AASHTO LRFD was shown in bold type when it was unconservative with respect to any test value in the same category.

In the following tables, five different entries are given for the AASHTO LRFD design code. In summary, Equations 6.1 and 6.4 gave the "Approximate Formula." The "Lever Rule" for both positions was described in Section 6.3.1. The "Rigid Body" method is described in Section 6.3.2. The AASHTO LRFD dictates that one would use the largest of these five values in design. The only AASHTO WSD entry was derived from Equation 6.7.

Recall that the notation for the vehicle tests was given in Table 1.2. The designation of D.T.1-2 signifies a dump truck test where the vehicle was located over girders 1 and 2 according to the notation presented in Figure 1.12. The suffixes "a" and "b" refer to either the first or second low speed test run. Average values for repeat dump truck runs using the same lateral location are given in the tables. The notation for the HETS test is simpler. A suffix of "1" or "2" indicate either the first or second low-speed test. The

notation "H.S." indicates a high-speed test down the center of the bridge for both test vehicles. A single average test value is given for HETS tests since the lateral location was the same in the HETS 1, HETS 2, and HETS H.S. tests.

Table 7.1: Moments and LLDFs for exterior girders in negative moment regions for dump truck tests

Test	Maximum Negative Moment (k-ft.)	LLDF at Negative Moment	Truck Position at Min. Design Moment (ft.)
D.T. 3-4 a&b	-136	0.372	120
D.T. 1-2 a&b	-126	0.364	120
BRUFEM	**-125**	0.383	120
LRFD:			
Approx. Formula	**-99**	0.299	116
Lever Rule (AASTHO)	-182	0.550	116
Lever Rule (Actual)	**-90**	0.273	116
Rigid Body (AASTHO)	-187	0.565	116
Rigid Body (Actual)	-142	0.429	116
WSD:			
AASTHO (S/7)	-157	0.476	116

Table 7.2: Moments and LLDFs for exterior girders in negative moment regions for HETS vehicle tests

Test	Maximum Negative Moment (k-ft.)	LLDF at Negative Moment	Truck Position at Min. Design Moment (ft.)
HETS 1,2, & H.S.	-142	0.224	139
BRUFEM	**-134**	0.225	139
LRFD:			
Approx. Formula	-178	0.299	141
Lever Rule (AASTHO)	-238	0.400	141
Lever Rule (Actual)	**-41**	0.069	141
Rigid Body (AASTHO)	-267	0.449	141
Rigid Body (Actual)	-151	0.254	141
WSD:			
AASTHO (S/7)	-284	0.476	141

Table 7.3: Moments and LLDFs for exterior girders in positive moment regions for dump truck tests

Test	Maximum Positive Moment (k-ft.)	LLDF at Positive Moment	Truck Position at Max. Design Moment (ft.)
D.T. 3-4 a&b	275	0.411	129
D.T. 1-2 a&b	253	0.413	129
BRUFEM	**218**	0.368	129
LRFD:			
Approx. Formula	**170**	0.286	129
Lever Rule (AASTHO)	326	0.550	129
Lever Rule (Actual)	**162**	0.273	129
Rigid Body (AASTHO)	335	0.565	129
Rigid Body (Actual)	**254**	0.429	129
WSD:			
AASTHO (S/7)	282	0.476	129

Table 7.4: Moments and LLDFs for exterior girders in positive moment regions for HETS vehicle tests

Test	Maximum Positive Moment (k-ft.)	LLDF at Positive Moment	Truck Position at Max. Design Moment (ft.)
HETS 1,2, & H.S.	244	0.278	155
BRUFEM	**197**	0.247	155
LRFD:			
Approx. Formula	**230**	0.286	153
Lever Rule (AASTHO)	321	0.400	153
Lever Rule (Actual)	**55**	0.069	153
Rigid Body (AASTHO)	361	0.449	153
Rigid Body (Actual)	**204**	0.254	153
WSD:			
AASTHO (S/7)	382	0.476	153

Table 7.5: Moments and LLDFs for interior girders in negative moment regions for dump truck tests

Test	Maximum Negative Moment (k-ft.)	LLDF at Negative Moment	Truck Position at Min. Design Moment (ft.)
D.T. 3-4 a&b	-121	0.349	107
D.T. 1-2 a&b	-115	0.345	107
BRUFEM	**-102**	0.328	107
LRFD Approx. Formula	**-99**	0.299	116
WSD AASHTO (S/7)	-157	0.476	116

Table 7.6: Moments and LLDFs for interior girders in negative moment regions for HETS vehicle tests

Test	Maximum Negative Moment (k-ft.)	LLDF at Negative Moment	Truck Position at Min. Design Moment (ft.)
HETS 1,2, & H.S.	-189	0.295	139
BRUFEM	**-159**	0.268	139
LRFD Approx. Formula	**-178**	0.299	141
WSD AASHTO (S/7)	-284	0.476	141

Table 7.7: Moments and LLDFs for interior girders in positive moment regions for dump truck tests

Test	Maximum Positive Moment (k-ft.)	LLDF at Positive Moment	Truck Position at Max. Design Moment (ft.)
D.T. 3-4 a&b	223	0.393	50
D.T. 1-2 a&b	198	0.324	129
BRUFEM	**200**	0.337	129
LRFD Approx. Formula	**170**	0.286	129
WSD AASHTO (S/7)	282	0.476	129

Table 7.8: Moments and LLDFs for interior girders in positive moment regions for HETS vehicle tests

Test	Maximum Positive Moment (k-ft.)	LLDF at Positive Moment	Truck Position at Max. Design Moment (ft.)
HETS 1,2, & H.S.	214	0.245	139
BRUFEM	**203**	0.255	155
LRFD Approx. Formula	230	0.286	153
WSD AASHTO (S/7)	382	0.476	153

7.3 OBSERVATIONS ON LLDFS AND DESIGN MOMENTS

Many observations were made based on the results tabulated in Section 7.2. There were noticeable patterns in the repeated test runs and the design and analysis values. Some of these trends were valid for all tests concerning all girders in all regions of moment action. Some showed certain behavior only for certain combinations. This section will summarize trends among the test data, BRUFEM output, and design values.

7.3.1 Trends in Measured Values

A few significant trends could be seen in the tables given in Section 7.2. The most striking observation initially made was that the maximum positive girder moments measured from the HETS vehicle were about the same as those measured from the dump truck. For example, in the case of exterior girders in negative moment regions (Tables 7.1 and 7.2) the governing moments for both vehicles fell within the 120-140k-ft range for tests at low-speed. Only the negative moments found in Tables 7.5 and 7.6 did not follow this trend. Other patterns noticed for each vehicle are cited in this section.

7.3.1.1 Dump Truck Tests

The values of moment and lateral load distribution factors for all the dump truck tests were close to each other in value. This indicated very repeatable data for the low-speed tests. The values from all the low-speed dump truck tests could be compared even though the truck was run in two different locations. Recall that the D.T. 1-2 tests and D.T. 3-4 tests were symmetric about the bridge centerline. Therefore, where girders 1 or 2 gave the maximum moments in the D.T. 1-2 tests, girders 3and 4 gave maximum moments for the D.T. 3-4 tests.

The maximum range of governing moments before an average was made was 36k-ft for interior girders and was 34k-ft. for the exterior girders. The range was large due to the behavior of the bridge under two different lateral locations of the vehicle. The maximum range was within 20% of the average moments measured. The corresponding LLDF values for all the slow tests were also similar to each other in value.

The high-speed dump truck test did not have the same lateral position as the other 4 dump truck tests. This was reflected in the values for the D.T.H.S. test. The LLDFs for the high-speed test were not as great since the vehicle was traveling down the center of the bridge. The governing moments could have been smaller for the high-speed test because the distribution of moment had a greater effect than did the impact of the vehicle.

7.3.1.2 HETS Vehicle Tests

The HETS test exhibited the highest degree of repeatability and did show evidence of dynamic effects. In general, the data from the HETS H.S. test matched well with its low-speed counterparts since the lateral location of the vehicle was the same in both tests. The maximum difference before averaging between any governing moments for HETS tests was 13k-ft (approximately 6% of the measured moments). Some evidence of dynamic effects was seen in all HETS moments except for the exterior girder in positive moment regions. However, the presentation of moments in each gauged section given in Section 4.3.2 shows better evidence of dynamic effects.

7.3.2 Comparison of BRUFEM Values

In general, the BRUFEM LLDF values did a satisfactory job approximating the LLDFs from the vehicle tests. BRUFEM LLDFs were greater than 8 of 16 average test values. However, the BRUFEM *moments* underestimated the actual moments from tests in 13 of the 16 cases. This phenomenon may have been caused more by the conservative nature of Fully Composite method to estimate the girder moments than an unconservative BRUFEM analysis.

7.3.3 Comparison of Design Values

The design methods used to estimate moments each have their own variables and degree of safety. The AASHTO Working Stress Design Code contains the least variables, and generally ends up being the most conservative way to distribute moment laterally. The newer AASHTO LRFD equations contain the most variables of any used in this research and attempt to more accurately model bridge behavior. This section cites the performance of all the design estimates with respect to the measured values.

7.3.3.1 AASHTO Working Stress Design

It was expected that the values given by the Working Stress Design code would be the most conservative. This was due in part to the location of the test truck. The dump truck was not located in the position that would give the largest moments on the exterior girder. The moment and LLDF values given by AASHTO WSD were the most conservative of all the design values with the exception of the lever rule for the AASHTO position of the dump truck. On average, AASHTO WSD moments were conservative by a factor of 1.3 for all the dump truck cases and by a factor of 1.7 for the HETS cases. It was notable

that the WSD value matched the values for the dump truck 3-4 tests in Table 7.3 within 7k-ft even though the dump truck was not as close to the curb as the AASHTO position dictates.

7.3.3.2 AASHTO LRFD Lever Rule and Rigid Body Analysis

The exterior girder methods gave different results depending on whether an AASHTO or actual position was considered. It is important to note that all of the lever rule values for the actual position gave unconservative values. The rigid body values for exterior girders using actual vehicle positions were unconservative as well. All of the lever rule and rigid body values for the AASHTO positions were conservative, which should have been expected since the dump truck was not in the AASHTO position during the test. The lever rule values of moment were conservative by a factor of 1.4 for the dump truck and 1.5 for the HETS. The rigid body analysis values were conservative by a factor of 1.4 for the dump truck and 1.7 for the HETS.

7.3.3.3 AASHTO Load and Resistance Factor Design

The LRFD equation gave unconservative values for moment in all cases involving the dump truck and for half of those involving the HETS. When the LRFD moment was unconservative, it was so by 24% on average. When conservative, the reduced moments were about 86% of what the LRFD equation predicted. The AASHTO LRFD LLDFs for the interior girders were closer to the measured values than were the AASHTO estimates for the exterior girders. This was due to the correction factor, *e*, in Equation 6.4. The correction factor was not greater than 1.0 and did not result in larger design moments for the exterior girders. Again, if a more accurate reduction method were used, it was believed that the LRFD moment values would fit quite well with the test values. Recall, that Section 4.3.1 stated that the Fully Composite reduction method was conservative by about 7.5% in regions of extreme moment.

7.4 MOMENT RANGES

The lateral load distribution factors reduced and summarized in this chapter were not only used to compare LLDF values and girder moments. The data was also used to investigate moment ranges. Calculation of moment ranges is done to estimate the potential for fatigue problems in a bridge. The results of this investigation are provided in the tables at the end of this section.

The design moment ranges for a girder were calculated using the LLDFs determined from the design codes and the maximum positive and negative static moments in the bridge. The LLDFs from the design codes do not account for the location of the vehicle relative to the section when a maximum effect occurs. In some cases, the location of the vehicle that gives the maximum moment range is far from the section considered. Therefore, it would be appropriate to use a LLDF that takes into consideration where the vehicle is longitudinally.

Section 5.1.2 shows the redistribution of moment among girders with increased vehicle distance. The actual girder moments and LLDFs were known for all of the seven representative vehicle locations for both the test data and the BRUFEM analysis. Figure 7.1 shows a moment history from test D.T. 3-4a for an exterior and interior girder. The two vehicle positions that cause the maximum positive and negative moment in those girders for the Midspan action show are 50’ and 120’ respectively. The moment range taken for each girder is the difference between the moments at each of these locations. Both ranges are shown on the plot.

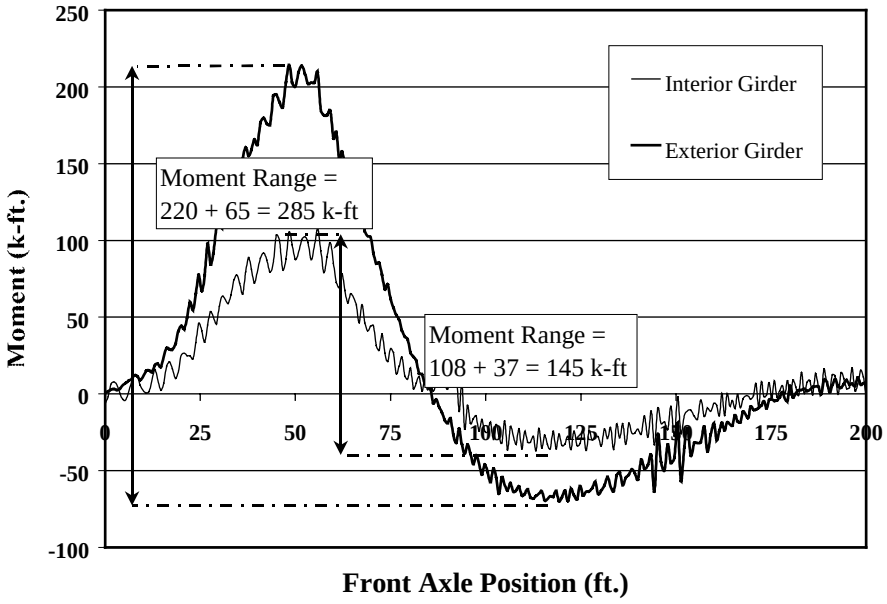

Figure 7.1: Example of girder moment ranges from test D.T. 3-4a

A moment range for a girder was calculated from the actual girder moments found in computer estimates and field tests and was found to be different than the design moment ranges.

7.4.1 Explanation of Moment Range Tables

Tables 7.9-7.12 show moment ranges for girders in the Midspan section for the HETS vehicle and girders in all three sections for the dump truck. Average values from the two low-speed HETS and from all four low-speed dump truck tests were considered. The table first gives the vehicle locations that cause the maximum positive and negative total moments. Notice that the one location is generally close to where the instrumentation was and the other is some distance from it. The next column gives the unfactored moment range in the section. These values are equal to the difference in maximum and minimum moments for all the design methods and field tests.

The fourth and sixth columns give two LLDF values. The first is the governing LLDF in the section for the first truck location; the second LLDF is the value that governs at the second truck position. Except for BRUFEM estimates and field tests, these values are the same for both vehicle locations. Treatment of exterior and interior girders is handled in separate columns. The fifth and seventh columns give the factored moment range for the governing girder. This value is either the product of the design LLDFs and the line girder moments or an actual moment range found in the BRUFEM output or vehicle test data.

For example, Table 7.9 shows values for the Midspan section for dump truck loading. Recall that the Midspan section was located 35’ from the beginning of the bridge. The second column shows that the maximum positive effect in the cross section occurred when the dump truck was at 50’ (close to the section of interest). It also shows that the maximum negative effect in the cross section occurred when the dump truck was at 120’ (far from the section). The line girder values taken from Figure 2.2 are 535k-ft at 50’ and -181k-ft at 120’. This gives an total moment range of 535 - (-181) = 716k-ft. The BRUFEM and field test ranges were obtained directly from computer output and reduced data at the same vehicle locations.

Considering the BRUFEM method in Table 7.9, the average LLDF for interior girders when the truck was at 50’ was 0.35. The factor was only 0.29 when the truck was at 120’. It is important to note that these LLDFs were calculated from moments estimated by BRUFEM and moments reduced from the field data

using the Fully Composite Method. The LLDFs are given only to compare with the design LLDFs from AASHTO, which do not change with vehicle position.

The factored moment ranges for the BRUFEM method are the actual range of moment experience by a single exterior or interior girder. In the case of Table 7.9, the maximum positive moment in an exterior girder for the truck at 50' was 196k-ft. The maximum negative moment in the same exterior girder occurred when the truck was at 120' and was equal to –67k-ft. This indicated a moment range estimated by BRUFEM of 196 + 67 = 263k-ft, which appears in the last column.

7.4.2 Presentation of Moment Range Tables

Tables 7.9-7.12 show moment ranges obtained using four different methods. This was done to show how the design, analysis, and field-testing methods compare in the estimation of moment ranges. The older AASHTO WSD code is represented as "S/7" in Tables 7.9-7.12. For the entries labeled "LRFD," the LLDF given is the largest of the "Approximate Formula," "Lever Rule," or "Rigid Body" methods, whichever is appropriate for the girder and section considered.

Table 7.9: Moment ranges in the Midspan Section found in girders from dump truck action

Method	Vehicle Locations for Maximum Positive and Negative Moment (ft.)	Total Bridge Moment Range (k-ft.)	Interior Girder		Exterior Girder	
			LLDFs at Both Locations	Moment Range for Girder (k-ft.)	LLDFs at Both Locations	Moment Range for Girder (k-ft.)
S/7	50 / 120	716	0.48 / 0.48	341	0.48 / 0.48	341
LRFD	50 / 120	716	0.29 / 0.29	205	0.57 / 0.57	405
BRUFEM	50 / 120	721	0.35 / 0.29	243	0.36 / 0.38	263
Field Test	50 / 120	739	0.34 / 0.28	245	0.40 / 0.38	292

Table 7.10: Moment ranges in the Support Section found in girders from dump truck action

Method	Vehicle Locations for Maximum Positive and Negative Moment (ft.)	Total Bridge Moment Range (k-ft.)	Interior Girder		Exterior Girder	
			LLDFs at Both Locations	Moment Range for Girder (k-ft.)	LLDFs at Both Locations	Moment Range for Girder (k-ft.)
S/7	200 / 120	405	0.48 / 0.48	193	0.48 / 0.48	193
LRFD	200 / 120	405	0.30 / 0.30	121	0.57 / 0.57	229
BRUFEM	200 / 120	398	0.30 / 0.31	122	0.38 / 0.39	155
Field Test	200 / 120	407	0.35 / 0.33	142	0.33 / 0.37	145

Table 7.11: Moment ranges in the River Section found in girders from dump truck action

Method	Vehicle Locations for Maximum Positive and Negative Moment (ft.)	Total Bridge Moment Range (k-ft.)	Interior Girder		Exterior Girder	
			LLDFs at Both Locations	Moment Range for Girder (k-ft.)	LLDFs at Both Locations	Moment Range for Girder (k-ft.)
S/7	129 / 57	699	0.48 / 0.48	333	0.48 / 0.48	333
LRFD	129 / 57	699	0.29 / 0.29	200	0.45 / 0.45	314
BRUFEM	129 / 57	699	0.33 / 0.29	229	0.37 / 0.38	261
Field Test	129 / 57	727	0.32 / 0.26	224	0.41 / 0.39	297

Table 7.12: Moment ranges in the Midspan Section found in girders from HETS vehicle action

Method	Vehicle Locations for Maximum Positive and Negative Moment (ft.)	Total Bridge Moment Range (k-ft.)	Interior Girder		Exterior Girder	
			LLDFs at Both Locations	Moment Range for Girder (k-ft.)	LLDFs at Both Locations	Moment Range for Girder (k-ft.)
S/7	57 / 139	976	0.48 / 0.48	465	0.48 / 0.48	465
LRFD	57 / 139	976	0.29 / 0.29	279	0.45 / 0.45	438
BRUFEM	57 / 139	981	0.27 / 0.25	256	0.23 / 0.25	234
Field Test	57 / 139	1013	0.30 / 0.28	297	0.24 / 0.26	250

7.4.3 Observations on Moment Ranges

Some observations were made based on Tables 7.9-7.12. They concern the moment ranges and the methods used to calculate them. This section will present the trends and generalizations that were made based on the results of the investigation into the range of moments for the girders of the Leon River Bridge. In general, although the moment ranges for all 4 cases were very close in value, the different methods gave a broad range of moment ranges for individual girders.

The ranges given by the S/7 method were the largest value in 6 of 8 cases. This was expected because the AASHTO WSD method is very conservative and contains simple LLDFs that do not account for vehicle position. The AASHTO LRFD LLDFs were also the same for all vehicle locations and were conservative in some areas as well.

The LLDFs used to determine the AASHTO LRFD moment ranges were different for interior and exterior girders. The governing LLDF was used in each case. This meant that the LRFD LLDF was used for the interior girders and that the rigid body LLDF was used for exterior girders. The AASHTO LRFD ranges for exterior girders were always larger than the BRUFEM and field-test ranges. No such trend existed for the LRFD design ranges for interior girders with respect to BRUFEM.

The BRUFEM estimates were significantly less than all WSD S/7 estimates and LRFD estimates for exterior girders. On average, the BRUFEM ranges were 33% lower than the WSD S/7 and LRFD design ranges. The BRUFEM estimates were, on average, smaller that the field measurements indicated. The values from field measurements were only 6.4% greater than the BRUFEM values on average. Recall from the end of Section 4.3.1 that the Fully Composite Method of reducing the field data was considered to be conservative by 7.5% on average with respect to line girder moments. The field measurements were smaller than all the design ranges except for the AASHTO LRFD ranges for interior girders. On average, the AASHTO LRFD and WSD exterior girder ranges were conservative with respect to the field test ranges by a factor of 1.4 in both cases.

CHAPTER 8: CONCLUSIONS AND RECOMMENDATIONS

This research was successful in investigating the distribution of moment laterally across the Leon River Bridge. It was also successful in investigating design methods, dynamic effects, and moment ranges in girders. Key elements in the completion of this research were testing the bridge in the field and modeling it using SAP2000 and BRUFEM. In general, BRUFEM predicted moment and behavior that were very close to measured values. The results of both field-testing and BRUFEM modeling showed the lateral distribution of moment and how that distribution was related to longitudinal vehicle position. The primary use of the measured LLDFs was for comparison against LLDFs from various design codes. The design values were conservative in most cases.

8.1 SUMMARY OF FINDINGS

There were a few observations made throughout the course of this research that are significant enough to repeat here. The first point that should be made is that the Leon River Bridge, although designed for noncomposite action, did not behave noncompositely. The calculated N.A. locations and the results of the Fully Composite Method of data reduction indicate some degree of composite action. Other points made in this section cover the quality of the methods used in this research, the repeatability and behavior found in the field tests, and trends found in the LLDFs and moment ranges.

8.1.1 Moment Reduction Method

The Fully Composite Method used to reduce the data was chosen for two reasons. First of all, the method recognized that the neutral axes of the girders were such that some composite action was present. The method gave the best estimate of moment values in regions of high strains. The other methods used gave values that indicated that some moment was unaccounted for in the cross-section. The method chosen was conservative in this respect and possibly gave values that would make the LRFD and BRUFEM values appear unconservative. The second reason why this method was chosen was its simplicity. Classical equations and basic spreadsheets were all the tools required to reduce the acquired strains into moments. A method of "partial composite action" is outlined in Jauregui (1999) but was not used in this research.

8.1.2 Repeatability

The range in values obtained from all tests was remarkably small. This indicated that the Leon River Bridge responded in a similar manner throughout all the tests. This also signifies that that procedure used to instrument and test the bridge was an acceptable method that gave accurate output. The data acquisition system used for this research was well designed. It also shows that the person using the manual switch, the driver of the vehicle, and the person running the data acquisition system practiced good communication skills throughout all the tests.

8.1.3 Dynamic Effects

Conclusions on dynamic effects could only be made from the series of HETS tests. Although additional vibration and oscillations were present in the high-speed HETS test, the filtered results showed an increase in moment response due to dynamic effects. Dynamic effects were most prevalent in the individual girder values and present to a lesser effect in total moment at a section. According to Tables 4.3 and 4.4, the average dynamic increase was 24% in *individual* girders and 13% for *total* moment at a section. This data fit well with the results of field tests used by AASHTO to determine impact factors. Section 3.6.2 of the AASHTO code indicates that the dynamic load allowance (IM) was based on dynamic truck effects that cause increases of 25%.

8.1.4 Moment Distribution as a Function of Distance

Figures 5.4 through 5.9 in Chapter 5 depict the change in moment distribution as a function of vehicle position. It was concluded that the girders that take the majority of the load in primary moment action, still support the majority of the load when the vehicle moved away onto an adjacent span. However the range between moment percentages became smaller as vehicle distance increased. BRUFEM performed well in estimating the LLDFs as a function of distance.

This was significant because the stress range a girder experienced was reduced because of this change in distribution. Section 7.4 showed how moment ranges from the AASHTO LRFD and WSD methods were conservative with respect to the BRUFEM estimates and field tests. The field tests were on average only 6.4% greater than the BRUFEM estimates. This was notable especially because the field tests were believed to be conservative by 7.5% in extreme moment action.

8.1.5 Trends in Lateral Load Distribution Factors

Overall, the tests gave results with a high level of repeatability and confidence. The BRUFEM and AASHTO LRFD LLDFs fit the test data reasonably well since the reduction method was considered conservative in nature. The degree to which the method was conservative could not be known for certain, but was probably about 7-8%. Tables 7.1-7.8 showed that the AASHTO LRFD moments were not as conservative as those calculated using the AASHTO WSD (S/7) approach.

Most of cases using AASHTO methods for exterior girders using the actual lateral location of the vehicle gave unconservative values. However, all of the values calculated using the AASHTO wheel locations (24" to curb) gave conservative design values. As expected, conservative values were also given by the older AASHTO WSD code in all cases.

8.2 PRACTICAL RESULTS

There were three types of practical results that were derived from this test. These included recommendations about the testing procedure, the quality of design methods, and insight into the Leon River Bridge behavior. The conclusions and recommendations drawn here are based strictly on the researched conducted.

8.2.1 Proposed Changes to the Bridge Instrumentation and Test Procedure

Adjustments to some of the strain gauging equipment have been made since the time of the Leon River Test. Labeling of all wires that lead from the gauge to the laptop was implemented to allow the repair of faulty channels in a more organized manner. A shunt calibration system was also added to each completion box in order to test each gauge with a predetermined strain. Based on the results of this research, no additional hardware changes could be proposed that would significantly improve the quality of data.

There was one change to the gauge layout that would result in better data reduction. In the future, concrete gauges should be used on the bridge deck and parapet portions of bridges of this type. These gauges would aid in determining the degree of composite action of the bridge deck with the girders even though non-composite action was expected. Strain data of this type would improve the quality of data reduced by either a classical composite method such as the one chosen in this research or the Moment-Couple Method presented, but not chosen. In addition, data from gauges placed at the curbs would allow for a better model of the contributing parapet portions.

A change to the lateral location of the dump truck would allow for more meaning full comparisons of LLDFs. Many of the lever rule and rigid body design moments given in Tables 7.1 and 7.3 appear conservative because the AASHTO position used to calculate the design LLDF was different than the actual position of the truck on the bridge. In future tests, the load vehicle should be placed in the

AASHTO position in order to make valid comparisons to the AASHTO design methods for exterior girders.

8.2.2 Use of Design Methods for LLDF Calculation

The BRUFEM analysis package is a useful tool for bridge analysis. The package contained appropriate modeling options that varied depending on the type of bridge system. It was relatively easy to obtain LLDF values from the BRUFEM output. The package was used mainly for this LLDF calculation and contributed greatly to this research.

The results given by BRUFEM matched the field data very well. This good correlation substantiated the modeling assumptions made in the BRUFEM model. It was believed that the solution used for non-standard vehicle modeling given in Section 2.3.2.2 and that to K-type diaphragm modeling given in Section 2.3.2.3 were satisfactory and had negligible impact on the results. In summary, BRUFEM can be used with confidence as a preliminary design tool for moment distribution in steel girder-slab bridges.

Considering the conservative nature of the Fully Composite method, the AASHTO LRFD equations did a satisfactory job in estimating truck moments for interior girders. The use of the AASHTO LRFD equations for exterior girders did not produce good estimates. The geometry of the Leon River Bridge was such that the LRFD correction factor for exterior girders had to be taken as 1.0. These poor estimates of exterior girder LLDFs would lead to very conservative design moments dictated by the AASHTO rigid body analysis LLDFs.

8.2.3 Insight into Bridge Behavior

The current AASHTO lever rule, rigid body, and old AASHTO WSD design methods for exterior girders were quite conservative in this case. The Leon River Bridge was tested with a heavy dump truck in the appropriate lanes and with an overload vehicle. Measured moments did not approach those predicted by most equations for exterior girder design. This was due perhaps to the participation of the deck slab in a degree of composite action that was not anticipated in the design of the bridge.

Most overweight vehicles are longer and wider than typical vehicles. The increased dimensions help reduce moment effects in two ways. The axles of the 61.7-foot long HETS vehicle were frequently in multiple spans, which reduces the maximum positive moment a span will experience. Also the increased width would warrant that the vehicle be driven down the center of the bridge. This caused the load to be distributed almost equally among the four girders. Therefore, most maximum individual girder moment values for the HETS were similar to those obtained for the dump truck.

The equalizing of distribution factors with distance had a profound effect on the design stress ranges for the girders. When the test vehicles progressed away from a section, the moment was reversed, but also more spread out. This is significant because an exterior girder may not take the as great a portion of the maximum positive moment as it would the maximum negative moment at the same location if the truck positions that cause the extremes differ by a large distance. The AASHTO LRFD design methods currently do not have a method of calculating stress ranges that takes this effect into consideration, therefore the stress ranges used in design were very conservative in most cases. The actual moment ranges were measured in this research and predicted by BRUFEM. The BRUFEM estimates were easy to attain and were remarkably close to the moment ranges taken directly from the field data. This effect should be studied further to properly understand and predict the range of stresses seen by bridge girders.

APPENDIX A

BRUFEM Input Files

This appendix contains the input files used in the BRUFEM analysis presented in this research. The HISTORY.PRE files are listed first. They contain all the information for the BRUFUM analyses. Six HISTORY.PRE files are listed, one for each type of analysis performed. The BAR.DAT file is presented next and contains the geometry of the girders on the Leon River Bridge. The VEH.DAT files used to model the non-standards vehicles are presented at the end of this appendix.

A.1. HISTORY.PRE FILES FOR ALL BRUFEM ANALYSES

A.1.1. HISTORY.PRE File for the CGM Using the Dump Truck:

```
BEGIN_HISTORY_FILE
-----<PROBLEM_TITLE>----------------------
DUMPTRUCK 3-4  CGMODEL (50,57,107,120,129,139,155)
-----<BRIDGE_TYPE_IBTYPE>-----------------
STL
-----<TYPE_OF_UNITS>----------------------
1
-----<VARIABLE/CONSTANT_SKEW>-------------
1
-----<PRIS_NONPRIS_IXSECT>----------------
2
-----<STL_BASIC_MODEL_DATA>---------------
4 6.6667 0
-----<ANALYSIS_TYPE_FULL/LIVE>------------
1
-----<COMPOSITE_MODEL_TYPE>---------------
2
-----<SLAB_THICK_STRENGTH>----------------
6 4
-----<NUM_ELEM_BTWN_GIRD>-----------------
4
-----<NUM_SPANS>--------------------------
3
-----<SPAN_LEN_&_NUM_Y_ELEMS>-------------
70 35
-----<SPAN_LEN_&_NUM_Y_ELEMS>-------------
90 45
-----<SPAN_LEN_&_NUM_Y_ELEMS>-------------
70 35
-----<STL_EFF_NEG_MOM>--------------------
100
-----<STL_DIA_TYPE>----------------------
2
-----<STL_DIA_CROSS_&_BTM_AREA>-----------
2.5 3.05
```

```
-----<STL_DIA_TOP_&_BTM_DIST>------------
1.5 4.5
-----<ADDED_DIA_YESNO>-------------------
Y
-----<ADDED_DIA_COUNT>-------------------
11
-----<ADDED_DIA_DIST>--------------------
20 40 55 85 100 115 130 145 175 190 210
-----<STL_HINGE_YESNO>-------------------
N
-----<EXTRA_MEMBERS_YESNO>---------------
N
-----<LEFT_EDGE_WIDTH_&_COUNT>-----------
2.8333 2
-----<RIGHT_EDGE_WIDTH_&_COUNT>----------
2.8333 2
-----<TRAVEL_CLEARANCE_L_&_R>------------
2.25 2.25
-----<VEH_LOAD_GROUP_01_YESNO>-----------
Y
-----<VEH_INPUT_FILE_INTER>--------------
F
-----<VEH_POSITION_METHOD>---------------
1
-----<VEH_POSITION_FWD/REV_X_Y>----------
F 164.5 607
-----<LANE_LOAD_DESC_YESNO>--------------
N
-----<LANE_LOAD_COUNT>-------------------
0
-----<MORE_LIVE_LOADS_01_YESNO>----------
Y
-----<VEH_LOAD_GROUP_02_YESNO>-----------
Y
-----<VEH_INPUT_FILE_INTER_SAME>---------
S
-----<VEH_POSITION_METHOD>---------------
1
-----<VEH_POSITION_FWD/REV_X_Y>----------
F 164.5 691
-----<LANE_LOAD_DESC_YESNO>--------------
N
-----<LANE_LOAD_COUNT>-------------------
0
-----<MORE_LIVE_LOADS_02_YESNO>----------
Y
-----<VEH_LOAD_GROUP_03_YESNO>-----------
Y
-----<VEH_INPUT_FILE_INTER_SAME>---------
S
-----<VEH_POSITION_METHOD>---------------
1
-----<VEH_POSITION_FWD/REV_X_Y>----------
F 164.5 1291
-----<LANE_LOAD_DESC_YESNO>--------------
N
-----<LANE_LOAD_COUNT>-------------------
```

```
0
-----<MORE_LIVE_LOADS_03_YESNO>-----------
Y
-----<VEH_LOAD_GROUP_04_YESNO>------------
Y
-----<VEH_INPUT_FILE_INTER_SAME>----------
S
-----<VEH_POSITION_METHOD>----------------
1
-----<VEH_POSITION_FWD/REV_X_Y>-----------
F 164.5 1447
-----<LANE_LOAD_DESC_YESNO>---------------
N
-----<LANE_LOAD_COUNT>--------------------
0
-----<MORE_LIVE_LOADS_04_YESNO>-----------
Y
-----<VEH_LOAD_GROUP_05_YESNO>------------
Y
-----<VEH_INPUT_FILE_INTER_SAME>----------
S
-----<VEH_POSITION_METHOD>----------------
1
-----<VEH_POSITION_FWD/REV_X_Y>-----------
F 164.5 1555
-----<LANE_LOAD_DESC_YESNO>---------------
N
-----<LANE_LOAD_COUNT>--------------------
0
-----<MORE_LIVE_LOADS_05_YESNO>-----------
Y
-----<VEH_LOAD_GROUP_06_YESNO>------------
Y
-----<VEH_INPUT_FILE_INTER_SAME>----------
S
-----<VEH_POSITION_METHOD>----------------
1
-----<VEH_POSITION_FWD/REV_X_Y>-----------
F 164.5 1675
-----<LANE_LOAD_DESC_YESNO>---------------
N
-----<LANE_LOAD_COUNT>--------------------

0
-----<MORE_LIVE_LOADS_06_YESNO>-----------
Y
-----<VEH_LOAD_GROUP_07_YESNO>------------
Y
-----<VEH_INPUT_FILE_INTER_SAME>----------
S
-----<VEH_POSITION_METHOD>----------------
1
-----<VEH_POSITION_FWD/REV_X_Y>-----------
F 164.5 1867
-----<LANE_LOAD_DESC_YESNO>---------------
N
-----<LANE_LOAD_COUNT>--------------------
```

```
0
-----<MORE_LIVE_LOADS_07_YESNO>-----------
N
-----<VEH_OMIT_NONCRIT_CASES_YESNO>-------
N
-----<FEM_OUTPUT_QUANTITY>----------------
2
-----<SELECTIVE_OUTPUT_FLAGS>-------------
Y
Y
Y
Y
Y
Y
Y
-----<GRAPHICS_PLOTTING_YESNO>------------
Y
END_HISTORY_FILE
```

A.1.2. HISTORY.PRE File for the EGM (With Diaphragms) Using the Dump Truck:

```
BEGIN_HISTORY_FILE
-----<PROBLEM_TITLE>----------------------
DUMPTRUCK 3-4 EGMODEL (50,57,107,120,129,139,155)
-----<BRIDGE_TYPE_IBTYPE>-----------------

STL
-----<TYPE_OF_UNITS>----------------------
1
-----<VARIABLE/CONSTANT_SKEW>-------------
1
-----<PRIS_NONPRIS_IXSECT>----------------
2
-----<STL_BASIC_MODEL_DATA>---------------
4 6.6667 0
-----<ANALYSIS_TYPE_FULL/LIVE>------------
1
-----<COMPOSITE_MODEL_TYPE>---------------
3
-----<SLAB_THICK_STRENGTH>----------------
6 4
-----<NUM_ELEM_BTWN_GIRD>-----------------
4
-----<NUM_SPANS>-------------------------
3
-----<SPAN_LEN_&_NUM_Y_ELEMS>-------------
70 35
-----<SPAN_LEN_&_NUM_Y_ELEMS>-------------
90 45
-----<SPAN_LEN_&_NUM_Y_ELEMS>-------------
70 35
-----<STL_EFF_NEG_MOM>--------------------
100
-----<STL_DIA_TYPE>----------------------
2
```

```
-----<STL_DIA_CROSS_&_BTM_AREA>-----------
2.5 3.05
-----<STL_DIA_TOP_&_BTM_DIST>------------
1.5 4.5
-----<ADDED_DIA_YESNO>-------------------
Y
-----<ADDED_DIA_COUNT>-------------------
11
-----<ADDED_DIA_DIST>--------------------
20 40 55 85 100 115 130 145 175 190 210
-----<STL_HINGE_YESNO>-------------------
N
-----<EXTRA_MEMBERS_YESNO>---------------
N
-----<LEFT_EDGE_WIDTH_&_COUNT>-----------
2.8333 2
-----<RIGHT_EDGE_WIDTH_&_COUNT>----------
2.8333 2
-----<TRAVEL_CLEARANCE_L_&_R>------------
2.25 2.25
-----<VEH_LOAD_GROUP_01_YESNO>-----------
Y
-----<VEH_INPUT_FILE_INTER>--------------
F
-----<VEH_POSITION_METHOD>---------------
1
-----<VEH_POSITION_FWD/REV_X_Y>----------
F 164.5 607
-----<LANE_LOAD_DESC_YESNO>--------------
N
-----<LANE_LOAD_COUNT>-------------------
0
-----<MORE_LIVE_LOADS_01_YESNO>----------
Y
-----<VEH_LOAD_GROUP_02_YESNO>-----------
Y
-----<VEH_INPUT_FILE_INTER_SAME>---------
S
-----<VEH_POSITION_METHOD>---------------
1
-----<VEH_POSITION_FWD/REV_X_Y>----------
F 164.5 691
-----<LANE_LOAD_DESC_YESNO>--------------
N
-----<LANE_LOAD_COUNT>-------------------
0
-----<MORE_LIVE_LOADS_02_YESNO>----------
Y
-----<VEH_LOAD_GROUP_03_YESNO>-----------
Y
-----<VEH_INPUT_FILE_INTER_SAME>---------
S
-----<VEH_POSITION_METHOD>---------------
1
-----<VEH_POSITION_FWD/REV_X_Y>----------
F 164.5 1291
-----<LANE_LOAD_DESC_YESNO>--------------
```

```
N
-----<LANE_LOAD_COUNT>--------------------
0
-----<MORE_LIVE_LOADS_03_YESNO>-----------
Y
-----<VEH_LOAD_GROUP_04_YESNO>------------
Y
-----<VEH_INPUT_FILE_INTER_SAME>----------
S
-----<VEH_POSITION_METHOD>----------------
1
-----<VEH_POSITION_FWD/REV_X_Y>-----------
F 164.5 1447
-----<LANE_LOAD_DESC_YESNO>---------------
N
-----<LANE_LOAD_COUNT>--------------------
0
-----<MORE_LIVE_LOADS_04_YESNO>-----------
Y
-----<VEH_LOAD_GROUP_05_YESNO>------------
Y
-----<VEH_INPUT_FILE_INTER_SAME>----------
S
-----<VEH_POSITION_METHOD>----------------
1
-----<VEH_POSITION_FWD/REV_X_Y>-----------
F 164.5 1555
-----<LANE_LOAD_DESC_YESNO>---------------
N
-----<LANE_LOAD_COUNT>--------------------
0
-----<MORE_LIVE_LOADS_05_YESNO>-----------
Y
-----<VEH_LOAD_GROUP_06_YESNO>------------
Y
-----<VEH_INPUT_FILE_INTER_SAME>----------
S
-----<VEH_POSITION_METHOD>----------------
1
-----<VEH_POSITION_FWD/REV_X_Y>-----------
F 164.5 1675
-----<LANE_LOAD_DESC_YESNO>---------------
N
-----<LANE_LOAD_COUNT>--------------------

0
-----<MORE_LIVE_LOADS_06_YESNO>-----------
Y
-----<VEH_LOAD_GROUP_07_YESNO>------------
Y
-----<VEH_INPUT_FILE_INTER_SAME>----------
S
-----<VEH_POSITION_METHOD>----------------
1
-----<VEH_POSITION_FWD/REV_X_Y>-----------
F 164.5 1867
-----<LANE_LOAD_DESC_YESNO>---------------
```

```
N
-----<LANE_LOAD_COUNT>--------------------
0
-----<MORE_LIVE_LOADS_07_YESNO>-----------
N
-----<VEH_OMIT_NONCRIT_CASES_YESNO>-------
N
-----<FEM_OUTPUT_QUANTITY>----------------
2
-----<SELECTIVE_OUTPUT_FLAGS>-------------
Y
Y
Y
Y
Y
Y
Y
-----<GRAPHICS_PLOTTING_YESNO>------------
Y
END_HISTORY_FILE
```

A.1.3. HISTORY.PRE File for the EGM (Without Diaphragms) Using the Dump Truck:

```
BEGIN_HISTORY_FILE
-----<PROBLEM_TITLE>----------------------
DUMPTRUCK 3-4 EGMODEL W/O DIAPHRAMS
-----<BRIDGE_TYPE_IBTYPE>-----------------

STL
-----<TYPE_OF_UNITS>----------------------
1
-----<VARIABLE/CONSTANT_SKEW>-------------
1
-----<PRIS_NONPRIS_IXSECT>----------------
2
-----<STL_BASIC_MODEL_DATA>---------------
4 6.6667 0
-----<ANALYSIS_TYPE_FULL/LIVE>------------
1
-----<COMPOSITE_MODEL_TYPE>---------------
3
-----<SLAB_THICK_STRENGTH>----------------
6 4
-----<NUM_ELEM_BTWN_GIRD>-----------------
4
-----<NUM_SPANS>--------------------------
3
-----<SPAN_LEN_&_NUM_Y_ELEMS>-------------
70 35
-----<SPAN_LEN_&_NUM_Y_ELEMS>-------------
90 45
-----<SPAN_LEN_&_NUM_Y_ELEMS>-------------
70 35
-----<STL_EFF_NEG_MOM>--------------------
100
```

```
-----<STL_DIA_TYPE>----------------------
2
-----<STL_DIA_CROSS_&_BTM_AREA>-----------
2.5 3.05
-----<STL_DIA_TOP_&_BTM_DIST>-------------
1.5 4.5
-----<ADDED_DIA_YESNO>--------------------
N
-----<STL_HINGE_YESNO>--------------------
N
-----<EXTRA_MEMBERS_YESNO>----------------
N
-----<LEFT_EDGE_WIDTH_&_COUNT>------------
2.8333 2
-----<RIGHT_EDGE_WIDTH_&_COUNT>-----------
2.8333 2
-----<TRAVEL_CLEARANCE_L_&_R>-------------
2.25 2.25
-----<VEH_LOAD_GROUP_01_YESNO>------------
Y
-----<VEH_INPUT_FILE_INTER>---------------
F
-----<VEH_POSITION_METHOD>----------------
1
-----<VEH_POSITION_FWD/REV_X_Y>-----------
F 164.5 607
-----<LANE_LOAD_DESC_YESNO>---------------
N
-----<LANE_LOAD_COUNT>--------------------
0
-----<MORE_LIVE_LOADS_01_YESNO>-----------
Y
-----<VEH_LOAD_GROUP_02_YESNO>------------
Y
-----<VEH_INPUT_FILE_INTER_SAME>----------
S
-----<VEH_POSITION_METHOD>----------------
1
-----<VEH_POSITION_FWD/REV_X_Y>-----------
F 164.5 691
-----<LANE_LOAD_DESC_YESNO>---------------
N
-----<LANE_LOAD_COUNT>--------------------
0
-----<MORE_LIVE_LOADS_02_YESNO>-----------
Y
-----<VEH_LOAD_GROUP_03_YESNO>------------
Y
-----<VEH_INPUT_FILE_INTER_SAME>----------
S
-----<VEH_POSITION_METHOD>----------------
1
-----<VEH_POSITION_FWD/REV_X_Y>-----------
F 164.5 1291
-----<LANE_LOAD_DESC_YESNO>---------------
N
-----<LANE_LOAD_COUNT>--------------------
```

```
0
-----<MORE_LIVE_LOADS_03_YESNO>-----------
Y
-----<VEH_LOAD_GROUP_04_YESNO>------------
Y
-----<VEH_INPUT_FILE_INTER_SAME>----------
S
-----<VEH_POSITION_METHOD>----------------
1
-----<VEH_POSITION_FWD/REV_X_Y>-----------
F 164.5 1447
-----<LANE_LOAD_DESC_YESNO>---------------
N
-----<LANE_LOAD_COUNT>--------------------
0
-----<MORE_LIVE_LOADS_04_YESNO>-----------
Y
-----<VEH_LOAD_GROUP_05_YESNO>------------
Y
-----<VEH_INPUT_FILE_INTER_SAME>----------
S
-----<VEH_POSITION_METHOD>----------------
1
-----<VEH_POSITION_FWD/REV_X_Y>-----------
F 164.5 1555
-----<LANE_LOAD_DESC_YESNO>---------------
N
-----<LANE_LOAD_COUNT>--------------------
0
-----<MORE_LIVE_LOADS_05_YESNO>-----------
Y
-----<VEH_LOAD_GROUP_06_YESNO>------------
Y
-----<VEH_INPUT_FILE_INTER_SAME>----------
S
-----<VEH_POSITION_METHOD>----------------
1
-----<VEH_POSITION_FWD/REV_X_Y>-----------
F 164.5 1675
-----<LANE_LOAD_DESC_YESNO>---------------
N
-----<LANE_LOAD_COUNT>--------------------

0
-----<MORE_LIVE_LOADS_06_YESNO>-----------
Y
-----<VEH_LOAD_GROUP_07_YESNO>------------
Y
-----<VEH_INPUT_FILE_INTER_SAME>----------
S
-----<VEH_POSITION_METHOD>----------------
1
-----<VEH_POSITION_FWD/REV_X_Y>-----------
F 164.5 1867
-----<LANE_LOAD_DESC_YESNO>---------------
N
-----<LANE_LOAD_COUNT>--------------------
```

```
0
-----<MORE_LIVE_LOADS_07_YESNO>-----------
N
-----<VEH_OMIT_NONCRIT_CASES_YESNO>-------
N
-----<FEM_OUTPUT_QUANTITY>----------------
2
-----<SELECTIVE_OUTPUT_FLAGS>-------------
Y
Y
Y
Y
Y
Y
Y
-----<GRAPHICS_PLOTTING_YESNO>------------
Y
END_HISTORY_FILE
```

A.1.4. HISTORY.PRE File for the CGM Using the HETS Vehicle:

```
BEGIN_HISTORY_FILE
-----<PROBLEM_TITLE>----------------------
HET CENTERED CGMODEL (50,57,107,120,129,139,155)
-----<BRIDGE_TYPE_IBTYPE>-----------------

STL
-----<TYPE_OF_UNITS>----------------------
1
-----<VARIABLE/CONSTANT_SKEW>-------------
1
-----<PRIS_NONPRIS_IXSECT>----------------
2
-----<STL_BASIC_MODEL_DATA>---------------
4 6.6667 0
-----<ANALYSIS_TYPE_FULL/LIVE>------------
1
-----<COMPOSITE_MODEL_TYPE>---------------
2
-----<SLAB_THICK_STRENGTH>----------------
6 4
-----<NUM_ELEM_BTWN_GIRD>-----------------
4
-----<NUM_SPANS>-------------------------
3
-----<SPAN_LEN_&_NUM_Y_ELEMS>-------------
70 35
-----<SPAN_LEN_&_NUM_Y_ELEMS>-------------
90 45
-----<SPAN_LEN_&_NUM_Y_ELEMS>-------------
70 35
-----<STL_EFF_NEG_MOM>--------------------
100
-----<STL_DIA_TYPE>----------------------
2
```

```
-----<STL_DIA_CROSS_&_BTM_AREA>-----------
2.5 3.05
-----<STL_DIA_TOP_&_BTM_DIST>------------
1.5 4.5
-----<ADDED_DIA_YESNO>-------------------
Y
-----<ADDED_DIA_COUNT>-------------------
11
-----<ADDED_DIA_DIST>--------------------
20 40 55 85 100 115 130 145 175 190 210
-----<STL_HINGE_YESNO>-------------------
N
-----<EXTRA_MEMBERS_YESNO>---------------
N
-----<LEFT_EDGE_WIDTH_&_COUNT>-----------
2.8333 2
-----<RIGHT_EDGE_WIDTH_&_COUNT>----------
2.8333 2
-----<TRAVEL_CLEARANCE_L_&_R>------------
2.25 2.25
-----<VEH_LOAD_GROUP_01_YESNO>-----------
Y
-----<VEH_INPUT_FILE_INTER>--------------
F
-----<VEH_POSITION_METHOD>---------------
1
-----<VEH_POSITION_FWD/REV_X_Y>----------
F 120 607
-----<LANE_LOAD_DESC_YESNO>--------------
N
-----<LANE_LOAD_COUNT>-------------------
0
-----<MORE_LIVE_LOADS_01_YESNO>----------
Y
-----<VEH_LOAD_GROUP_02_YESNO>-----------
Y
-----<VEH_INPUT_FILE_INTER_SAME>---------
S
-----<VEH_POSITION_METHOD>---------------
1
-----<VEH_POSITION_FWD/REV_X_Y>----------
F 120 691
-----<LANE_LOAD_DESC_YESNO>--------------
N
-----<LANE_LOAD_COUNT>-------------------
0
-----<MORE_LIVE_LOADS_02_YESNO>----------
Y
-----<VEH_LOAD_GROUP_03_YESNO>-----------
Y
-----<VEH_INPUT_FILE_INTER_SAME>---------
S
-----<VEH_POSITION_METHOD>---------------
1
-----<VEH_POSITION_FWD/REV_X_Y>----------
F 120 1291
-----<LANE_LOAD_DESC_YESNO>--------------
```

```
N
-----<LANE_LOAD_COUNT>--------------------
0
-----<MORE_LIVE_LOADS_03_YESNO>-----------
Y
-----<VEH_LOAD_GROUP_04_YESNO>------------
Y
-----<VEH_INPUT_FILE_INTER_SAME>----------
S
-----<VEH_POSITION_METHOD>----------------
1
-----<VEH_POSITION_FWD/REV_X_Y>-----------
F 120 1447
-----<LANE_LOAD_DESC_YESNO>---------------
N
-----<LANE_LOAD_COUNT>--------------------
0
-----<MORE_LIVE_LOADS_04_YESNO>-----------
Y
-----<VEH_LOAD_GROUP_05_YESNO>------------
Y
-----<VEH_INPUT_FILE_INTER_SAME>----------
S
-----<VEH_POSITION_METHOD>----------------
1
-----<VEH_POSITION_FWD/REV_X_Y>-----------
F 120 1555
-----<LANE_LOAD_DESC_YESNO>---------------
N
-----<LANE_LOAD_COUNT>--------------------
0
-----<MORE_LIVE_LOADS_05_YESNO>-----------
Y
-----<VEH_LOAD_GROUP_06_YESNO>------------
Y
-----<VEH_INPUT_FILE_INTER_SAME>----------
S
-----<VEH_POSITION_METHOD>----------------
1
-----<VEH_POSITION_FWD/REV_X_Y>-----------
F 120 1675
-----<LANE_LOAD_DESC_YESNO>---------------
N
-----<LANE_LOAD_COUNT>--------------------

0
-----<MORE_LIVE_LOADS_06_YESNO>-----------
Y
-----<VEH_LOAD_GROUP_07_YESNO>------------
Y
-----<VEH_INPUT_FILE_INTER_SAME>----------
S
-----<VEH_POSITION_METHOD>----------------
1
-----<VEH_POSITION_FWD/REV_X_Y>-----------
F 120 1867
-----<LANE_LOAD_DESC_YESNO>---------------
```

```
N
-----<LANE_LOAD_COUNT>--------------------
0
-----<MORE_LIVE_LOADS_07_YESNO>-----------
N
-----<VEH_OMIT_NONCRIT_CASES_YESNO>-------
N
-----<FEM_OUTPUT_QUANTITY>----------------
2
-----<SELECTIVE_OUTPUT_FLAGS>-------------
Y
Y
Y
Y
Y
Y
Y
-----<GRAPHICS_PLOTTING_YESNO>------------
Y
END_HISTORY_FILE
```

A.1.5. HISTORY.PRE File for the EGM (With Diaphragms) Using the HETS Vehicle:

```
BEGIN_HISTORY_FILE
-----<PROBLEM_TITLE>----------------------
HET CENTERED EGMODEL (50,57,107,120,129,139,155)
-----<BRIDGE_TYPE_IBTYPE>-----------------

STL
-----<TYPE_OF_UNITS>----------------------
1
-----<VARIABLE/CONSTANT_SKEW>-------------
1
-----<PRIS_NONPRIS_IXSECT>----------------
2
-----<STL_BASIC_MODEL_DATA>---------------
4 6.6667 0
-----<ANALYSIS_TYPE_FULL/LIVE>------------
1
-----<COMPOSITE_MODEL_TYPE>---------------
3
-----<SLAB_THICK_STRENGTH>----------------
6 4
-----<NUM_ELEM_BTWN_GIRD>-----------------
4
-----<NUM_SPANS>-------------------------
3
-----<SPAN_LEN_&_NUM_Y_ELEMS>-------------
70 35
-----<SPAN_LEN_&_NUM_Y_ELEMS>-------------
90 45
-----<SPAN_LEN_&_NUM_Y_ELEMS>-------------
70 35
-----<STL_EFF_NEG_MOM>--------------------
100
```

```
-----<STL_DIA_TYPE>----------------------
2
-----<STL_DIA_CROSS_&_BTM_AREA>-----------
2.5 3.05
-----<STL_DIA_TOP_&_BTM_DIST>-------------
1.5 4.5
-----<ADDED_DIA_YESNO>--------------------
Y
-----<ADDED_DIA_COUNT>--------------------
11
-----<ADDED_DIA_DIST>---------------------
20 40 55 85 100 115 130 145 175 190 210
-----<STL_HINGE_YESNO>--------------------
N
-----<EXTRA_MEMBERS_YESNO>----------------
N
-----<LEFT_EDGE_WIDTH_&_COUNT>------------
2.8333 2
-----<RIGHT_EDGE_WIDTH_&_COUNT>-----------
2.8333 2
-----<TRAVEL_CLEARANCE_L_&_R>-------------
2.25 2.25
-----<VEH_LOAD_GROUP_01_YESNO>------------
Y
-----<VEH_INPUT_FILE_INTER>---------------
F
-----<VEH_POSITION_METHOD>----------------
1
-----<VEH_POSITION_FWD/REV_X_Y>-----------
F 120 607
-----<LANE_LOAD_DESC_YESNO>---------------
N
-----<LANE_LOAD_COUNT>--------------------
0
-----<MORE_LIVE_LOADS_01_YESNO>-----------
Y
-----<VEH_LOAD_GROUP_02_YESNO>------------
Y
-----<VEH_INPUT_FILE_INTER_SAME>----------
S
-----<VEH_POSITION_METHOD>----------------
1
-----<VEH_POSITION_FWD/REV_X_Y>-----------
F 120 691
-----<LANE_LOAD_DESC_YESNO>---------------
N
-----<LANE_LOAD_COUNT>--------------------
0
-----<MORE_LIVE_LOADS_02_YESNO>-----------
Y
-----<VEH_LOAD_GROUP_03_YESNO>------------
Y
-----<VEH_INPUT_FILE_INTER_SAME>----------
S
-----<VEH_POSITION_METHOD>----------------
1
-----<VEH_POSITION_FWD/REV_X_Y>-----------
```

```
F 120 1291
-----<LANE_LOAD_DESC_YESNO>--------------
N
-----<LANE_LOAD_COUNT>-------------------
0
-----<MORE_LIVE_LOADS_03_YESNO>-----------
Y
-----<VEH_LOAD_GROUP_04_YESNO>------------
Y
-----<VEH_INPUT_FILE_INTER_SAME>----------
S
-----<VEH_POSITION_METHOD>----------------
1
-----<VEH_POSITION_FWD/REV_X_Y>-----------
F 120 1447
-----<LANE_LOAD_DESC_YESNO>--------------
N
-----<LANE_LOAD_COUNT>-------------------
0
-----<MORE_LIVE_LOADS_04_YESNO>-----------
Y
-----<VEH_LOAD_GROUP_05_YESNO>------------
Y
-----<VEH_INPUT_FILE_INTER_SAME>----------
S
-----<VEH_POSITION_METHOD>----------------
1
-----<VEH_POSITION_FWD/REV_X_Y>-----------
F 120 1555
-----<LANE_LOAD_DESC_YESNO>--------------
N
-----<LANE_LOAD_COUNT>-------------------
0
-----<MORE_LIVE_LOADS_05_YESNO>-----------
Y
-----<VEH_LOAD_GROUP_06_YESNO>------------
Y
-----<VEH_INPUT_FILE_INTER_SAME>----------
S
-----<VEH_POSITION_METHOD>----------------
1
-----<VEH_POSITION_FWD/REV_X_Y>-----------
F 120 1675
-----<LANE_LOAD_DESC_YESNO>--------------
N
-----<LANE_LOAD_COUNT>-------------------

0
-----<MORE_LIVE_LOADS_06_YESNO>-----------
Y
-----<VEH_LOAD_GROUP_07_YESNO>------------
Y
-----<VEH_INPUT_FILE_INTER_SAME>----------
S
-----<VEH_POSITION_METHOD>----------------
1
-----<VEH_POSITION_FWD/REV_X_Y>-----------
```

```
F 120 1867
-----<LANE_LOAD_DESC_YESNO>--------------
N
-----<LANE_LOAD_COUNT>-------------------
0
-----<MORE_LIVE_LOADS_07_YESNO>-----------
N
-----<VEH_OMIT_NONCRIT_CASES_YESNO>-------
N
-----<FEM_OUTPUT_QUANTITY>----------------
2
-----<SELECTIVE_OUTPUT_FLAGS>-------------
Y
Y
Y
Y
Y
Y
Y
-----<GRAPHICS_PLOTTING_YESNO>------------
Y
END_HISTORY_FILE
```

A.1.6. HISTORY.PRE File for the EGM (Without Diaphragms) Using the HETS Vehicle:

```
BEGIN_HISTORY_FILE
-----<PROBLEM_TITLE>---------------------
HET MODEL (EGM W/OUT DIAPHRAMS)
-----<BRIDGE_TYPE_IBTYPE>-----------------

STL
-----<TYPE_OF_UNITS>---------------------
1
-----<VARIABLE/CONSTANT_SKEW>-------------
1
-----<PRIS_NONPRIS_IXSECT>----------------
2
-----<STL_BASIC_MODEL_DATA>---------------
4 6.6667 0
-----<ANALYSIS_TYPE_FULL/LIVE>------------
1
-----<COMPOSITE_MODEL_TYPE>---------------
3
-----<SLAB_THICK_STRENGTH>----------------
6 4
-----<NUM_ELEM_BTWN_GIRD>-----------------
4
-----<NUM_SPANS>-------------------------
3
-----<SPAN_LEN_&_NUM_Y_ELEMS>-------------
70 35
-----<SPAN_LEN_&_NUM_Y_ELEMS>-------------
90 45
-----<SPAN_LEN_&_NUM_Y_ELEMS>-------------
70 35
```

```
-----<STL_EFF_NEG_MOM>--------------------
100
-----<STL_DIA_TYPE>----------------------
2
-----<STL_DIA_CROSS_&_BTM_AREA>-----------
2.5 3.05
-----<STL_DIA_TOP_&_BTM_DIST>-------------
1.5 4.5
-----<ADDED_DIA_YESNO>--------------------
N
-----<STL_HINGE_YESNO>--------------------
N
-----<EXTRA_MEMBERS_YESNO>----------------
N
-----<LEFT_EDGE_WIDTH_&_COUNT>------------
2.8333 2
-----<RIGHT_EDGE_WIDTH_&_COUNT>-----------
2.8333 2
-----<TRAVEL_CLEARANCE_L_&_R>-------------
2.25 2.25
-----<VEH_LOAD_GROUP_01_YESNO>------------
Y
-----<VEH_INPUT_FILE_INTER>---------------
F
-----<VEH_POSITION_METHOD>----------------
1
-----<VEH_POSITION_FWD/REV_X_Y>-----------
F 120 607
-----<LANE_LOAD_DESC_YESNO>---------------
N
-----<LANE_LOAD_COUNT>--------------------
0
-----<MORE_LIVE_LOADS_01_YESNO>-----------
Y
-----<VEH_LOAD_GROUP_02_YESNO>------------
Y
-----<VEH_INPUT_FILE_INTER_SAME>----------
S
-----<VEH_POSITION_METHOD>----------------
1
-----<VEH_POSITION_FWD/REV_X_Y>-----------
F 120 691
-----<LANE_LOAD_DESC_YESNO>---------------
N
-----<LANE_LOAD_COUNT>--------------------
0
-----<MORE_LIVE_LOADS_02_YESNO>-----------
Y
-----<VEH_LOAD_GROUP_03_YESNO>------------
Y
-----<VEH_INPUT_FILE_INTER_SAME>----------
S
-----<VEH_POSITION_METHOD>----------------
1
-----<VEH_POSITION_FWD/REV_X_Y>-----------
F 120 1291
-----<LANE_LOAD_DESC_YESNO>---------------
```

```
N
-----<LANE_LOAD_COUNT>--------------------
0
-----<MORE_LIVE_LOADS_03_YESNO>-----------
Y
-----<VEH_LOAD_GROUP_04_YESNO>------------
Y
-----<VEH_INPUT_FILE_INTER_SAME>----------
S
-----<VEH_POSITION_METHOD>----------------
1
-----<VEH_POSITION_FWD/REV_X_Y>-----------
F 120 1447
-----<LANE_LOAD_DESC_YESNO>---------------
N
-----<LANE_LOAD_COUNT>--------------------
0
-----<MORE_LIVE_LOADS_04_YESNO>-----------
Y
-----<VEH_LOAD_GROUP_05_YESNO>------------
Y
-----<VEH_INPUT_FILE_INTER_SAME>----------
S
-----<VEH_POSITION_METHOD>----------------
1
-----<VEH_POSITION_FWD/REV_X_Y>-----------
F 120 1555
-----<LANE_LOAD_DESC_YESNO>---------------
N
-----<LANE_LOAD_COUNT>--------------------
0
-----<MORE_LIVE_LOADS_05_YESNO>-----------
Y
-----<VEH_LOAD_GROUP_06_YESNO>------------
Y
-----<VEH_INPUT_FILE_INTER_SAME>----------
S
-----<VEH_POSITION_METHOD>----------------
1
-----<VEH_POSITION_FWD/REV_X_Y>-----------
F 120 1675
-----<LANE_LOAD_DESC_YESNO>---------------
N
-----<LANE_LOAD_COUNT>--------------------

0
-----<MORE_LIVE_LOADS_06_YESNO>-----------
Y
-----<VEH_LOAD_GROUP_07_YESNO>------------
Y
-----<VEH_INPUT_FILE_INTER_SAME>----------
S
-----<VEH_POSITION_METHOD>----------------
1
-----<VEH_POSITION_FWD/REV_X_Y>-----------
F 120 1867
-----<LANE_LOAD_DESC_YESNO>---------------
```

```
N
-----<LANE_LOAD_COUNT>--------------------
0
-----<MORE_LIVE_LOADS_07_YESNO>-----------
N
-----<VEH_OMIT_NONCRIT_CASES_YESNO>-------
N
-----<FEM_OUTPUT_QUANTITY>----------------
2
-----<SELECTIVE_OUTPUT_FLAGS>-------------
Y
Y
Y
Y
Y
Y
Y
-----<GRAPHICS_PLOTTING_YESNO>------------
Y
END_HISTORY_FILE
```

A.2. BAR.DAT FILE FOR LEON RIVER BRIDGE GIRDER:

```
CROSS SECTIONS:   Required Header
ENGLISH
3:                3 Sections
1 6 3:            Section 1 TSlabG = 6", 3 Plates
11.510 0.855:     Top Flange
0.580 31.38:      Web
11.510 .855:      Bottom Flange
2 6 5
10.5 .5:          Top Cover Plate
11.510 .855:      Top Flange
.580 31.38:       Web
11.510 .855:      Bottom Flange
10.5 .5:          Bottom Cover Plate
3 6 3
11.535 .960
.605 31.38
11.535 .960
14:               14 Section ID Locations
1:                Section 1 at start
64 1:             64 feet to end of section 1
0 2:              0 feet to start of 2
12 2:             12 feet to end of 2 Ignoring tapered ends
0 1:              0 feet to start of 1
14 1:             14 feet to end of 1
0 3
50 3
0 1
14 1
0 2
12 2
0 1
64 1
```

```
END-DATA
```

A.3. VEH.DAT FILES FOR TEST VEHICLES

A.3.1. VEH.DAT File for the Dump Truck:

```
VEHICLE DATA
ENGLISH:       English Units
1:             # of Vehicles
1:             FIRST Vehicle Properties, # of axles
10.12 6.6 0 2: First Axle Properties
18.17:         Second Axle weight
5:             Wheel Gage
1:             Wheel Spacing
4:             Wheels on Axle
2:             # of Axles
13.4:          Spacing between axle groups
4.5:           Spacing between axles
END-DATA
```

A.3.2. VEH.DAT File for the Army HETS Vehicle:

```
VEHICLE DATA
ENGLISH:                  English Units
1:                        # of Vehicles
4:                        FIRST Vehicle Properties, # of axle groups
19.40 6.833 0 2:          First Axle Properties
11.80 11.58 11.55 11.16:  Subsequent Axle weights
6.833 6.833 6.833 4.83:   Wheel Gages
0 0 0 2.67:               Wheel Spacings
2 2 2 4:                  Wheels on Axles (Note 4 instead of 8)
1 1 1 5:                  # of Axles in each group
12.917 5 5 15.104:        Spacing between axle groups
0 0 0 5.938:              Spacing between axles
END-DATA
```

REFERENCES

American Association of State Highway and Transportation Officials (AASHTO). (1998). *LRFD Bridge Design Specifications*, 2nd Edition, Washington D.C.

American Association of State Highway and Transportation Officials (AASHTO). (1992). *Standard Specification for Highway Bridges*, 15th Edition, Washington D.C.

Computers and Structures, Inc. (1997). "SAP2000 Analysis Reference–Volumes I and II." Version 6.1.

Computers and Structures, Inc. (1997). "SAP2000 Getting Started–Basic Analysis Reference." Version 6.1.

Hays Jr., C. O., Consolazio, G. R., Hoit, M.I., and Kakhandiki, A. (1994). "Bridge Rating of Girder-Slab Bridges Using Automated Finite Element Technology." *Structures Research Report No. 94-1*, Department of Civil Engineering, University of Florida at Gainesville.

Jauregui, D. V. (1999). "Measurement-Based Evaluation of Non-Composite Steel Girder Bridges." Doctorial Dissertation, University of Texas at Austin.

McIlrath, D. S. (1999). "Improving Bridge Rating and Truck Permitting Procedures Through Finite Element Analysis." Master's Thesis, University of Texas at Austin.